

The 19th International Symposium on Nonlinear Acoustics

May 21 – May 24, 2012

International Conference Center of
Waseda University, Tokyo, Japan

19th IS

Tokyo Japan 2012



International Symposium on Nonlinear Acoustics

Program and Abstracts



Hosted by
Nonlinear Acoustics Society of Japan



and Sponsored by
Acoustical Society of Japan (ASJ)
Acoustical Society of America (ASA)
International Union of Pure and Applied Physics (IUPAP)
The University of Electro-Communications (UEC)

<http://www.isna19.com>

The 19th International Symposium on Nonlinear Acoustics

May 21 – May 24, 2012

International Conference Center of
Waseda University, Tokyo, Japan

19th IS

Tokyo Japan 2012



International Symposium on Nonlinear Acoustics

Co-chaired by

Tomoo KAMAKURA

Member of International Organizing Committee of ISNA

and

Nobumasa SUGIMOTO

President of Nonlinear Acoustics Society of Japan

About ISNA

Although the origin of nonlinear acoustics dates back to the pioneering work by great mathematicians and physicists in 18th and 19th centuries, a new surge emerged in 1960's to research various problems associated with acoustic waves of finite amplitude from a unified point of view as "nonlinear acoustics." In 1968, the meeting devoted to discuss exclusively nonlinear acoustics was held at the Navy Underwater Sound Laboratory, New London, Connecticut, USA. This meeting has since been labeled the first International Symposium on Nonlinear Acoustics (ISNA).† Since then, the ISNA was held every year or every two years in Denmark, France, the Soviet Union, the United Kingdom and the United States until 1978. After this year, the ISNA has been held every three years. The following table lists the year and location where the ISNA was held in the past.

ISNA-1	1968	New London, USA
ISNA-2	1969	Austin, USA
ISNA-3	1971	Birmingham, Great Britain
ISNA-4	1972	Buffalo, USA
ISNA-5	1973	Copenhagen, Denmark
ISNA-6	1975	Moscow, USSR
ISNA-7	1976	Blacksburg, USA
ISNA-8	1978	Paris, France
ISNA-9	1981	Leeds, Great Britain
ISNA-10	1984	Kobe, Japan
ISNA-11	1987	Novosibirsk, USSR
ISNA-12	1990	Austin, USA
ISNA-13	1993	Bergen, Norway
ISNA-14	1996	Nanjing, China
ISNA-15	1999	Goettingen, Germany
ISNA-16	2002	Moscow, Russia
ISNA-17	2005	State College, USA
ISNA-18	2008	Stockholm, Sweden

† Nonlinear Acoustics (eds. Mark F. Hamilton & David T. Blackstock), Academic Press (1998).

CONTENTS

Welcome to the 19th International Symposium on Nonlinear Acoustics	1
Organization and Sponsors	2
Scope of the Symposium	4
Invited Lectures and Organized Sessions	5
General Information / Contact Information	7
Floor Map	10
Program at a Glance	11
Scientific Program	14
Program	19
Abstracts	41
Author Index	112
Session Chair Index	115

Welcome to the 19th International Symposium on Nonlinear Acoustics

It is our great pleasure to hold the International Symposium on Nonlinear Acoustics at the International Conference Center of Waseda University in Tokyo, Japan. This is the 19th symposium since 1968, and is hosted by the Nonlinear Acoustics Society of Japan.

Although the symposium was originally scheduled to be held from August 1 to 4 in 2011, it was postponed due to the aftermath of the terrible disasters by the very powerful earthquake and tsunamis on March 11, 2011, and the accidents at Fukushima nuclear power plants. In view of progresses in restoration and in securing safety, the symposium has been decided to be held after nine months of delay. Because of this delay, resubmission of abstracts was newly called for from October to November, 2011, with the abstracts submitted initially before February, 2011 held effective. While some of the abstracts were canceled, we were pleased to find that many abstracts were resubmitted in the original form or renewed one, and some abstracts were newly submitted.

The symposium consists of the Invited Lectures by the eminent scientists in plenary sessions, the Invited Papers in six pre-nominated sessions on hot topics organized by experts, and the contributed papers in oral and poster presentation. All the abstracts received were peer-reviewed and screened for presentation from a viewpoint of quality and also of the Scope of the Symposium. Efforts of review by the members of the International Scientific Committee and of the Local Organizing Committees are greatly acknowledged. The number of papers is just suitable for the three-and-half-day symposium so that appropriate time may be allocated to each presentation.

All members of the Nonlinear Acoustics Society of Japan welcome you cordially to the symposium by providing a forum for eminent scientists and engineers, and students to discuss problems and exchange ideas in academic atmosphere. We are expecting that this symposium will contribute greatly not only to advancement of nonlinear acoustics itself but also to international collaboration and cooperation in research, especially among young researchers and students.

As Tokyo is one of the busiest capitals in the world and the conference site is located just in the heart of the metropolitan area, you will be able to observe and experience both modern and traditional aspects of Japanese life. You may also discover beautiful scenery and many features of interest in the countryside. We hope you may partake in some sightseeing or travel by yourself and enjoy your stay in Japan in addition to participating in the symposium.

We would like to appreciate all the support of sponsors, academic organizations, partner societies, foundations and companies. We would also like to express our thanks to the Waseda University for providing us with its facility of the International Conference Center. Without their generous supports, this symposium would not be held.

Finally we are hoping that this year's symposium and your stay in Tokyo will be most pleasant and rewarding.

Sincerely

Tomoo Kamakura,
Nobumasa Sugimoto,
Co-Chairpersons of the 19th ISNA

Organization and Sponsors

■ Co-Chairpersons:

Tomoo Kamakura (The University of Electro-Communications, Tokyo)

Nobumasa Sugimoto (Osaka University, Osaka)

■ Members of International Organizing Committee:

M. F. Hamilton (USA), General Secretary

A. A. Atchley (USA)

Ph. Blanc-Benon (France)

L. A. Crum (USA)

B. O. Enflo (Sweden)

X. F. Gong (China)

H. Hobæk (Norway)

P. A. Johnson (USA)

T. Kamakura (Japan)

V. K. Kedrinskii (Russia)

W. Lauterborn (Germany)

W. G. Mayer (USA)

K. A. Naugolnykh (USA/Russia)

L. A. Ostrovsky (USA/Russia)

O. A. Sapozhnikov (Russia)

I. Yu. Solodov (Germany/Russia)

■ Members of International Scientific Committee:

T. Kamakura (Japan), Co-chairman

N. Sugimoto (Japan), Co-chairman

A. A. Atchley (USA)

Ph. Blanc-Benon (France)

F. Coulouvrat (France)

L. A. Crum (USA)

M. F. Hamilton (USA)

C. M. Hedberg (Sweden)

P. A. Johnson (USA)

V. K. Kedrinski (Russia)

V. A. Khokhlova (USA/Russia)

D. Lohse (Netherlands)

R. Mettin (Germany)

O. A. Sapozhnikov (Russia)

I. Yu. Solodov (Germany/Russia)

Y. Watanabe (Japan)

T. Yano (Japan)

K. Yasui (Japan)

■ Members of Local Organizing Committee:

A. Nakamura (Honorary Member, Osaka)

T. Kamakura (Co-Chairman, The University of Electro-Communications, Tokyo)

N. Sugimoto (Co-Chairman, Osaka University, Osaka)

I. Akiyama (Doshisha University, Kyoto)

S. Biwa (Kyoto University, Kyoto)

T. Biwa (Tohoku University, Sendai)

P. Choi (Meiji University, Tokyo)

S. Hatanaka (The University of Electro-Communications, Tokyo)

J. Kondoh (Shizuoka University, Hamamatsu)

D. Koyama (Doshisha University, Kyoto)

T. Kozuka (National Institute of AIST, Nagoya)

E. Kurihara (Oita University, Oita)

Y. Matsumoto (The University of Tokyo, Tokyo)

H. Mitome (National Institute of AIST, Nagoya)

H. Nomura (The University of Electro-Communications, Tokyo)

Y. Oikawa (Waseda University, Tokyo)

Y. Ouchi (Waseda University, Tokyo)

S. Saito (Tokai University, Shimizu)

S. Sakamoto (The University of Shiga Prefecture, Hikone)

T. Tsuchiya (Doshisha University, Kyoto)

Y. Watanabe (Doshisha University, Kyoto)

K. Yamanaka (Tohoku University, Sendai)

Y. Yamazaki (Waseda University, Tokyo)

T. Yano (Osaka University, Osaka)

K. Yasui (National Institute of AIST, Nagoya)

Host

Nonlinear Acoustics Society of Japan

Sponsors

■ Academic organizations:

Acoustical Society of Japan (ASJ)
Acoustical Society of America (ASA)
International Union of Pure and Applied Physics (IUPAP)
The University of Electro-Communications (UEC)

■ Partner Academic Societies:

Japan Society of Sonochemistry
Marine Acoustics Society of Japan
The Institute of Electronics, Information and Communication Engineers
The Japan Society for Non-Destructive Inspection
The Japan Society of Applied Physics
The Japan Society of Fluid Mechanics
The Japan Society of Ultrasonics in Medicine

■ Foundations:

Inoue Foundation for Science
Kato Foundation for Promotion of Science
The Kajima Foundation
The Murata Science Foundation

■ Companies:

Do Produce
Fuji Ultrasonic Engineering Co., Ltd.
Japan Probe Co. Ltd.
KANSAI Automation Co., Ltd.
KGK Co., Ltd.
Mitsubishi Electric Corporation
Mitsubishi Electric Engineering Co. Ltd
Semiconductor Energy Laboratory Co., Ltd.
Tokyo Keiki Inc.

Scope of the Symposium

■ Categories and topics intended for the symposium

1. General theory of nonlinear acoustics

Analytical methods, numerical methods, ray theory, scattering theory, shocks, solitons, chaos, bifurcation, localization, phase conjugation, etc.

2. Nonlinear acoustics in fluids

Sound beams, parametric arrays, resonators, acoustic streaming, radiation pressure, acoustic levitation, etc.

3. Nonlinear acoustics in multiphase and porous media, and cavitation phenomena

Bubbly liquid, cavitation, sonoluminescence, sonochemistry, etc.

4. Nonlinear acoustics in solids and structures

Elastic waves, viscoelastic waves, surface waves, nonlinear acousto-electronics, non-destructive evaluation and testing, etc.

5. Nonlinear acoustics of reacting, relaxing media, and physical kinetics

Nonlinear acoustics in superfluid helium, waves in rarefied gases, micro-acoustics, nano-acoustics, quantum effects, sonic crystals, metamaterials, etc.

6. Nonlinear acoustics in medicine and biology

Shock wave therapy, diagnostic ultrasound, ultrasound propagation in bone and biological tissue, nonlinear acoustics in speech, etc.

7. Thermoacoustics

Energy conversion and their devices, aero-thermoacoustics, combustion noise and oscillations, etc.

8. Nonlinear acoustics of atmosphere, ocean, and earth, and nonlinear underwater acoustics

Shock wave, sonic boom, aircraft noise, intense noise generated by ground transportation, infrasound, acoustic-gravity waves, explosions, earthquakes, etc.

9. Nonlinear aero- and hydroacoustics

Vortex sound, jets, turbulence, flow-induced sound, etc.

10. Nonlinear acoustics and optics

Laser generation of acoustic waves, optoacoustical spectroscopy, magneto-acoustics, etc.

11. General experimental methods

Measurements, instrumentations, etc.

12. Devices and industrial applications of nonlinear acoustics

Musical acoustics is included here.

13. Other topics in nonlinear acoustics

Invited Lectures

A wide variety of nonlinear acoustic effects associated with a small kidney stone

Oleg Sapozhnikov, *Moscow State University (Russia) & University of Washington (USA)*

Sources and propagation of atmospheric acoustic shock waves

François Coulouvrat, *University of Pierre and Marie Curie (France)*

Nonlinear aspects of modern ultrasound applications in medicine

Vera A. Khokhlova, *Moscow State University (Russia) & University of Washington (USA)*

Understanding of thermoacoustic phenomena and their applications

Tetsushi Biwa, *Tohoku University (Japan)*

Nonlinear acoustic/seismic waves in earthquake processes

Paul A. Johnson, *Los Alamos National Laboratory (USA)*

Conditions inside a collapsing bubble

Kenneth S. Suslick, *University of Illinois at Urbana Champaign (USA)*

Organized Sessions and Organizers

Cavitation and bubble dynamics

Organizers: Kyuichi Yasui (Japan) & Shinichi Hatanaka (Japan)

Invited Paper:

News from bubble dynamics: high static pressures, shock waves and interior dynamics

Werner Lauterborn, Thomas Kurz, Philipp Koch, Mohsen Alizadeh, Hendrik Söhnholz, Daniel Schanz, *Universität Göttingen (Germany)*

Sonochemistry and sonoluminescence

Organizers: Kyuichi Yasui (Japan) & Shinichi Hatanaka (Japan)

Invited Papers:

Observing multi-bubble sonoluminescence in phosphoric acid

Kai Yang¹, Maimaititusong Maimaitiming^{1,2}, Cui Ying Zhang^{1,3}, Qi Rong Zhu¹, Yu An¹

¹*Tsinghua University*, ²*Hetian Institute of Education*, ³*Hulunbeir University (China)*

Generation and aggregation of BaTiO₃ nanoparticle under ultrasound

Kyuichi Yasui, Toru Tuziuti, Kazumi Kato, *National Institute of AIST (Japan)*

Acoustic/elastic nonlinearity in media with complex structures

Organizers: Paul A. Johnson (USA) & Lev A. Ostrovsky (USA)

Invited Papers:

Nonlinear spectroscopy of closed delaminations and surface breaking cracks: finite element simulations of clapping and nonlinear air-coupled emission

Steven Delrue, Koen Van Den Abeele, *K.U.Leuven Campus Kortrijk (Belgium)*

Nonlinear dynamical processes in media with relaxation

Lev A. Ostrovsky^{1,2}, Andrey V. Lebedev², ¹*Zel Technologies & University of Colorado (USA)*, ²*Institute of Applied Physics (Russia)*

Medical application of acoustic radiation force

Organizers: Iwaki Akiyama (Japan) & Tsuyoshi Shiina (Japan)

Invited Paper:

Principles of shear wave elastography: challenges and opportunities

Jacques Souquet, Jeremy Bercoff, Claude Cohen-Bacrie, *SuperSonic Imagine (France)*

Nonlinear acoustics in the atmosphere

Organizers: Philippe Blanc-Benon (France) & Yoshikazu Makino (Japan)

Invited Paper:

A sonic boom propagation model including mean flow atmospheric effects

Joe Salamone, Victor Sparrow, *Pennsylvania State University (USA)*

Parametric acoustic array

Organizers: Gan Woon Seng (Singapore) & Tomoo Kamakura (Japan)

Invited Paper:

Actively created quiet zones by parametric loudspeaker as control sources in the sound field

Chao Ye, Ming Wu, Jun Yang, *Institute of Acoustics, Chinese Academy of Sciences (China)*

General Information

■ Dates and venue of the symposium:

The 19th International Symposium on Nonlinear Acoustics (19th ISNA) is held from May 21 (Mon) to May 24 (Thu), 2012 at the International Conference Center of Waseda University (address: Nishi-Waseda 1-20-14, Shinjuku, Tokyo 169-0051, Japan).

■ Website of the symposium:

The official website of the symposium is <http://www.isna19.com>.

■ Registration:

All participants in the symposium except accompanying person(s) should make registration on our web or on site. Registration fee is JPY60,000 and fee for student is JPY30,000. On-site registration begins from 16:00 (to 19:00) on May 20 (Sun) at the entrance on the first (ground) floor of the International Conference Center.

■ Accommodation:

A block of rooms is reserved at Rihga Royal Hotel Tokyo, Hotel Sunroute at Takadanobaba, Sunshine City Prince Hotel and Hotel Bellclassic Tokyo. For details, visit our website or contact our travel agent KNT (see p.9).

■ Transportation and access to the venue:

The International Conference Center of Waseda University is located in the western campus of Waseda University. You may walk from JR Takadanobaba station on Yamanote line or Waseda station on Tokyo Metro Tozai line. It will take 15 minutes or 10 minutes, respectively. For details, please visit our website. You may follow the path on Google Map.

Bus service is available from JR Takadanobaba station. Please take Tokyo city bus #2 bound for Sodai-seimon (Waseda University Main Gate) and get off at Nish(west)-Waseda bus stop (second stop). Fare is JPY170. Taxi is available from JR Takadanobaba station or JR Shinjuku station. It costs JPY710 per 2 km.

■ Presentation of paper:

The symposium consists of four types of presentation, one type being the Invited Lecture in the plenary session, another the Invited Paper in the Organized Sessions (OS), and the contributed papers in oral and poster presentation. The Invited Lectures are given in Ibuka Hall (main hall) on the first (ground) floor. The Invited Papers and contributed papers in oral presentation are given in either one of three lecture rooms designated as A, B or C on the third (second) floor. The contributed papers in poster presentation are displayed in Foyer on the third (second) floor.

■ Language and length of presentation:

Official language is English. The invited lectures are given 60 minutes, 50 minutes for presentation and 10 minutes for discussion. During the invited lectures, the other sessions are adjourned. The Invited Papers are given 40 minutes, 35 minutes for presentation and 5 minutes for discussion and changeover. Contributed papers in oral presentation are given 20 minutes, 15 minutes for presentation and 5 minutes for discussion and changeover.

■ Audio/Visual equipment:

Presenters should bring their own IBM PC-compatible computers. LCD projectors are available in Ibuka Hall and all lecture rooms. No overhead projectors are available. Before each session starts, all presenters in the session are advised to connect their own computers to a switcher connecting to LCD. Mac users should prepare their own connectors and cables. In case audio facility is needed, please contact us by no later than May 18 via isna19@isna19.com. Electric power is supplied of 100 V in 50 Hz, and a plug is of flat type (two plates usually without ground).

■ Instruction of poster presentation:

Poster session is scheduled on May 22 from 16:40 to 17:40 in Foyer on the third floor. No other sessions are held during the poster session. Each presenter should prepare a poster and post it on board with a proper paper number well in advance before the session starts. The poster should be displayed throughout this session. The maximum size of the poster is 120 cm in height and 80 cm in width. The poster is attached on the board by pushpins.

■ Instruction of preparation of paper:

All authors are invited to submit their papers to the conference proceedings to be published in one volume of the Conference Proceedings Series by the American Institute of Physics (AIP). They are asked to prepare the PDF files of their papers according to the 6x9 inch single column format. The templates and guidelines for Microsoft Word or for LaTeX are available from the following website: <http://proceedings.aip.org/outline/6x9>. Please follow the link to find the instructions, MS Word templates and LaTeX classes in several different formats.

Papers should be prepared within the following page limits in accordance with the types of presentations:

- Invited lecture: 8 to 10 pages
- Invited paper: 6 to 8 pages
- Contributed paper (both oral and poster presentations): 4 pages.

Color graphics may be reproduced in electronic version of the Proceedings on DVD. However, all original graphics will be converted to black and white in printed version of the Proceedings. The maximum size of the PDF file is **10 MB**.

■ Submission of paper for the Proceedings:

Before submission, please print out the PDF file for your final check, looking for any blank/black or garbles which would result from missing fonts, and make sure that all fonts are appropriately embedded in the PDF file.

The file name should be the family name of the presenting author followed by the abstract ID number in parentheses, for example, kamakura (1000).pdf. Please submit the paper by uploading it to the ISNA19 website until May 24, 2012.

On submission of paper, you should also submit Transfer of Copyright Agreement which is also available from the AIP website. If any figures or tables are taken in their entirety from other sources, you are requested to submit Executed Permission to Reprint Published Material from the publisher and/or author. These materials are also to be uploaded in a single PDF file. If you have a difficulty in creating the PDF file, you may send them via isna19@isna19.com.

The deadline of submission of the paper, Transfer of Copyright Agreement, and if necessary, Executed Permission is **May 24, 2012**.

■ Internet connection:

Wireless internet connection is available in Foyer on the third floor.

For connection, please use the following ID, key and protocol:

network name: isna2012
security key: isna2012japan,
security protocol: WPA2.

■ Messages:

Please check regularly the message board in front of Symposium Office on the third floor.

■ Reception and banquet:

Reception is held in the evening on May 21 from 18:30 at Chinzanso, Four Seasons Hotel near Rihga Royal Hotel Tokyo (a 10-minute walk from the Conference Center). Participants registered and their accompanying persons are cordially invited. Dinners are served in buffet style. Banquet is held in the evening on May 23 from 18:30 at Royal Hall on the third floor of Rihga Royal Hotel Tokyo. A ticket is available at JPY10,000 per person. Both reception and banquet are informal.

■ Optional tours:

During the symposium, no social activity other than reception and banquet are planned. But you may partake in optional tours. Please contact our travel agent KNT or consult at KNT travel desk.

■ Security and safety:

Tokyo is safe even in late night. But please be careful in crowded, public places. When earthquake hits, do not be panic. Modern buildings are earthquake-proof. Please secure your evacuation route in emergency when you check in your hotel.

Radioactivity level is normal and well below the safe limit except for restricted area of radius 20 km centered about Fukushima #1 nuclear power plants, 220km northeast of Tokyo. Please feel easy about all foods because production in contaminated area is prohibited and very strict inspection is performed.

■ Medical facility:

Medical service is available at the hospital of the National Center of Global Health and Medicine (<http://www.ncgm.go.jp/>, Office hour: 8:30-11:00 on Monday to Friday, Phone number: (03) 3202-7181, Address: Toyama 1-21-1, Shinjuku, Tokyo 162-8655). This center is located close to the International Conference Center of Waseda University (a 15-minute walk). In case you need a medical service, please consult our staff member.

■ Smoking:

Smoking is prohibited in the inside of the building of International Conference Center.

■ Annular solar eclipse on May 21, 2012:

We will see fully annular, solar eclipse in the morning at 07h 34m 30s for about three hours from 06h 19m. Don't look at the sun without protecting your eyes. Sunglasses are not enough.

Contact Information

■ Symposium office:

The Symposium office is located on the third floor of the International Conference Center (Phone: 080-2275-7959).

■ Symposium secretariat:

Graduate School of Informatics and Engineering
The University of Electro-Communications
1-5-1 Chofugaoka, Chofu, Tokyo 182-8285, Japan
E-mail: isna19@isna19.com, Phone: +81-42-443-5161

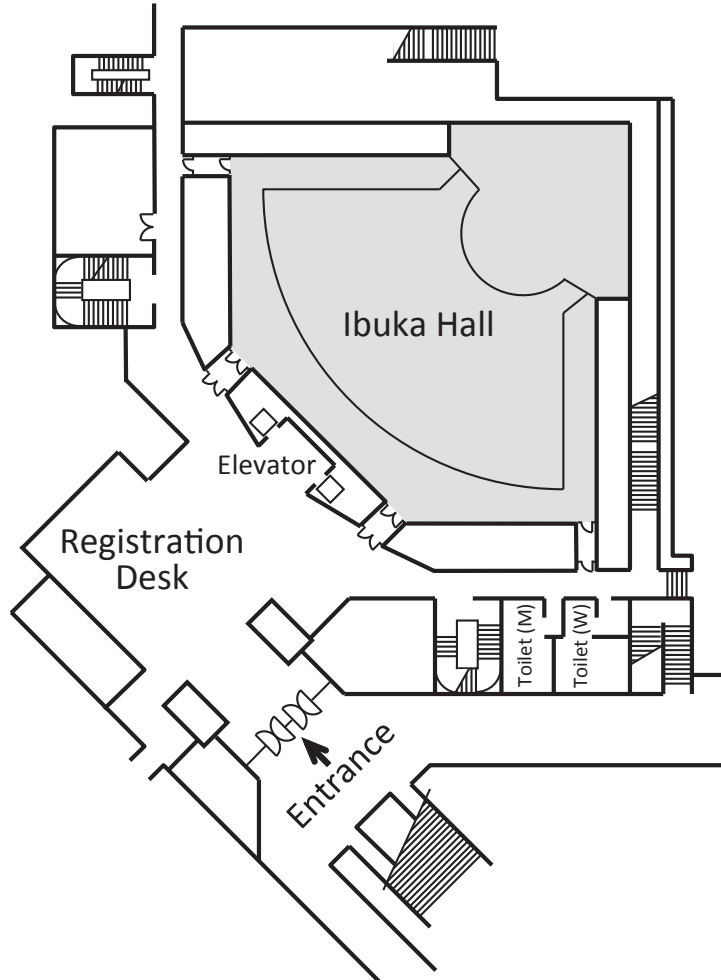
■ Official travel agent:

Kinki Nippon Tourist Co., Ltd. (KNT)
Global Business Management Branch, 12F Kanda-Izumi-cho Bldg.
Kanda Izumi-cho 1-12, Chiyoda, Tokyo 101-0024, Japan
E-mail: isna19-gbm@or.knt.co.jp, Phone: +81-3-6891-9600, Fax: +81-3-6891-9599

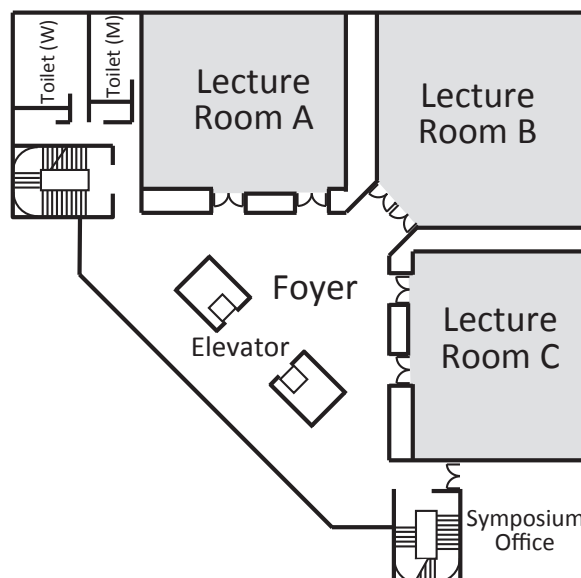
Floor Map

International Conference Center, Waseda University

■ 1st Floor (Ground Floor)



■ 3rd Floor (2nd Floor)



19th IS



Program at a Glance

Tokyo Japan 2012

International Symposium on Nonlinear Acoustics

Overview

■ May 21 (Mon):

8:50 - 9:30 : Opening ceremony

9:30 - 10:30 : Ibuka Hall: **Opening Lecture “A wide variety of nonlinear acoustic effects associated with a small kidney stone” by Oleg Sapozhnikov**

11:00 - 12:00 : Lecture Room A : Nonlinear acoustics in atmosphere 1 (OS)

Lecture Room B : Nonlinear acoustics and optics/ Device and industrial applications

Lecture Room C : Nonlinear acoustics in solids and structures 1

13:40 - 15:00 : Lecture Room A : Nonlinear acoustics in atmosphere 2 (OS)

Lecture Room B : Medical application of microbubbles

Lecture Room C : Nonlinear acoustics in solids and structures 2

15:30 - 16:30 : Ibuka Hall : **Invited Lecture “Sources and propagation of atmospherical acoustic shock waves” by François Coulouvrat**

16:40 - 17:40 : Lecture Room A : General theory of nonlinear acoustics 1

Lecture Room B : Nonlinear acoustics in fluids 1

Lecture Room C : General theory of nonlinear acoustics 2 / General experimental method

■ May 22 (Tue):

8:50 - 10:30 : Lecture Room A : Nonlinear acoustics in atmosphere 3 (OS)

Invited Paper : “A sonic boom propagation model including mean flow atmospheric effects” by Joe Salamone

Lecture Room B : Nonlinear acoustics in clinical medicine

Lecture Room C : General theory of nonlinear acoustics 3

11:00 - 12:00 : Ibuka Hall : **Invited Lecture “Nonlinear aspects of modern ultrasound applications in medicine” by Vera A. Khokhlova**

13:40 - 15:00 : Lecture Room A : Nonlinear acoustics in multiphase

Lecture Room B : Medical application of acoustic radiation force 1 (OS)

Invited Paper : “Principles of shear wave elastography: challenges and opportunities” by Jacques Souquet

Lecture Room C : Nonlinear acoustics in fluids 2

15:30 - 16:30 : Lecture Room A : Cavitation and bubble dynamics 1 (OS)

Lecture Room B : Medical application of acoustic radiation force 2 (OS)

Lecture Room C : General theory of nonlinear acoustics 4

16:40 - 17:40 : Poster session

■ **May 23 (Wed):**

8:50 - 10:30 : Lecture Room A : Cavitation and bubble dynamics 2 (OS)
Lecture Room B : Acoustic/elastic nonlinearity in media with complex structures 1 (OS)
Invited Paper : "Nonlinear spectroscopy of closed delaminations and surface breaking cracks: finite element simulations of clapping and nonlinear air-coupled emission" by Koen Van Den Abeele
Lecture Room C : Thermoacoustics 1

11:00 - 12:00 : Ibuka Hall: **Invited Lecture "Understanding of thermoacoustic phenomena and their applications" by Tetsushi Biwa**

13:40 - 15:00 : Lecture Room A : Cavitation and bubble dynamics 3 (OS)
Invited Paper : "News from bubble dynamics: high static pressures, shock waves and interior dynamics" by Werner Lauterborn
Lecture Room B : Acoustic/elastic nonlinearity in media with complex structures 2 (OS)
Invited Paper : "Nonlinear dynamical processes in media with relaxation" by Lev A. Ostrovsky
Lecture Room C : Thermoacoustics 2

15:30 - 16:30 : Ibuka Hall: **Invited Lecture "Nonlinear acoustic/seismic waves in earthquake processes "by Paul A. Johnson**

16:40 - 17:40 : Lecture Room A : Sonochemistry and sonoluminescence 1 (OS)
Invited Paper : "Observing multi-bubble sonoluminescence in phosphoric acid" by Yu An
Lecture Room B : Acoustic/elastic nonlinearity in media with complex structures 3 (OS)
Lecture Room C : Thermocoustics 3/ Nonlinear aeroacoustics

■ **May 24 (Thu):**

8:30 - 10:30 : Lecture Room A : Nonlinear acoustics in medicine and biology/ Sonochemistry and sonoluminescence 2 (OS)
Invited Paper : "Generation and aggregation of BaTiO₃ nanoparticle under ultrasound" by Kyuichi Yasui,
Lecture Room B : Acoustic/elastic nonlinearity in media with complex structures 4 (OS)
Lecture Room C : Parametric acoustic array (OS)
Invited Paper : "Actively created quiet zones by parametric loudspeaker as control sources in the sound field" by Jun Yang

11:00 - 12:00 : Ibuka Hall : **Closing Lecture "Conditions inside a collapsing bubble" by Kenneth S. Suslick**

12:00 - Closing ceremony

May 21 (Monday)

8:50	Welcome & Opening Ceremony (Ibuka Hall)		
9:30	Chair : T. Kamakura		
	1a L1. Opening Lecture A wide variety of nonlinear acoustic effects associated with a small kidney stone Oleg Sapozhnikov		
10:30	Coffee break		
	Lecture Room A	Lecture Room B	Lecture Room C
	Nonlinear acoustics in atmosphere 1	Nonlinear acoustics and optics/ Device and industrial applications	Nonlinear acoustics in solids and structures 1
	Chair : Ph. Blanc-Benon	Chair : K. Nakamura	Chair : S. Biwa
11:00	1a A01. Computational fluid dynamics simulations of infrasound generated process by meteorites François Coulouvrat	1a B01. Acoustic effects at interaction of laser radiation with a liquid accompanied by optical breakdown A. V. Bulanov	1a C01. Anharmonic properties of CaO Krishna Murti Raju
11:20	1a A02. Interference patterns in non-homogeneous flow over the obstacles Janna Lvovna Maltseva	1a B02. Three-dimensional focus scanning by an acoustic variable-focus optical liquid lens Daisuke Koyama	1a C02. Nonlinear approach for evaluation properties of materials at elevated temperature Iosif E Shkolnik
11:40	1a A03. Acoustic waves in the atmosphere and ground generated by volcanic activities Mie Ichihara	1a B03. Observation of acoustic streaming in water/sensor plate/thin water layer/ 128YX-LiNbO3 for realizing disposable digital microfluidic system Jun Kondoh	1a C03. Non-linear elasto-plastic shock wave simulation in high-velocity compaction by discrete element method Leif Kari
12:00	Lunch		
	Lecture Room A	Lecture Room B	Lecture Room C
	Nonlinear acoustics in atmosphere 2	Medical application of microbubbles	Nonlinear acoustics in solids and structures 2
	Chair : Y. Makino	Chair : V. A. Khokhlova	Chair : C. M. Hedberg
13:40	1p A04. Nonlinear propagation of acoustic pulses through the atmosphere with the anisotropic wind velocity and temperature nonhomogeneities Igor Chunchuzov		1p C04. Subharmonic wave analysis in crack using the developed FEM Tsuyoshi Mihara
14:00	1p A05. Numerical simulation of shock wave propagation in flows Régis Marchiano	1p B05. Effects of the liposomal formulation on the behavior and physical characteristics of acoustic liposomes Nicolas Sax	1p C05. Two dimensional model for subharmonic generation at closed cracks with damped double nodes Kazushi Yamanaka
14:20	1p A06. Global variation of sonic boom overpressure due to seasonal changes in atmosphere Hiroshi Yamashita	1p B06. Analysis of a bubble deformation process in a microcapsule by shock waves for developing DDS Masaaki Tamagawa	1p C06. Formation and evaluation of closed stress corrosion cracks in Ni-based alloy weld metal for nuclear power plants Yoshikazu Ohara
14:40		1p B07. Enhancement of cavitation inception by second-harmonic superimposition Shin Yoshizawa	1p C07. Analysis of harmonic generation in Lamb waves by finite-difference time-domain method Naoki Matsuda
15:00	Coffee break		
15:30	Chair : Ph. Blanc-Benon		
16:30	1p L2. Invited Lecture Sources and propagation of atmospherical acoustic shock waves François Coulouvrat		
	Lecture Room A	Lecture Room B	Lecture Room C
	General theory of nonlinear acoustics 1	Nonlinear acoustics in fluids 1	General theory of nonlinear acoustics 2/ General experimental method
	Chair : T. Yano	Chair : J. Kondoh	Chair : Y. Watanabe
16:40	1p A08. Derivation of exact solutions of the inhomogeneous Burgers equation using the Darboux transformations Oleg Sapozhnikov	1p B08. Nonlinear and dispersive effects in the propagation of a finite-amplitude sound wave in a waveguide Pablo Luis Rendon	1p C08. Nonlinearity parameter B/A and scattering of sound by sound Kiran Shanker
17:00	1p A09. On the evolution of a spherical short pulse in nonlinear acoustics Bengt O. Enflo	1p B09. Peculiarities of shocks forming in high intensity acoustic beams in the presence of soft boundary at interaction area Dmitry A Kasyanov	1p C09. Validation of planar wave incidence technique for measurement of transmission-loss Koichi Mori
17:20	1p A10. Whether there can be something general between methods of classical linear wave equation solving and a finding of analytical solutions of nonlinear acoustical equations? Yury Nikolaevich Makov	1p B10. Nonlinear shear visco-elastic properties of liquids Bair Damdinov	1p C10. Acoustic micromanipulation in a microchannel Teruyuki Kozuka
17:40			
18:30	Reception (Chinzanso)		

May 22 (Tuesday)

	Lecture Room A	Lecture Room B	Lecture Room C
	Nonlinear acoustics in atmosphere 3	Nonlinear acoustics in clinical medicine	General theory of nonlinear acoustics 3
	Chair : Y. Makino & Ph. Blanc-Benon	Chair : H. Hasegawa	Chair : K. Yoshimura
8:50	2a A01. Invited Paper A sonic boom propagation model including mean flow atmospheric effects		
9:10	Joe Salamone	2a B02. Nonlinear modeling of 3D ultrasound fields of HIFU arrays Vera A Khokhlova	2a C02. Localization and interaction of small inclusions with phase transformations in acoustic field Vladimir A. Bulanov
9:30	2a A03. Numerical simulations for sonic boom propagation through an inhomogeneous atmosphere with winds Masafumi Yamamoto	2a B03. Effective bandwidth extension by combined harmonics Gregory Thomas Clement	2a C03. Ultrafast solitons measurement in crystalline semiconductor wafers by femtosecond laser ultrasonics Nicolas Chuecos
9:50	2a A04. Infrasound propagation in realistic atmosphere using nonlinear ray theory Olaf Gainville	2a B04. Linearization strategies for the iterative nonlinear contrast source method for full-wave simulation of nonlinear ultrasound fields Martin D Verweij	2a C04. Low-frequency intrinsic localized modes in a spatially periodic and articulated structure of rigid members with elastic supports Yosuke Watanabe
10:10	2a A05. Numerical and asymptotic solutions of generalised Burgers equation John Michael Schofield	2a B05. Coded excitation in detection of polymer-shelled ultrasound contrast agents: in vitro study Veera Venkata Satya Narayana Kothapalli	2a C05. A study on bifurcations and structure of phase space concerning intrinsic localized modes in a nonlinear magneto-mechanical lattice Masayuki Kimura
10:30	Coffee break		
11:00	Chair : M. F. Hamilton		
12:00	2a L3. Invited Lecture: Nonlinear aspects of modern ultrasound applications in medicine Vera A. Khokhlova		
12:00	Lunch		
	Lecture Room A	Lecture Room B	Lecture Room C
	Nonlinear acoustics in multiphase	Medical application of acoustic radiation force 1	Nonlinear acoustics in fluids 2
	Chair : H. Takahira	Chair : I. Akiyama	Chair : Bengt O. Enflo
13:40	2p A06. Sound propagation in saturated gas-vapor-droplet mixtures with evaporation and nonlinear particle relaxation Max Kandula	2p B06. Invited Paper Principles of shear wave elastography: challenges and opportunities	2p C06. Molecular dynamics study of sound propagation in a gas Takeru Yano
14:00	2p A07. Instability and breakup of a gas-cored viscous annular jet Takao Yoshinaga	Jacques Souquet	2p C07. Resonant gas oscillation with evaporation and condensation Masashi Inaba
14:20	2p A08. Focused ultrasound induced free-surface breakup and damage in acrylic plates Yukio Tomita	2p B08. Endoscopic optical coherence elastography using acoustic radiation force and a vibrating fiber scanner Kentaro Nakamura	2p C08. Numerical simulation of non linear acoustic streaming in a standing wave resonator Diana Baltean-Carlès
14:40	2p A09. Bubble dynamics and decompression wave structure in a magmatic melt: diffusion effects Valeriy Kirillovich Kedrinskiy	2p B09. Ultrasonic actuation of biological tissues using dual acoustic radiation force for assessment of elastic properties Hideyuki Hasegawa	2p C09. Experimental study of acoustic streaming in a high level standing wave guide: influence of mean temperature and higher harmonics distribution Ida Reytt
15:00	Coffee break		
	Lecture Room A	Lecture Room B	Lecture Room C
	Cavitation and bubble dynamics 1	Medical application of acoustic radiation force 2	General theory of nonlinear acoustics 4
	Chair : E. Kurihara	Chair : G. T. Clement	Chair : Leif Kari
15:30	2p A10. Theoretical study on the shape instability of an encapsulated bubble in an ultrasound field Shu Takagi	2p B10. Acoustic radiation force on a gas bubble in tissue Mark F. Hamilton	2p C10. Existence and stability of localized modes in one-dimensional nonlinear lattices Kazuyuki Yoshimura
15:50	2p A11. Pattern formation on the wall of acoustically driven gas bubble Alexey Maksimov	2p B11. Experimental study on temperature rise of acoustic radiation force elastography Marie Tabaru	2p C11. Modulational instability and chaotic breathers in two dimensional Fermi-Pasta-Ulam lattices Yusuke Doi
16:20	2p A12. Direct numerical simulations of nonspherical bubble collapse with nonequilibrium phase transition by the improved ghost fluid method Hiroyuki Takahira	2p B12. Temperature elevation of biological tissue model exposed by focused ultrasound with acoustic radiation force Naotaka Nitta	2p C12. Controlled translation of an intrinsic localized mode Masayuki Sato
16:40	Poster Session (Foyer on 3rd Floor)		
17:40			

May 23 (Wednesday)

	Lecture Room A	Lecture Room B	Lecture Room C
	Cavitation and bubble dynamics 2	Acoustic/elastic nonlinearity in media with complex structures 1	Thermoacoustics 1
	Chair : Yu An	Chair : L. A. Ostrovsky	Chair : K. Ishii
8:50	3a A01. Stability thresholds for multi-bubble systems David Sinden	3a B01. Invited Paper Nonlinear spectroscopy of closed delaminations and surface breaking cracks: finite element simulations of clapping and nonlinear air-coupled emission	3a C01. Improvement of energy conversion efficiency of thermoacoustic engine by a multistage stack with multiple pore radii Kohei Yanagimoto
9:10	3a A02. Derivation of nonlinear wave equations for ultrasound beam in nonuniform bubbly liquids Tetsuya Kanagawa	Koen Van Den Abeele	3a C02. Thermoacoustics design using stems of goose down stack Irna - Farikhah
9:30	3a A03. A model for coupled bubble dynamics between thin elastic tissue layers Todd A. Hay	3a B03. Nonlinear resonant ultrasound spectroscopy (NRUS) applied to fatigue damage evaluation in a pure copper Yutaka Ishii	3a C03. Amplitude dependence of thermoacoustic properties of stacked wire meshes Atsushi Obayashi
9:50	3a A04. Nonlinear interaction among oscillating non-spherical bubbles Eru Kurihara	3a B04. A quantitative imaging of bonding strength at the bonded solid-solid interface obtained by nonlinear test Jianjun Chen	3a C04. Investigation of the acoustic field in a standing wave thermoacoustic refrigerator using time-resolved particle image velocimetry Philippe Blanc-Benon
10:10	3a A05. Orbital motions of bubbles in an acoustic field Minori Shiota	3a B05. Evaluation of the concrete structure integrity via nonlinear ultrasonic measurements Marta Korenska	3a C05. High-amplitude acoustic oscillations externally induced in a thermoacoustic engine Yuki Ueda
10:30	Coffee break		
11:00	Chair : A. A. Atchley		
12:00	3a L4. Invited Lecture	Understanding of thermoacoustic phenomena and their applications Tetsushi Biwa	
12:00	Lunch		
	Lecture Room A	Lecture Room B	Lecture Room C
	Cavitation and bubble dynamics 3	Acoustic/elastic nonlinearity in media with complex structures 2	Thermoacoustics 2
	Chair : V. K. Kedrinskiy	Chair : K. Van Den Abeele	Chair : Ph. Blanc-Benon
13:40	3p A06. Studying acoustic and shock wave effects accompanying the optical breakdown of water and some alcohols by 1,064 nm nanosecond radiations Grigory Toker	3p B06. Invited Paper Nonlinear dynamical processes in media with relaxation	3p C06. Account of heat convection by Rayleigh streaming in the description of wave amplitude growth and stabilization in a standing wave thermoacoustic prime-mover Guillaume Penelet
14:00	3p A07. Peak gas density during shock driven cavity collapse Nicholas Hawker	Lev A. Ostrovsky	3p C07. Numerical analysis of thermoacoustic spontaneous oscillations in a 2D rectangular and an axisymmetric closed tube Masahiro Ishigaki
14:20	3p A08. Invited Paper News from bubble dynamics: high static pressures, shock waves and interior dynamics Werner Lauterborn	3p B08. Localization of a nonlinear source in the bulk of a solid Pierre-Yves Le Bas	3p C08. Numerical simulations of thermoacoustic oscillations in a looped tube Dai Shimizu
14:40			
15:00	Coffee break		
15:30	Chair : N. Sugimoto		
16:30	3p L5. Invited Lecture	Nonlinear acoustic/seismic waves in earthquake processes Paul A. Johnson	
	Lecture Room A	Lecture Room B	Lecture Room C
	Sonochemistry and sonoluminescence 1	Acoustic/elastic nonlinearity in media with complex structures 3	Thermoacoustics 3/ Nonlinear aeroacoustics
	Chair : K. S. Suslick	Chair : O. Sapozhnikov	Chair : M. F. Hamilton
16:40	3p A10. Invited Paper Observing multi-bubble sonoluminescence in phosphoric acid Yu An	3p B10. Dilatance and acoustic nonlinearity of dry and saturated marine sand Nora A. Vilchinska	3p C10. Asymptotic analysis of thermoacoustic effects near the critical point Pierre Carles
17:00		3p B11. Comparative study of two wideband nonlinear methods applied to an experimental model of prostheses osseointegration Jacques Riviere	3p C11. Nonlinearity analysis of model-scale jet noise Anthony A. Atchley
17:20	3p A12. Two components of Na atom emission from collapsing bubbles in surfactant solutions Yuichi Hayashi	3p B12. Imaging of partial plastic deformation in thin steel plate by immersion nonlinear ultrasonic resonance Koichiro Kawashima	3p C12. Numerical study of a silencer Mikael A Langthjem
17:40			
18:30	Banquet (Rihga Royal Hotel)		

May 24 (Thursday)

	Lecture Room A	Lecture Room B	Lecture Room C
	Nonlinear acoustics in medicine and biology/Sonochemistry and sonoluminescence 2	Acoustic/elastic nonlinearity in media with complex structures 4	Parametric acoustic array
	Chair : P.-K Choi	Chair : P. A. Johnson	Chair : W-S. Gan & H. Nomura
8:30	4a A01. Tissue lesion created by HIFU in continuous scanning mode Dong Zhang		4a C01. Invited Paper Actively created quiet zones by parametric loudspeaker as control sources in the sound field
8:50	4a A02. Real-time sonoporation through HeLa cells Spiros Kotopoulos	4a B02. An analysis on the second-order nonlinear effect of focused acoustic wave around a scatterer in an ideal fluid Gang Liu	Jun Yang
9:10	4a A03. Sonoluminescence, sonochemistry and bubble dynamics of single bubble cavitation Shin-ichi Hatanaka	4a B03. Slow variations of mechanical and electrical properties of dielectrics at high-intensity ultrasonic irradiation Claes M. Hedberg	4a C03. Estimation of parametric sound field controlled by source amplitudes and phases using numerical simulation Hideyuki Nomura
9:30	4a A04. Invited Paper Generation and aggregation of BaTiO ₃ nanoparticles under ultrasound	4a B04. Shear waves in a cubic nonlinear inhomogeneous resonator Timofey Borisovich Krit	4a C04. Modeling the directivity of parametric loudspeaker Chuang Shi
9:50	Kyuichi Yasui	4a B05. Simulation of multi-cracks in solid using harmonics filtering with a time reversal process Xiaozhou Liu	4a C05. Inverse system design based on the Volterra modeling of a parametric loudspeaker system W-S. Gan
10:10	4a A06. Autoreduction of tetrachloride gold(III) ions and spontaneous formation of gold nanoparticles in sonicated water Toshio Sakai		4a C06. 3D Simulation of parametric ultrasound fields Fabrice Prieur
10:30	Coffee break		
11:00	Chair : Y. Matsumoto		
12:00	4a L6. Closing Lecture Conditions inside a collapsing bubble Kenneth S. Suslick		
12:00	Closing Ceremony (Ibuka Hall)		

Poster Session on May 22(Tuesday)

16:40 - 17:40	2p P01. The nonlinear multifrequency sonars for underwater navigation	Vadim Yur'evich Voloshchenko
	2p P02. A novel method for detecting second harmonic ultrasonic components generated from fastened bolts	Makoto Fukuda
	2p P03. Droplet propulsion on non-piezoelectric substrates induced by Lamb waves	Wei Liang
	2p P04. Finite difference calculation of acoustic streaming including the boundary layer phenomena in an ultrasonic air pump on graphics processing unit array	Yuji Wada
	2p P05. Spectral hole burning in piezoelectric resonators	Fujio Tsuruoka
	2p P06. Measurement of temperature gradient in a stack of a prime mover in a loop-tube-type thermoacoustic cooling system	Shin-ichi Sakamoto
	2p P07. Consideration of nonlinear vibration characteristic of object for irradiating high-intensity ultrasonic waves by a point-convergence-type aerial ultrasonic source	Ayumu Osumi
	2p P08. On the two-dimensional patterning of inorganic particles in resin using ultrasound	Toru Tuziuti
	2p P09. Dynamics of second harmonics in nonlinear surface acoustic waves and a proposal of its device application	Koji Aizawa
	2p P10. Acoustic harmonic generation in a multilayered structure with nonlinear interfaces	Yosuke Ishii
	2p P11. Laser induced stress waves emerged by laser-target interaction	Motoaki Nishiwaki
	2p P12. The numerical simulation of evolution of finite-amplitude noise pulses	Igor Yu. Demin

19th IS



Tokyo Japan 2012

International Symposium on Nonlinear Acoustics

Program

May 21 (Monday)

9:30 - 10:30

Ibuka Hall

Opening LectureChair: T. Kamakura (*The University of Electro-Communications, Tokyo, Japan*)

9:30 - 10:30

1a L1. A wide variety of nonlinear acoustic effects associated with a small kidney stoneOleg Sapozhnikov^{1,2}¹Department of Acoustics, Faculty of Physics, Moscow State University, Leninskie Gory, Moscow 119991, Russia,²Center for Industrial and Medical Ultrasound, Applied Physics Laboratory, University of Washington, Seattle, WA 98105, USA

May 21 (Monday)

11:00 - 12:00

Lecture Room A

Nonlinear acoustics in atmosphere 1Chair: Ph. Blanc-Benon (*Ecole Centrale de Lyon, Lyon, France*)

11:00 - 11:20

1a A01. Computational fluid dynamics simulations of infrasound generation process by meteoritesMartin Henneton^{1,2}, Philippe Delorme¹, Olaf Gainville³, François Coulouvrat²¹ONERA, DSNA, France, ²Université Pierre et Marie Curie - UMR CNRS 7190, France, ³CEA, DAM, DIF, France

11:20 - 11:40

1a A02. Interference patterns in non-homogeneous flow over the obstaclesNikolay Ivanovich Makarenko^{1,2}, Janna Lvovna Maltseva^{1,2}¹Lavrentyev Institute of Hydrodynamics, Russia, ²Novosibirsk State University, Russia

11:40 - 12:00

1a A03. Acoustic waves in the atmosphere and ground generated by volcanic activitiesMie Ichihara¹, John Lyons², Jun Oikawa¹, Minoru Takeo¹¹Earthquake Research Institute, University of Tokyo, Japan, ²Instituto Geofísico, Escuela Politécnica Nacional, Ecuador

Lecture Room B

Nonlinear acoustics and optics/Device and industrial applicationsChair: K. Nakamura (*Tokyo Institute of Technology, Tokyo, Japan*)

11:00 - 11:20

1a B01. Acoustic effects at interaction of laser radiation with a liquid accompanied by optical breakdown

Alexey V. Bulanov

V.I. Il'ichev Pacific Oceanological Institute, Far Eastern Branch of Russian Academy of Sciences, Russia

11:20 - 11:40

1a B02. Three-dimensional focus scanning by an acoustic variable-focus optical liquid lens

Daisuke Koyama, Ryoichi Isago, Kentaro Nakamura

Precision and Intelligence Laboratory, Tokyo Institute of Technology, Japan

11:40 - 12:00

1a B03. Observation of acoustic streaming in water/sensor plate/thin water layer/ 128YX-LiNbO3 for realizing disposable digital microfluidic system

Jun Kondoh, Hitoshi Toyozumi
Shizuoka University, Japan

Lecture Room C

Nonlinear acoustics in solids and structures 1

Chair: S. Biwa (Kyoto University, Kyoto, Japan)

11:00 - 11:20

1a C01. Anharmonic properties of CaO

Krishna Murti Raju
BNV PG College, Hamirpur, India

11:20 - 11:40

1a C02. Nonlinear approach for evaluation properties of materials at elevated temperature

Iosif E Shkolnik, Huseyin R Hiziroglu
Kettering University, United States

11:40 - 12:00

1a C03. Non-linear elasto-plastic shock wave simulation in high-velocity compaction by discrete element method

Muhammad Shoaib, Leif Kari
The Marcus Wallenberg Laboratory for Sound and Vibration Research, Royal Institute of Technology, Sweden

May 21 (Monday)

13:40 - 15:00

Lecture Room A

Nonlinear acoustics in atmosphere 2

Chair: Y. Makino (Japan Aerospace Exploration Agency, Tokyo, Japan)

13:40 - 14:00

1p A04. Nonlinear propagation of acoustic pulses through the atmosphere with the anisotropic wind velocity and temperature nonhomogeneities

Igor Chunchuzov¹, Sergey Kulichkov¹, Oleg Popov¹, Roger Waxler², Jelle Assink²
¹Obukhov Institute of Atmospheric Physics, 119017 Moscow, Russia,
²National Center for Physical Acoustics, University of Mississippi, MS 38677, United States

14:00 - 14:20

1p A05. Numerical simulation of shock wave propagation in flows

Mathieu Rénier¹, Régis Marchiano¹, Eric Gaudard¹, Louis-Jonardan Gallin^{1,3}, François Coulouvrat^{1,2}
¹Université Pierre et Marie Curie, France, ²Centre National de la Recherche Scientifique, France,
³CEA, DAM, DIF, F - 91297 Arpajon, France, France

14:20 - 14:40

1p A06. Global variation of sonic boom overpressure due to seasonal changes in atmosphere

Hiroshi Yamashita¹, Shigeru Obayashi²

¹Formerly Institute of Fluid Science, Tohoku University and Currently Department of Aerospace Engineering, Nagoya University, Japan, ²Institute of Fluid Science, Tohoku University, Japan

Lecture Room B

Medical application of microbubbles

Chair: V. A. Khokhlova (Moscow State University, Moscow, Russia & University of Washington, Seattle, USA)

14:00 - 14:20

1p B05. Effects of the liposomal formulation on the behavior and physical characteristics of acoustic liposomes

Nicolas Sax¹, Sachiko Horie¹, Li Li¹, Shenwei Li¹, Takashi Kochi^{1,2}, Rui Chen¹, Yukiko Watanabe¹, Yoko Yagishita^{1,3}, Maya Sakamoto⁴, Shiro Mori⁴, Tetsuya Kodama¹

¹Graduate School of Biomedical Engineering, Tohoku University, Japan,

²Graduate School of Medicine, Tohoku University, Japan, ³Graduate School of Dentistry, Tohoku University, Japan,

⁴Tohoku University Hospital, Japan

14:20 - 14:40

1p B06. Analysis of a bubble deformation process in a microcapsule by shock waves for developing DDS

Masaaki Tamagawa, Kenshi Morimoto

Kyushu Institute of Technology, Japan

14:40 - 15:00

1p B07. Enhancement of cavitation inception by second-harmonic superimposition

Shin-ichiro Umemura, Ryo Takagi, Jun Yasuda, Shin Yoshizawa

Tohoku University, Japan

Lecture Room C

Nonlinear acoustics in solids and structures 2

Chair: C. M. Hedberg (Blekinge Institute of Technology, Karlskrona, Sweden)

13:40 - 14:00

1p C04. Subharmonic wave analysis in crack using the developed FEM

Tsuyoshi Mihara¹, Koji Shimaya¹, Yasushi Ikegami², Takashi Furukawa³, Ichiro Komura³

¹University of Toyama, Japan, ²ITOCHU Techno-Solutions Co., Japan, ³JAPEIC, Japan

14:00 - 14:20

1p C05. Two dimensional model for subharmonic generation at closed cracks with damped double nodes

Kazushi Yamanaka, Yohei Shintaku, Yoshikazu Ohara

Tohoku University, Japan

14:20 - 14:40

1p C06. Formation and evaluation of closed stress corrosion cracks in Ni-based alloy weld metal for nuclear power plants

Yoshikazu Ohara, Yohei Shintaku, Satoshi Horinouchi, Kazushi Yamanaka
Tohoku University, Japan

14:40 - 15:00

1p C07. Analysis of harmonic generation in Lamb waves by finite-difference time-domain method

Naoki Matsuda, Shiro Biwa
Graduate School of Engineering, Kyoto University, Japan

May 21 (Monday)

15:30 - 16:30

Ibuka Hall

Invited Lecture

Chair: Ph. Blanc-Benon (*Ecole Centrale de Lyon, Lyon, France*)

15:30 - 16:30

1p L2. Sources and propagation of atmospherical acoustic shock waves

François Coulouvrat
Université Pierre et Marie Curie, UMR CNRS 7190, F-75005 Paris, France

May 21 (Monday)

16:40 - 17:40

Lecture Room A

General theory of nonlinear acoustics 1

Chair: T. Yano (*Osaka University, Osaka, Japan*)

16:40 - 17:00

1p A08. Derivation of exact solutions of the inhomogeneous Burgers equation using the Darboux transformations

Oleg Sapozhnikov¹, Andrey Kudryavtsev²
¹*Department of Acoustics, Faculty of Physics, Moscow State University, Russia,*
²*Institute of Applied Mechanics of the Russian Academy of Sciences, Russia*

17:00 - 17:20

1p A09. On the evolution of a spherical short pulse in nonlinear acoustics

Bengt O. Enflo¹, Claes M. Hedberg²
¹*Royal Institute of Technology, Stockholm, Sweden,* ²*Blekinge Institute of Technology, Karlskrona, Sweden*

17:20 - 17:40

1p A10. Whether there can be something general between methods of classical linear wave equation solving and a finding of analytical solutions of nonlinear acoustical equations?

Yury Nikolaevich Makov
Moscow State University, Department of Acoustics, Faculty of Physics, Russia

Lecture Room B

Nonlinear acoustics in fluids 1

Chair: J. Kondoh (*Shizuoka University, Hamamatsu, Japan*)

16:40 - 17:00

1p B08. Nonlinear and dispersive effects in the propagation of a finite-amplitude sound wave in a waveguide

Pablo Luis Rendon

CCADET, Universidad Nacional Autonoma de Mexico, Mexico

17:00 - 17:20

1p B09. Peculiarities of shocks forming in high intensity acoustic beams in the presence of soft boundary at interaction area

Dmitry A Kasyanov¹, Mikhail S Deriabin¹, Vasily V Kurin²

¹*Radiophysical Research Institute, Russia,* ²*Nizhny Novgorod State University, Russia*

17:20 - 17:40

1p B10. Nonlinear shear visco-elastic properties of liquids

Bair Damdinov, Dagzama Makarova, Tuyana Dembelova, Badma Badmaev

Buryat scientific center of RAS, Russia

Lecture Room C

General theory of nonlinear acoustics 2/General experimental method

Chair: Y. Watanabe (*Doshisha University, Kyoto, Japan*)

16:40 - 17:00

1p C08. Nonlinearity parameter B/A and scattering of sound by sound

Kiran Shanker

Physics Dept-CMP College, University of Allahabad, India

17:00 - 17:20

1p C09. Validation of planar wave incidence technique for measurement of transmission-loss

Koichi Mori, Yoshiaki Nakamura

Department of Aerospace Engineering, Nagoya University, Japan

17:20 - 17:40

1p C10. Acoustic micromanipulation in a microchannel

Teruyuki Kozuka¹, Kyuichi Yasui¹, Shin-ichi Hatanaka²

¹*National Institute of Advanced Industrial Science and Technology (AIST), Japan,*

²*The University of Electro-Communications, Japan*

May 22 (Tuesday)

8:50 - 10:30

Lecture Room A

Nonlinear acoustics in atmosphere 3

Chair: Y. Makino (*Japan Aerospace Exploration Agency, Tokyo, Japan*)

Ph. Blanc-Benon (*Ecole Centrale de Lyon, Lyon, France*)

8:50 - 9:30

Invited Paper

2a A01. A sonic boom propagation model including mean flow atmospheric effects

Joe Salamone, Victor Sparrow

Pennsylvania State University, United States

9:30 - 9:50

2a A03. Numerical simulations for sonic boom propagation through an inhomogenous atmosphere with winds

Masafumi Yamamoto¹, Atsushi Hashimoto², Takashi Takahashi², Tomoo Kamakura³, Takeharu Sakai⁴

¹Research Center of Computational Mechanics, Inc., Japan, ²Japan Aerospace Exploration Agency, Japan,

³University of Electro-Communications, Japan, ⁴Nagoya University, Japan

9:50 - 10:10

2a A04. Infrasound propagation in realistic atmosphere using nonlinear ray theory

Philippe Blanc-Benon¹, Olaf Gainville², Julian Scott¹

¹CNRS, LMFA UMR 5509, Ecole centrale de Lyon, France, ²CEA, DAM, DIF, France

10:10 - 10:30

2a A05. Numerical and asymptotic solutions of generalised Burgers equation

John Michael Schofield, Paul William Hammerton

University of East Anglia, United Kingdom

Lecture Room B

Nonlinear acoustics in clinical medicine

Chair: H. Hasegawa (*Tohoku University, Sendai, Japan*)

9:10 - 9:30

2a B02. Nonlinear modeling of 3D ultrasound fields of HIFU arrays

Petr V Yuldashev^{1,2}, Vera A Khokhlova^{1,3}

¹Moscow State University, Russia, ²Ecole Centrale de Lyon, France, ³University of Washington, United States

9:30 - 9:50

2a B03. Effective bandwidth extension by combined harmonics

Gregory Thomas Clement^{1,2}, Hideyuki Nomura², Hideo Adachi², Tomoo Kamakura²

¹Harvard Medical School, United States, ²University of Electro-Communications, Japan

9:50 - 10:10

2a B04. Linearization strategies for the iterative nonlinear contrast source method for full-wave simulation of nonlinear ultrasound fields

Martin D Verweij, Libertario Demi, Koen WA van Dongen

Laboratory of Acoustical Imaging, Faculty of Applied Sciences, Delft University of Technology, Netherlands

10:10 - 10:30

2a B05. Coded excitation in detection of polymer-shelled ultrasound contrast agents: in vitro studyVeera Venkata Satya Narayana Kothapalli¹, Dmitry Grishenkov¹, Gaio Paradossi², Lars-Ake Brodin¹¹Medical Engineering, School of Technology and Health, KTH, Alfred Nobels Allé 10, SE-14152 Huddinge, Stockholm, Sweden,²Dipartimento di Chimica, Università di Roma Tor Vergata, 00133 Rome, Italy

Lecture Room C

General theory of nonlinear acoustics 3Chair: K. Yoshimura (*NTT Communication Science Laboratories, Kyoto, Japan*)

9:10 - 9:30

2a C02. Localization and interaction of small inclusions with phase transformations in acoustic field

Vladimir A. Bulanov

V.I. Il'ichev Pacific Oceanological Institute, Far Eastern Branch of Russian Academy of Sciences, Russia

9:30 - 9:50

2a C03. Ultrafast solitons measurement in crystalline semiconductor wafers by femtosecond laser ultrasonics

Nicolas Chuecos, Émmanuel Péronne, Bernard Perrin

Institut des NanoSciences de Paris, CNRS UMR 7588 - Université Pierre et Marie Curie, France

9:50 - 10:10

2a C04. Low-frequency intrinsic localized modes in a spatially periodic and articulated structure of rigid members with elastic supports

Yosuke Watanabe, Sojiro Awata, Nobumasa Sugimoto

Osaka University, Japan

10:10 - 10:30

2a C05. A study on bifurcations and structure of phase space concerning intrinsic localized modes in a nonlinear magneto-mechanical latticeMasayuki Kimura¹, Takashi Hikiyama²¹The University of Shiga Prefecture, Japan, ²Kyoto University, Japan

May 22 (Tuesday)

11:00 - 12:00

Ibuka Hall

Invited LectureChair: M. F. Hamilton (*The University of Texas at Austin, Texas, USA*)

11:00 - 12:00

2a L3. Nonlinear aspects of modern ultrasound applications in medicineVera A. Khokhlova^{1,2}¹Dept. of Acoustics, Faculty of Physics, M.V. Lomonosov Moscow State University, Moscow 119991, Russia,²Center for Industrial and Medical Ultrasound, Applied Physics Laboratory, University of Washington, 1013 NE 40th Street, Seattle, WA 98105

May 22 (Tuesday)

13:40 - 15:00

Lecture Room A

Nonlinear acoustics in multiphaseChair: H. Takahira (*Osaka Prefecture University, Osaka, Japan*)

13:40 - 14:00

2p A06. Sound propagation in saturated gas-vapor-droplet mixtures with evaporation and nonlinear particle relaxationMax Kandula*ESC - Team QNA, United States*

14:00 - 14:20

2p A07. Instability and breakup of a gas-cored viscous annular jetTakao Yoshinaga*Osaka University, Japan*

14:20 - 14:40

2p A08. Focused ultrasound induced free-surface breakup and damage in acrylic platesYukio Tomita, Shigenori Tanaka*Hokkaido University of Education, Hakodate, Japan*

14:40 - 15:00

2p A09. Bubble dynamics and decompression wave structure in a magmatic melt: diffusion effectsValeriy Kirillovich Kedrinskiy*Lavrentyev Institute of Hydrodynamics, SB Russian Academy of Sciences, Russia*

Lecture Room B

Medical application of acoustic radiation force 1Chair: I. Akiyama (*Doshisha University, Kyoto, Japan*)

13:40 - 14:20

Invited Paper >**2p B06. Principles of shear wave elastography: challenges and opportunities**Jacques Souquet, Jeremy Bercoff, Claude Cohen-Bacrie*SuperSonic Imagine, France*

14:20 - 14:40

2p B08. Endoscopic optical coherence elastography using acoustic radiation force and a vibrating fiber scannerRyoichi Isago, Daisuke Koyama, Kentaro Nakamura*Precision and Intelligence Laboratory, Tokyo Institute of Technology, Japan*

14:40 - 15:00

2p B09. Ultrasonic actuation of biological tissues using dual acoustic radiation force for assessment of elastic propertiesHideyuki Hasegawa, Jun Yamaguchi, Hiroshi Kanai*Tohoku University, Japan*

Lecture Room C

Nonlinear acoustics in fluids 2Chair: Bengt O. Enflo (*Royal Institute of Technology, Stockholm, Sweden*)

13:40 - 14:00

2p C06. Molecular dynamics study of sound propagation in a gasTakeru Yano*Osaka University, Japan*

14:00 - 14:20

2p C07. Resonant gas oscillation with evaporation and condensationMasashi Inaba¹, Takeru Yano², Masao Watanabe¹, Kazumichi Kobayashi¹, Shigeo Fujikawa¹¹*Hokkaido University, Japan*, ²*Osaka University, Japan*

14:20 - 14:40

2p C08. Numerical simulation of non linear acoustic streaming in a standing wave resonatorVirginie Daru^{1,3}, Diana Baltean-Carlès^{1,2}, Catherine Weisman^{1,2}¹*LIMSI-CNRS, France*, ²*Université Pierre et Marie Curie, France*, ³*Arts et Métiers ParisTech, France*

14:40 - 15:00

2p C09. Experimental study of acoustic streaming in a high level standing wave guide: influence of mean temperature and higher harmonics distributionIda Rey¹, Solenn Moreau^{1,2}, Hélène Bailliet¹, Jean-Christophe Valière¹¹*Institut Pprime, CNRS - Université de Poitiers - ENSMA, Département Fluides - Thermique - Combustion, France*,²*Laboratoire Roberval UMR UTC-CNRS No. 6253 - Université de Technologie de Compiègne, France*

May 22 (Tuesday)

15:30 - 16:30

Lecture Room A

Cavitation and bubble dynamics 1Chair: E. Kurihara (*Oita University, Oita, Japan*)

15:30 - 15:50

2p A10. Theoretical study on the shape instability of an encapsulated bubble in an ultrasound fieldYunqiao Liu, Kazuyasu Sugiyama, Shu Takagi, Yoichiro Matsumoto*The University of Tokyo, Japan*

15:50 - 16:10

2p A11. Pattern formation on the wall of acoustically driven gas bubbleAlexey Maksimov¹, Timothy Leighton²¹*Pacific Oceanological Institute FEBRAS, Russia*,²*Institute of Sound and Vibration Research, University of Southampton, United Kingdom*

16:10 - 16:30

2p A12. Direct numerical simulations of nonspherical bubble collapse with nonequilibrium phase transition by the improved ghost fluid methodYoshinori Jinbo, Hiroyuki Takahira*Osaka Prefecture University, Japan*

Lecture Room B

Medical application of acoustic radiation force 2

Chair: G. T. Clement (*Harvard Medical School, Boston, USA & The University of Electro-Communications, Tokyo, Japan*)

15:30 - 15:50

2p B10. Acoustic radiation force on a gas bubble in tissue

Yurii A. Ilinskii, Evgenia A. Zabolotskaya, Mark F. Hamilton
University of Texas at Austin, United States

15:50 - 16:10

2p B11. Experimental study on temperature rise of acoustic radiation force elastography

Marie Tabaru, Hideki Yoshikawa, Takashi Azuma, Rei Asami, Kunio Hashiba
CRL, Hitachi Ltd., Japan

16:10 - 16:30

2p B12. Temperature elevation of biological tissue model exposed by focused ultrasound with acoustic radiation force

Naotaka Nitta¹, Nobuki Kudo², Iwaki Akiyama³
¹*Human Technology Research Institute, National Institute of Advanced Industrial Science and Technology (AIST), Japan,*
²*Laboratory of Biomedical Engineering, Graduate School of Information Science and Technology, Hokkaido University, Japan,*
³*Department of Human and Environmental Science, Shonan Institute of Technology, Japan*

Lecture Room C

General theory of nonlinear acoustics 4

Chair: Leif Kari (*Royal Institute of Technology, Stockholm, Sweden*)

15:30 - 15:50

2p C10. Existence and stability of localized modes in one-dimensional nonlinear lattices

Kazuyuki Yoshimura
NTT Communication Science Laboratories, Japan

15:50 - 16:10

2p C11. Modulational instability and chaotic breathers in two dimensional Fermi-Pasta-Ulam lattices

Yusuke Doi, Akihiro Nakatani
Department of Adaptive Machine Systems, Graduate School of Engineering, Osaka University, Japan

16:10 - 16:30

2p C12. Controlled translation of an intrinsic localized mode

Masayuki Sato¹, Naoki Fujita¹, Souichi Nishimura¹, Yuichi Takao¹, Yurina Sada¹, Weihua Shi¹, A. J. Sievers²
¹*Graduate School of Natural Science and Technology, Kanazawa University, Japan,*
²*Laboratory of Atomic and Solid State Physics, Cornell University, United States*

May 22 (Tuesday)

16:40 - 17:40

Foyer on 3rd Floor

Poster Session

2p P01. The nonlinear multifrequency sonars for underwater navigationVadim Yur'evich Voloshchenko*Department of Engineering Drawing and Computer Design, Taganrog Institute of Technology, South Federal University (TIT SFedU), Russia***2p P02. A novel method for detecting second harmonic ultrasonic components generated from fastened bolts**Makoto Fukuda, Kazuhiko Imano*Department of Electrical and Electronic Engineering, Graduate School of Engineering and Resource Science, Akita University, Japan***2p P03. Droplet propulsion on non-piezoelectric substrates induced by Lamb waves**Wei Liang*ISAT, Coburg University of Applied Sciences, Germany***2p P04. Finite difference calculation of acoustic streaming including the boundary layer phenomena in an ultrasonic air pump on graphics processing unit array**Yuji Wada, Daisuke Koyama, Kentaro Nakamura*Precision and Intelligence Laboratory, Tokyo Institute of Technology, Japan***2p P05. Spectral hole burning in piezoelectric resonators**Fujio Tsuruoka*Kurume university, Japan***2p P06. Measurement of temperature gradient in a stack of a prime mover in a loop-tube-type thermoacoustic cooling system**Shin-ichi Sakamoto¹, Ryoichi Isago¹, Yoshitaka Inui¹, Yoshiaki Watanabe²¹University of Shiga Prefecture, Japan, ²Doshisha University, Japan**2p P07. Consideration of nonlinear vibration characteristic of object for irradiating high-intensity ultrasonic waves by a point-convergence-type aerial ultrasonic source**Ayumu Osumi, Youichi Ito*Nihon University, Japan***2p P08. On the two-dimensional patterning of inorganic particles in resin using ultrasound**Toru Tuziuti*National Institute of Advanced Industrial Science and Technology (AIST), Japan***2p P09. Dynamics of second harmonics in nonlinear surface acoustic waves and a proposal of its device application**Koji Aizawa, Yoshiaki Tokunaga*Kanazawa Institute of Technology, Japan*

2p P10. Acoustic harmonic generation in a multilayered structure with nonlinear interfaces

Yosuke Ishii, Shiro Biwa
Kyoto University, Japan

2p P11. Laser induced stress waves emerged by laser-target interaction

Yoshiaki Tokunaga, Motoaki Nishiwaki, Mieko Kogi, Koji Aizawa
Kanazawa Institute of Technology, Japan

2p P12. The numerical simulation of evolution of finite-amplitude noise pulses

Igor Yu. Demin, Sergey N. Gurbatov, Nikolay V. Pronchatov-Rubtsov
Nizhny Novgorod State University, Russia

May 23 (Wednesday)

8:50 - 10:30

Lecture Room A

Cavitation and bubble dynamics 2

Chair: Yu An (*Tsinghua University, Beijing, China*)

8:50 - 9:10

3a A01. Stability thresholds for multi-bubble systems

David Sinden, Eleanor Stride, Nader Saffari
Dept Mechanical Engineering, University College London, United Kingdom

9:10 - 9:30

3a A02. Derivation of nonlinear wave equations for ultrasound beam in nonuniform bubbly liquids

Tetsuya Kanagawa¹, Takeru Yano², Junya Kawahara³, Kazumichi Kobayashi³, Masao Watanabe³,
Shigeo Fujikawa³
¹The University of Tokyo, Japan, ²Osaka University, Japan, ³Hokkaido University, Japan

9:30 - 9:50

3a A03. A model for coupled bubble dynamics between thin elastic tissue layers

Todd A. Hay, Yurii A. Ilinskii, Evgenia A. Zabolotskaya, Mark F. Hamilton
Applied Research Laboratories, The University of Texas at Austin, Austin, TX 78713-8029, United States

9:50 - 10:10

3a A04. Nonlinear interaction among oscillating non-spherical bubbles

Eru Kurihara
Oita University, Japan

10:10 - 10:30

3a A05. Orbital motions of bubbles in an acoustic field

Minori Shirota, Kou Yamashita, Takao Inamura
Faculty of Science and Technology, Hirosaki University, Japan

Lecture Room B

Acoustic/elastic nonlinearity in media with complex structures 1

Chair: L. A. Ostrovsky (*Zel Technologies & University of Colorado, Boulder, USA*)

8:50 - 9:30

Invited Paper

3a B01. Nonlinear spectroscopy of closed delaminations and surface breaking cracks: finite element simulations of clapping and nonlinear air-coupled emission

Steven Delrue, Koen Van Den Abeele
K.U.Leuven Campus Kortrijk, Belgium

9:30 - 9:50

3a B03. Nonlinear resonant ultrasound spectroscopy (NRUS) applied to fatigue damage evaluation in a pure copper

Toshihiro Ohtani, Yutaka Ishii
Shonan Institute of Technology, Japan

9:50 - 10:10

3a B04. A quantitative imaging of bonding strength at the bonded solid-solid interface obtained by nonlinear test

Jianjun Chen, De Zhang, Yiwei Mao
The Institute of Acoustics, Nanjing University, China

10:10 - 10:30

3a B05. Evaluation of the concrete structure integrity via nonlinear ultrasonic measurements

Marta Korenska, Monika Manychova, Michal Matysik
Brno University of Technology, Faculty of Civil Engineering, Czech Republic

Lecture Room C

Thermoacoustics 1

Chair: K. Ishii (*Nagoya University, Nagoya, Japan*)

8:50 - 9:10

3a C01. Improvement of energy conversion efficiency of thermoacoustic engine by a multistage stack with multiple pore radii

Kohei Yanagimoto¹, Shin-ichi Sakamoto², Kentaro Kuroda¹, Yosuke Nakano³, Yoshiaki Watanabe¹
¹*Faculty of Life and Medical Sciences, Doshisha University, Japan,*
²*Department of Electronic Systems Engineering, University of Shiga Prefecture, Japan,*
³*Faculty of Science and Engineering, Doshisha University, Japan*

9:10 - 9:30

3a C02. Thermoacoustics design using stems of goose down stack

Irna - Farikhah
IKIP PGRI SEMARANG, Indonesia

9:30 - 9:50

3a C03. Amplitude dependence of thermoacoustic properties of stacked wire meshes

Atsushi Obayashi, Tetsushi Biwa
Tohoku University, Japan

9:50 - 10:10

3a C04. Investigation of the acoustic field in a standing wave thermoacoustic refrigerator using time-resolved particle image velocimetryPhilippe Blanc-Benon¹, Gaëlle Poignand², Emmanuel Jondeau¹¹LMFA UMR CNRS 5509, France, ²LAUM UMR CNRS 6613, France

10:10 - 10:30

3a C05. High-amplitude acoustic oscillations externally induced in a thermoacoustic engine

Hideki Seki, Masataka Sakamoto, Yuki Ueda

Tokyo University of A&T, Japan

May 23 (Wednesday)

11:00 - 12:00

Ibuka Hall

Invited LectureChair: A. A. Atchley (*The Pennsylvania State University, Pennsylvania, USA*)

11:00 - 12:00

3a L4. Understanding of thermoacoustic phenomena and their applications

Tetsushi Biwa

Tohoku University, Japan

May 23 (Wednesday)

13:40 - 15:00

Lecture Room A

Cavitation and bubble dynamics 3Chair: V. K. Kedrinskiy (*Lavrentyev Institute of Hydrodynamics, Novosibirsk, Russia*)

13:40 - 14:00

3p A06. Studying acoustic and shock wave effects accompanying the optical breakdown of water and some alcohols by 1,064 nm nanosecond radiations

Grigory Toker

Research Prof., Chemical Dept., Technion, Israel

14:00 - 14:20

3p A07. Peak gas density during shock driven cavity collapse

Nicholas Hawker, Yiannis Ventikos

Dept of Engineering Science, University of Oxford, United Kingdom

14:20 - 15:00

Invited Paper >

3p A08. News from bubble dynamics: high static pressures, shock waves and interior dynamics

Werner Lauterborn, Thomas Kurz, Philipp Koch, Mohsen Alizadeh, Hendrik Söhnholz, Daniel Schanz

Drittes Physikalisches Institut, Universität Göttingen, Germany

Lecture Room B

Acoustic/elastic nonlinearity in media with complex structures 2Chair: K. Van Den Abeele (*K.U. Leuven Campus Kortrijk, Belgium*)

13:40 - 14:20

Invited Paper

3p B06. Nonlinear dynamical processes in media with relaxationLev A. Ostrovsky^{1,2}, Andrey V. Lebedev²¹Zel Technologies and University of Colorado, United States, ²Institute of Applied Physics, Russia

14:20 - 14:40

3p B08. Localization of a nonlinear source in the bulk of a solidPierre-Yves Le Bas¹, Timothy J Ulrich¹, Paul A Johnson¹, Brian E Anderson²¹Los Alamos National Laboratory, United States, ²Brigham Young University, United States

Lecture Room C

Thermoacoustics 2Chair: Ph. Blanc-Benon (*Ecole Centrale de Lyon, Lyon, France*)

13:40 - 14:00

3p C06. Account of heat convection by Rayleigh streaming in the description of wave amplitude growth and stabilization in a standing wave thermoacoustic prime-moverGuillaume Penelet¹, Matthieu Guedra¹, Vitalyi Gusev²¹Laboratoire d'Acoustique de l'Université du Maine, France, ²Laboratoire de Physique de l'Etat Condense, France

14:00 - 14:20

3p C07. Numerical analysis of thermoacoustic spontaneous oscillations in a 2D rectangular and an axisymmetric closed tubeMasahiro Ishigaki¹, Koichiro Shirai², Shizuko Adachi³, Katsuya Ishii^{2,4}¹Japan Atomic Energy Agency, Japan,²Department of Computational Science and Engineering, Graduate School of Engineering, Nagoya University, Japan,³School of Business and Commerce, Tokyo International University, Japan,⁴Information Technology Center, Nagoya University, Japan

14:20 - 14:40

3p C08. Numerical simulations of thermoacoustic oscillations in a looped tube

Dai Shimizu, Kohei Nishikawa, Nobumasa Sugimoto

Department of Mechanical Science, Graduate School of Engineering Science, University of Osaka, Japan

May 23 (Wednesday)

15:30 - 16:30

Ibuka Hall

Invited LectureChair: N. Sugimoto (*Osaka University, Osaka, Japan*)

15:30 - 16:30

3p L5. Nonlinear acoustic/seismic waves in earthquake processes

Paul A. Johnson

Geophysics Group, Los Alamos National Laboratory, Los Alamos, New Mexico 87544, USA

May 23 (Wednesday)

16:40 - 17:40

Lecture Room A

Sonochemistry and sonoluminescence 1

Chair: K. S. Suslick (*The University of Illinois at Urbana-Champaign, Illinois, USA*)

16:40 - 17:20

Invited Paper

3p A10. Observing multi-bubble sonoluminescence in phosphoric acid

Kai Yang¹, Maimaititusong Maimaitiming^{1,2}, Cui Ying Zhang^{1,3}, Qi Rong Zhu¹, Yu An¹

¹Department of Physics, Tsinghua University, China, ²Hetian Institute of Education, China,

³College of Physics and Electronic Information, Hulunbeir University, China

17:20 - 17:40

3p A12. Two components of Na atom emission from collapsing bubbles in surfactant solutions

Yuichi Hayashi, Pak-Kon Choi

Meiji University, Japan

Lecture Room B

Acoustic/elastic nonlinearity in media with complex structures 3

Chair: O. Sapozhnikov (*Moscow State University, Moscow, Russia*) & *University of Washington, Seattle, USA*)

16:40 - 17:00

3p B10. Dilatance and acoustic non linearity of dry and saturated marine sand

Nora A. Vilchinska

LAA-Latvian Acoustics Association, Latvia

17:00 - 17:20

3p B11. Comparative study of two wideband nonlinear methods applied to an experimental model of prostheses osseointegration

Jacques Riviere¹, Sylvain Hupert¹, Pascal Laugier¹, Paul Johnson²

¹UPMC Univ Paris 6 & CNRS, Laboratoire d'Imagerie Paramétrique, France,

²EES-17, Los Alamos National Laboratory, United States

17:20 - 17:40

3p B12. Imaging of partial plastic deformation in thin steel plate by immersion nonlinear ultrasonic resonance

Koichiro Kawashima¹, Ryusuke Imanishi¹, Fumio Fujita², Takumi Aida²

¹Nonlinear Ultrasonic Lab. Ltd., Japan, ²Insight k.k., Japan

Lecture Room C

Thermoacoustics 3/Nonlinear aeroacoustics

Chair: M. F. Hamilton (*The University of Texas at Austin, Texas, USA*)

16:40 - 17:00

3p C10. Asymptotic analysis of thermoacoustic effects near the critical point

Pierre Carles^{1,2}

¹Université Pierre et Marie Curie (Paris 06), France, ²Case Western Reserve University, Cleveland, Ohio, United States

17:00 - 17:20

3p C11. Nonlinearity analysis of model-scale jet noiseKent L. Gee¹, Anthony A. Atchley², Lauren E. Falco², Micah R. Shepherd³¹Dept. of Physics and Astronomy, Brigham Young University, United States,²Graduate Program in Acoustics, The Pennsylvania State University, United States,³Applied Research Laboratory, The Pennsylvania State University, United States

17:20 - 17:40

3p C12. Numerical study of a silencerMikael A Langthjem¹, Masami Nakano²¹Yamagata University, Japan, ²Tohoku University, Japan

May 24 (Thursday)

8:30 - 10:30

Lecture Room A

Nonlinear acoustics in medicine and biology/Sonochemistry and sonoluminescence 2

Chair: P. -K Choi (Meiji University, Tokyo, Japan)

8:30 - 8:50

4a A01. Tissue lesion created by HIFU in continuous scanning mode

Dong Zhang, TingBo Fan

Institute of Acoustics, Nanjing Univ, China, China

8:50 - 9:10

4a A02. Real-time sonoporation through HeLa cellsAnthony Delalande¹, Spiros Kotopoulos¹, Chantal Pichon², Michiel Postema¹¹University of Bergen, Norway, ²University of Orléans, France

9:10 - 9:30

4a A03. Sonoluminescence, sonochemistry and bubble dynamics of single bubble cavitation

Shin-ichi Hatanaka

Department of Engineering Science, University of Electro-Communications, Japan

9:30 - 10:10

Invited Paper >

4a A04. Generation and aggregation of BaTiO₃ nanoparticles under ultrasound

Kyuichi Yasui, Toru Tuziuti, Kazumi Kato

National Institute of Advanced Industrial Science and Technology (AIST), Japan

10:10 - 10:30

4a A06. Autoreduction of tetrachloride gold(III) ions and spontaneous formation of gold nanoparticles in sonicated water

Toshio Sakai, Shoichi Miwa, Tomohiko Okada, Shozi Mishima

Shinshu University, Japan

Lecture Room B

Acoustic/elastic nonlinearity in media with complex structures 4Chair: P. A. Johnson (*Los Alamos National Laboratory, New Mexico, USA*)**8:50 - 9:10****4a B02. An analysis on the second-order nonlinear effect of focused acoustic wave around a scatterer in an ideal fluid**Gang Liu¹, Boo Cheong Khoo^{1,2}, Pahala Gedara Jayathilake^{1,2}¹National University of Singapore, Singapore, ²Singapore-MIT Alliance, Singapore**9:10 - 9:30****4a B03. Slow variations of mechanical and electrical properties of dielectrics at high-intensity ultrasonic irradiation**Claes M. Hedberg, Oleg V. Rudenko*Blekinge Institute of Technology, Sweden***9:30 - 9:50****4a B04. Shear waves in a cubic nonlinear inhomogeneous resonator**Timofey Borisovich Krit, Valery Georgievich Andreev, Oleg Anatol'evich Sapozhnikov*Department of Acoustics, Faculty of Physics, MSU, Russia***9:50 - 10:10****4a B05. Simulation of multi-cracks in solid using harmonics filtering with a time reversal process**Xiaozhou Liu, Ying Zhang, Jinlin Zhu, Xiufen Gong*Institute of Acoustics, Nanjing University, China*

Lecture Room C

Parametric acoustic arrayChair: W-S. Gan (*Nanyang Technological University, Singapore*)H. Nomura (*The University of Electro-Communications, Tokyo, Japan*)**8:30 - 9:10****Invited Paper** ▶**4a C01. Actively created quiet zones by parametric loudspeaker as control sources in the sound field**Chao Ye, Ming Wu, Jun Yang*Institute of Acoustics, Chinese Academy of Sciences, China***9:10 - 9:30****4a C03. Estimation of parametric sound field controlled by source amplitudes and phases using numerical simulation**Hideyuki Nomura¹, Claes M. Hedberg², Tomoo Kamakura¹¹The University of Electro-Communications, Japan, ²Blekinge Institute of Technology, Sweden

9:30 - 9:50

4a C04. Modeling the directivity of parametric loudspeaker

Chuang Shi, Woon-Seng Gan
Nanyang Technological University, Singapore

9:50 - 10:10

4a C05. Inverse system design based on the Volterra modeling of a parametric loudspeaker system

Wei Ji, Woon-Seng Gan
Nanyang Technological University, Singapore

10:10 - 10:30

4a C06. 3D Simulation of parametric ultrasound fields

Fabrice Prieur
University of Oslo, Norway

May 24 (Thursday)

11:00 - 12:00

Ibuka Hall

Closing Lecture

Chair: Y. Matsumoto (*The University of Tokyo, Tokyo, Japan*)

11:00 - 12:00

4a L6. Conditions inside a collapsing bubble

Kenneth S. Suslick
University of Illinois, United States

19th IS



Tokyo Japan 2012

International Symposium on Nonlinear Acoustics

Abstracts

Opening Lecture**1a L1.****A wide variety of nonlinear acoustic effects associated with a small kidney stone****Oleg Sapozhnikov**^{1,2}¹*Department of Acoustics, Faculty of Physics, Moscow State University, Leninskie Gory, Moscow 119991, Russia,*²*Center for Industrial and Medical Ultrasound, Applied Physics Laboratory, University of Washington, Seattle, WA 98105, USA*

The International Symposium on Nonlinear Acoustics showcases research in the applications of a broad spectrum of nonlinear phenomena. This talk focuses on the various nonlinear effects as they relate to one specific application – kidney stones.

Urinary stones have plagued mankind for millennia and even been found in Egyptian mummies. Still it is an active research area as to how they occur much less how to prevent or cure them. And in fact it encompasses many diseases, and many types of stones form. Only hydration, diluting the urinary salts, works across the board. Now it is expected from 3 to 10% of the world population will suffer from stones, and the percent is on the rise. Acoustics plays an important role every day in dealing with the disease although there is still much to be learned.

As a physical object, a kidney stone is a polycrystalline hard concretion usually formed of calcium oxalate, with an inhomogeneous structure that frequently contains voids and cracks. The stone is 2-10 millimeters across or even larger and is surrounded by a liquid (urine) and soft tissue (kidney parenchyma) that are acoustically similar to water. Various types of acoustic waves are used in diagnosis and treatment of the kidney stone disease, ranging from low-amplitude diagnostic pulses to longer and more intense Doppler pulses, even more intense continuous focused ultrasound, and shock waves with up to 100 MPa peak pressure. A variety of nonlinear acoustic effects arise in such fields around the stone and inside it. To name some of them: In the procedure called shock wave lithotripsy the incident acoustic waves are so strong that they fracture the stone. As the stone surface contains many crevices, acoustic cavitation is frequently developed in the surrounding liquid. Because of absorption of the ultrasound, acoustic streaming in the liquid can be excited as well. Because the stone is a good sound scatterer, a significant acoustic radiation force may be created when the intense ultrasound beam is directed on the stone.

Although ultrasound is already a recognized tool in the treatment of kidney stones, there is room for improvement and understanding. A hard concretion would seem a perfect target for diagnostic ultrasound, yet still in the US most stones are diagnosed with x-ray CT, despite new mandates to reduce ionizing radiation exposure to patients. Developing new stone-specific diagnostic modes

would lead to better resolution of kidney images. Shock waves generated outside or inside the body are the primary tool for breaking stones so they will pass or can be removed. But today just a little more than half of shock wave lithotripsy treatments solve the problem. Research is underway to use radiation force to expel stones and fragments after lithotripsy from the kidney. This requires sufficient force to move stones, ability to steer the stones in the designed direction, and a need to not injury kidney tissue. All those problems need deeper insight in the physical phenomena involved, which cannot be done without use of the methods of nonlinear acoustics.

Work is supported by the National Institutes of Health (DK43881, DK92197), the National Space Biomedical Research Institute through NASA NCC 9-58, and the Russian Foundation for Basic Research (RFBR 11-02-01189, 12-02-00114).

1a A01.**Computational fluid dynamics simulations of infrasound generation process by meteorites****Martin Henneon^{1,2}, Philippe Delorme¹, Olaf Gainville³, François Coulouvrat²**¹ONERA, DSNA, France, ²Université Pierre et Marie Curie - UMR CNRS 7190, France, ³CEA, DAM, DIF, France

The worldwide installation of the International Monitoring System is performed to verify the Comprehensive nuclear Test-Ban Treaty which outlaws nuclear explosions. Its aim is to detect with certainty any nuclear test explosion of at least 1 kiloton (100F-0 tons TNT equivalent). The stations of this network, which record infrasound, often detect meteorite entries. It is essential to know if recorded signals correlate with a meteoritic entry or another phenomenon such as explosions, earthquakes or volcanic eruptions. The main objective of this work is to model the emission and the propagation of infrasound generated by meteorites. This is done by combining CFD simulations of shock waves with acoustic atmospheric propagation models. In a first step the trajectory of the meteorite is investigated. Newton's laws of motion are applied, in addition to the ablation phenomenon. It appears that input parameters (velocity, altitude, angle of entry, ...) controlling the trajectory are difficult to evaluate, so a sensitivity analysis of the influence of these parameters on the trajectory has therefore been conducted. This initial study provides the range of key parameters (velocity, density, evolution of the Mach, Reynolds and Knudsen number...) during the entry. In a second step, the pressure field in the vicinity of the meteorite is simulated using Euler equations, which are solved using a finite volume method (elsA©, ONERA). The influence of the parameters such as the diameter and the velocity of the meteorite on the pressure signal, at different radial distances away from the trajectory, is quantified and compared to an empirical line-source shock model. Finally the pressure signal is propagated at very long distances using a nonlinear ray tracing method. The matching of the CFD and acoustics models is performed at a distance where the shock is locally cylindrical and weakly nonlinear. The distance at which this matching is performed is discussed. This computational method is carried out in the case of the meteorite of Carancas, which impacted in Peru in the 15th September 2007.

1a A02.**Interference patterns in non-homogeneous flow over the obstacles****Nikolay Ivanovich Makarenko^{1,2}, Janna Lvovna Maltseva^{1,2}**¹Lavrentyev Institute of Hydrodynamics, Russia, ²Novosibirsk State University, Russia

An analytical model of weakly non-homogeneous fluid flow over the topography formed by isolated group of obstacles is considered. Attention is focused on the wave patterns and wave trains generated downstream the obstacles. Our method involves the perturbation procedure using two dimensionless parameters. One of them is the Boussinesq parameter which characterizes small slope of the density profile, and another parameter gives typical dimensionless height of single obstacle. Wave solutions corresponding to sinusoidal topography with finite number of peaks are calculated and examined. The interference patterns localized in the flow domain confined directly above the topography are calculated. Strongly modulated harmonic waves were observed for relatively short sinusoidal obstacles with 5-12 peaks. The wave modulation sharpened due to substantial influence of the end peaks by the transition from forced waves over the barrier to the lee waves behind of the obstacles. This effect was not observed for long sinusoidal-bottom domains. For such domains, the near-bottom region of boundary-trapped waves of small amplitude is clearly separated from the upper region of a slowly modulated waves having maximal amplitude at the mid-height of the fluid layer. The wave amplification was also found by the variation of upstream flow parameters. The work was supported by the Russian Foundation of Basic Research (grant No 09-01-00447) and the Program RAS No 20 (Project No 4).

1a A03.**Acoustic waves in the atmosphere and ground generated by volcanic activities****Mie Ichihara¹, John Lyons², Jun Oikawa¹, Minoru Takeo¹**¹*Earthquake Research Institute, University of Tokyo, Japan,*²*Instituto Geofisico, Escuela Politecnica Nacional, Ecuador*

Active volcanoes generates a variety of oscillation in the ground and in the air. Among them is what is called 'harmonic tremor'. As the name indicates, a harmonic tremor is a sustained oscillation consisting of a fundamental mode and its overtones. Because the spectral feature is similar to that of sounds generated by musical instruments, source mechanisms of the volcanic harmonic tremors have been considered in comparison with the physics of musical instruments. Although the unique feature of the oscillation has attracted researchers for decades, the source has not been exclusively determined for any observed cases. This paper reports an interesting sequence of harmonic tremors observed in the 2011 eruption of Shinmoedake Volcano, southern Japan. The main eruptive activities started with ash-cloud forming explosive eruptions, followed by lava effusion. Harmonic tremors were transmitted into the ground and observed as seismic waves at the last stage of the effusive eruption. The tremors observed at this stage had unclear and fluctuating harmonic modes. In the atmosphere, on the other hand, many impulsive acoustic waves indicating small surface explosions were observed. When the effusion stopped and the erupted lava was shrinking, harmonic tremor started to be transmitted also to the atmosphere and observed as acoustic waves. Then the harmonic modes became clearer and more stable. This sequence of harmonic tremors is interpreted as a process in which volcanic gas tries to make a path through the erupted lava to the atmosphere. In order to test this hypothesis, a laboratory experiment was performed and the essential feature was successfully reproduced.

1a B01.**Acoustic effects at interaction of laser radiation with a liquid accompanied by optical breakdown****Alexey V. Bulanov***V.I. Il'ichev Pacific Oceanological Institute, Far Eastern Branch of Russian Academy of Sciences, Russia*

Different mechanisms of plasma fronts supersonic expansion are known at the present time: a fast ionization wave (FIW), laser supported radiation wave (LSRW), laser supported detonation wave (LSDW), breakdown and electronic thermal conductivity mechanism. The study of mechanisms of laser plasma expansion is caused by different reasons including specially the research of laser plasma spectral characteristics and plasma fronts interaction for different mechanisms. We have determined the mechanism of plasma expansion for the case of an optical breakdown and low-threshold breakdown by laser wavelength $\lambda = 1.06 \mu\text{m}$ within intensities range of $5 \cdot 10^8 - 10^{11} \text{ W/cm}^2$ in a normal atmosphere. In a case of near-threshold laser intensities close to breakdown threshold of air, $I \sim (5 - 10) \cdot 10^{10} \text{ W/cm}^2$, we have restricted to reviewing of a case of sharp-focused laser beam. In whole, the determination of plasma expansion mechanism have produced by comparison of velocities of three mechanisms: the FWI, the LSDW and the LSRW. Besides the experimental data for speeds of laser fronts were compared with theoretical calculations. Plasma experiments were performed by using 532 nm (180 mJ) and 1064 nm (360 mJ) pulses from Brilliant B Nd:YAG laser. The spectral features of breakdown (including time-dependent intensities of absorption, molecular and atomic lines) have been performed. Researches of the acoustic effects accompanying optical breakdown in a liquid, generated by the focused laser radiation have been carried out at interaction with a liquid surface. Researches have been spent on the first and the second harmonics of Nd:Yag laser. Time laser radiation in a mode of the modulated quality was equal to 10 nanoseconds. Density of power for laser impulse was 10^{11} W/cm^2 . Various modes of movement of plasma fronts have simultaneously been investigated at various focusings of laser radiation. Estimations of acoustic radiation power were spent and dynamics of spectral structure of acoustic radiation have been investigated at various modes of plasma fronts movement.

1a B02.**Three-dimensional focus scanning by an acoustic variable-focus optical liquid lens****Daisuke Koyama, Ryoichi Isago, Kentaro Nakamura***Precision and Intelligence Laboratory, Tokyo Institute of Technology, Japan*

Compact variable-focus lenses whose focal points can be varied in the axial direction are used in optical devices, such as mobile electronic devices with built-in cameras, and the camera lens and its actuator occupy a large volume. We have been investigating the variable-focus liquid lens by acoustic radiation force without a mechanical moving part. Our liquid lens was more compact and had faster response than conventional mechanical lens, and the variable-focus lens with a fast response can realize high-speed focus scanning at 1 kHz in the axial direction. It can be applied to confocal microscopy with a large depth of field that can be used to image non-flat objects under a microscope. Wide-field confocal images can be obtained in real time by sweeping the focal point of a lens in the axial and radial directions and rapidly integrating the images obtained. This paper describes a liquid lens whose focal point can be varied in both the axial and radial directions. The liquid lens consists of an acrylic cylindrical cell with the inner diameter of 10 mm and the thickness of 3 mm, two immiscible liquids with different refractive index (water and silicone oil), and an annular PZT transducer with four-divided electrodes. The center of the transducer and the top of the lens were sealed using circular quartz plates so that light can propagate through the lens in the axial direction. The oil-water interface acting as the lens surface can be deformed by the acoustic radiation force from the transducer, and the lens acts as a variable-focus lens. The variation of the oil-water interface was observed by changing the driving condition of the transducer and using optical coherence tomography which images differences in the refractive index. The path of the laser beam transmitted through the lens was calculated by ray-tracing simulations. The oil-water interface could be deformed from the oil to water sides and the focal point could be changed three-dimensionally by controlling the input voltage. The displacement angle in the radial direction was approximately 3 degrees in the case that only two divide electrodes were excited with the input voltage of 45 V at 1 MHz. The dynamic performance of the lens was investigated by using a high-speed camera. By exciting with AM signals, the hemispherical water droplet oscillated and the focus scanning in the axial and radial directions could be achieved.

1a B03.**Observation of acoustic streaming in water/sensor plate/thin water layer/128YX-LiNbO₃ for realizing disposable digital microfluidic system****Jun Kondoh, Hitoshi Toyoizumi***Shizuoka University, Japan*

Surface acoustic wave (SAW) devices are extensively used as analog electrical filters for mobile and wireless communications. The SAW has an elliptical displacement on the surface. When liquid is loaded on the Rayleigh-SAW propagating surface, the Rayleigh-SAW becomes a leaky-SAW and a longitudinal wave is radiated into the liquid. While this phenomenon is unfavorable for SAW device applications, such as filters, new applications have been created based on it. If the SAW amplitude increases, the liquid shows non-linear dynamics, such as droplet vibration, droplet manipulation, and small droplet flying from a droplet. This phenomenon is well known as SAW streaming. If a sensor is integrated on the SAW propagating surface, droplet manipulating and measuring system is realized. In other word, novel digital microfluidic system is realized by using SAW device. Purpose of the system is to measure immunoreaction, hybridization of deoxyribonucleic acid (DNA), enzyme reaction and so on. As it is difficult to keep clean surface after measuring bio-reactions, disposable device is required for a microfluidic system. Realization of a disposable system using SAW device is difficult. Therefore, we have proposed three-layer structures of sensor plate/thin water layer/128YX-LiNbO₃. We have succeeded in droplets manipulation, mixing, and measuring on the three-layer device. For optimization, it is important to understand an acoustic streaming on the device. In this paper, the acoustic streaming on the three-layer structure device is discussed on the basis of experimental results. Acoustic streaming is observed in a water tank. The beam width on the proposed structure is wider than it on the 128YX-LiNbO₃. Acoustic streaming velocity was obtained from particle image velocimetry (PIV) as a function of thickness of thin water layer. Cover glasses of different thickness and polymer plate were used as sensor plates. Relationship between the maximum streaming velocity and thickness of thin water layer is linear. The streaming velocity decreases with increasing glass thickness. For the same thickness, the velocity for the polymer plate is slower than it for the cover glass. The obtained results suggest that the droplet manipulation speed on the proposed structure is influenced by material and thickness of a sensor plate. Also, streaming in the water thin layer is observed. Profiles are depended on the layer thickness. Above 1 mm thickness, vortex is observed.

1a C01.

Anharmonic properties of CaO

Krishna Murti Raju

BNV PG College, Hamirpur, India

The knowledge of elastic constants is essential to interpret the thermodynamic and elastic dimensions of solids at high temperatures. The elasticity offers more information than the volume in interpreting the temperature dependence of equation of state because the compressibility is defined by the derivative of volume. The elastic constants also provide a ground for examining of Earth's deep interior. The electrostatic and Born-Mayer repulsive potentials method was used to calculate the higher order elastic constants and pressure derivatives of alkaline-earth oxide CaO in a wide temperature range (100-1000 K). The first order pressure derivatives of second and third order elastic constants, the second order pressure derivatives of second order elastic constants and partial contractions are also evaluated at different temperatures. The different results of the calculations are compared with experimental data and discussed. Data on elastic constants and associated properties at high temperature for CaO crystal are presented and discussed starting from primary physical parameters viz. nearest neighbor distance (r) and hardness parameter (q) assuming long- and short-range potentials. The factors r and q are the primary physical parameters used in this study. When the values of the higher order elastic constants are known for a crystal, many of the anharmonic properties of the crystal can be treated within the limit of the continuum approximation in a quantitative manner. If the values of second order elastic constants and density at a particular temperature are known for any substance, one may obtain ultrasonic velocities for longitudinal and shear waves which give an important information about its internal structure, inherent and anharmonic properties. This study will be useful in characterisation of the material and it will give a clear picture of elastic behaviour in CaO. It is found that the elastic constants, in general, decrease with temperature. The new data may offer an additional possibility to improve the theoretical models developed recently for the interpretation of the behavior of elastic constants in elevated temperature region. Our whole theoretical approach can be applied to the evaluation of related parameters to study the anharmonic properties of CaO. Thus the results of the elastic properties of this alkaline earth oxide computed with the help of the present theory are satisfactory and are comparable to the results obtained by various first-principle studies.

1a C02.

Nonlinear approach for evaluation properties of materials at elevated temperature

Iosif E Shkolnik, Huseyin R Hiziroglu

Kettering University, United States

Temperature-dependent electrical and mechanical properties are very important in the analysis of materials in operating environments with changing temperatures. It has been observed that high temperature may adversely affect the performance of insulators and lead to its rapid aging and unexpected failure. The heterogeneous of structure, local overstress on real materials under loading lead to the deviation from Ohm's law as well as from Hook's law (even at infinitesimal deformations) and also significantly affect the behavior of materials at elevated temperature. There are standards and many experimental techniques that can predict thermal failure of materials. However, these experiments are not only tedious but also expensive and quite time consuming. Main objective of this paper consists in estimation of dielectric and mechanical properties of different materials (solders, polymers, concrete, and polymer-concrete) at elevated temperature by using corresponding data at room temperature and results of measurements by static and nonlinear nondestructive acoustical methods. Presented investigations are based on three fundamental relationships for materials: "modulus of elasticity-temperature", "strength-temperature" (according to the kinetic nature of solids strength), and nonlinear "stress-strain" dependency. It is shown that, in agreement with existing standards and experiments for different solders, polymers, concrete and polymer concrete insulators, the dielectric as well as mechanical properties decrease with temperature. Preliminary results are promising for predicting mechanical strength of materials at room temperature, dielectric strength and time to failure of insulators at elevated temperature.

1a C03.**Non-linear elasto-plastic shock wave simulation in high-velocity compaction by discrete element method****Muhammad Shoaib, Leif Kari***The Marcus Wallenberg Laboratory for Sound and Vibration Research, Royal Institute of Technology, Sweden*

Non-linear elasto-plastic shock waves in particle systems at high-velocity compaction are simulated by the discrete element method. The contact laws applied between the spherical metal particles include non-linear elastic and plastic loading, adhesion and elastic unloading. Of particular interest is to study the transmission and reflection of non-linear shock waves through a particle system using different particle sizes and materials, with and without voids between the particles and with and without adhesion at the contacts. Several interesting results are presented in the paper including the particle deformation at incident and reflected shocks, particle velocity oscillations as a result of voids and possible particle separations at unloading stage and their dependence upon the applied adhesion at the contacts. The study of non-linear elasto-plastic shock waves in particle systems has a strong practical relevance including high-velocity compaction of metal powder.

1p A04.**Nonlinear propagation of acoustic pulses through the atmosphere with the anisotropic wind velocity and temperature nonhomogeneities****Igor Chunchuzov¹, Sergey Kulichkov¹, Oleg Popov¹, Roger Waxler², Jelle Assink²**¹*Obukhov Institute of Atmospheric Physics, 119017 Moscow, Russia,*²*National Center for Physical Acoustics, University of Mississippi, MS 38677, United States*

The nonlinear distortion of the acoustic pulses propagating from point explosive sources (surface explosions, volcanoes) to the upper atmosphere in a presence of the anisotropic wind velocity and temperature nonhomogeneities is studied. Due to such distortion the pulses transform at high altitudes into N-waves, whose amplitudes and durations are estimated at different altitudes of the atmosphere (up to 120 km). The scattering of N-waves by atmospheric anisotropic nonhomogeneities in the stratosphere and lower thermosphere is analyzed with the use of a parabolic equation method. The calculated wave forms, amplitudes and durations of the stratospheric and thermospheric arrivals are compared with those observed in the experiments. It is shown that the acoustic field scattered from anisotropic nonhomogeneities may be responsible for some of the arrivals of the acoustic pulses observed in the acoustic shadow zones

1p A05.

Numerical simulation of shock wave propagation in flows

Mathieu Rénier¹, Régis Marchiano¹, Eric Gaudard¹, Louis-Jonardan Gallin^{1,3},
 François Coulouvrat^{1,2}

¹Université Pierre et Marie Curie, France, ²Centre National de la Recherche Scientifique, France,

³CEA, DAM, DIF, F – 91297 Arpajon, France, France

Acoustical shock waves propagate through flows in many situations. The sonic boom produced by a supersonic aircraft influenced by winds, or the so-called Buzz-Saw-Noise produced by turbo-engine fan blades when rotating at supersonic speeds, are two examples of such a phenomenon. In this work, an original method called FLHOWARD, acronym for FLOW and Heterogeneous One-Way Approximation for Resolution of Diffraction, is presented. It relies on a scalar nonlinear wave equation, which takes into account propagation in a privileged direction (one-way approach), with diffraction, flow, heterogeneous and nonlinear effects. Theoretical comparison of the dispersion relations between that equation and parabolic equations (standard or wide angle) shows that this approach is more precise than the parabolic approach because there are no restrictions about the angle of propagation. A numerical procedure based on the standard split-step technique is used. It consists in splitting the nonlinear wave equation into simpler equations. Each of these equations is solved thanks to an analytical solution when it is possible, and a finite differences scheme in other cases. The advancement along the propagation direction is done with an implicit scheme. The validity of that numerical procedure is assessed by comparisons with analytical solutions of the Lilley's equation in waveguides for uniform or shear flows in linear regime. Attention is paid to the advantages and drawbacks of that method. Finally, the numerical code is used to simulate the propagation of sonic boom through a piece of atmosphere with flows and heterogeneities. The effects of the various parameters are analysed.

1p A06.

Global variation of sonic boom overpressure due to seasonal changes in atmosphere

Hiroshi Yamashita¹, Shigeru Obayashi²

¹Formerly Institute of Fluid Science, Tohoku University and Currently Department of Aerospace Engineering, Nagoya University, Japan, ²Institute of Fluid Science, Tohoku University, Japan

This paper presents the global variation in sonic boom overpressure due to seasonal changes in atmosphere. The variation of overpressure at the ground according to difference in seasons and geographic positions was focused. The seasonally varying atmosphere employed in the simulation was computed from the raw observational data by the following steps: The upper-air meteorological raw observation data were processed by data filtering, vertical interpolation of the observations, and the seasonal average obtained by averaging the observations for three months. Sonic boom was calculated using the near-field pressure wave of Sears-Haack body obtained from Computational Fluid Dynamics (CFD) calculations in inviscid flow (Euler) mode. The sonic boom was extrapolated through all seasonal atmospheric gradients around the world by the Waveform Parameter Method. The distribution maps of sonic boom overpressure around the world were produced from the extrapolated waves. The differences in altitude were taken into consideration. However, the effects of wind and atmospheric turbulence were not taken into account. The results demonstrated that sonic boom overpressure varies widely with season and geographic position due to difference in the atmospheric gradients. The results revealed the tendencies of the global variation in overpressure. The results also showed the potential benefit of conducting the sonic boom estimation by taking local atmospheric conditions and terrains into the consideration. The estimation is useful to determine the optimal flight profiles for low-boom flight, which is important for the development of an environmentally acceptable supersonic aircraft.

1p B05.**Effects of the liposomal formulation on the behavior and physical characteristics of acoustic liposomes**

Nicolas Sax¹, Sachiko Horie¹, Li Li¹, Shenwei Li¹, Takashi Kochi^{1,2}, Rui Chen¹, Yukiko Watanabe¹, Yoko Yagishita^{1,3}, Maya Sakamoto⁴, Shiro Mori⁴, Tetsuya Kodama¹

¹Graduate School of Biomedical Engineering, Tohoku University, Japan,

²Graduate School of Medicine, Tohoku University, Japan,

³Graduate School of Dentistry, Tohoku University, Japan, ⁴Tohoku University Hospital, Japan

Ultrasound contrast agents (UCAs) are nano/microbubbles that contain air or a high-molecular-weight, low-solubility gas (e.g., C₃F₈, C₄F₁₀ or SF₆) encapsulated in a lipid or albumin shell. The diameters of UCAs vary from 100 nm to 10 μm and their behavior primarily depends on the ultrasound characteristics. Previous studies have developed acoustic liposomes (ALs), liposomes that encapsulate perfluoropropane (C₃F₈) gas. These ALs can be used as just UCAs, for early diagnostic, observation of angiogenesis, and evaluation of the therapeutic effect of various molecules. They also have the potential to be used for localized drug delivery, through their ultrasound-induced destruction in a target region leading to permeabilization of the neighboring cells by sonoporation. However, the stability of the gas encapsulation, as well as the fine structure of the ALs remain to be investigated. Here we show that the stability of ALs is affected by fluidity changes in the membrane induced by cholesterol or unsaturated phospholipids, in a quite different way from that of non-acoustic liposomes. Ultrasound B-Mode images show that liposomes sonicated in the presence of C₃F₈ gas have a high echogenicity and a good *in vitro* lifetime compared to ALs encapsulating air, but still suffer from a short lifetime *in vivo*. Further research aims at improving the stability of the gas encapsulation by surface modification and coating of the liposomes, and *in vivo* observation of the EPR effect through real-time visualization of the accumulation of such liposomes at tumor sites.

1p B06.**Analysis of a bubble deformation process in a microcapsule by shock waves for developing DDS**

Masaaki Tamagawa, Kenshi Morimoto

Kyushu Institute of Technology, Japan

This paper describes development of microcapsule including a bubble using underwater shock waves for shock wave drug delivery systems, especially the trial of making smaller microcapsules and analysis of a bubble deformation process in a microcapsule to have higher efficiency of disintegration. In our proposed drug delivery systems (DDS) using shock waves, microcapsules including gas bubbles are flown in the blood vessel, and they are broken by shock induced microjet, then drug is reached to the affected part in the body. For developing microcapsules including gas bubbles, the penetration force of microjet should be controlled by shock wave strength (power), wave form of pressure, and capsule geometry and material properties. Especially the mechanical properties of membrane and geometry of the membrane (membrane properties) are important parameters for changing the penetration strength of microjet in the microcapsule. To observe the bubble deformation process in a capsule is very important work for understanding disintegration of microcapsules by shock wave or pressure wave with changing these membrane parameters. In this paper, the bubble (less than 100μm) deformation process is observed in a microcapsule on the microscope using micro-holder. The worked pressure wave is generated by horn shaped piezoelectric pressure generator, and the maximum pressure is 0.16MPa, which is under the disintegration of capsule. In this investigation, the frequencies of sine pressure wave are 44 kHz and 77 kHz. As a result, the typical bubble deformation process was obtained. It is found that the bubble has an acute angle part with large deformation in the case that the ratio (air diameter/water diameter) is 0.53. In the case that this ratio is almost 1, it is clearly found that there are no acute-angle parts of a bubble. Effects of other parameters are also discussed. From these results and other ones, it is concluded that there should be optimum parameter to have strong micro-jet even in less than 100μm scale by shock waves and pressure waves.

1p B07.

Enhancement of cavitation inception by second-harmonic superimposition

Shin-ichiro Umemura, Ryo Takagi, Jun Yasuda, Shin Yoshizawa

Tohoku University, Japan

Microbubbles, whether administered or ultrasonically generated, accelerate the thermal as well as mechanical effects of therapeutic ultrasound. Furthermore, they are essential for the sonochemical effects. We have proposed "Triggered HIFU (High Intensity Focused Ultrasound)" exposure sequence, in which microbubble clouds are generated by short, extremely high intensity "trigger" pulses and accelerate the effect of following continuous heating waves with similar intensity and duration as conventional HIFU for therapeutic treatment. Because the heating effect is induced by synergy of the trigger pulses and the heating waves, which are both focused, the triggered HIFU treatment may have higher spatial selectivity as well as higher energy efficiency than conventional HIFU treatment. This paper presents our researches underway on improving the trigger pulses to increase their cavitation inception efficiency. The peak negative acoustic pressure, the most important acoustic parameter for cavitation inception, can be enhanced by superimposing the second-harmonic to the fundamental. Employing coaxially aligned co-focal PZT transducers at 1.14 and 2.28 MHz, the effectiveness of the second-harmonic superimposition was examined in water. Among the several short exposure sequences tested, the sequence, starting with the second-harmonic superimposed pulse waves enhancing the peak negative pressure, and followed by those enhancing the peak positive pressure, demonstrated the highest efficiency in cavitation inception. A high speed camera showed that the negative-pressure enhanced pulse waves produced a small cloud of cavitated microbubbles at the first stage and that the positive-pressure enhanced pulse waves expanded the microbubble cloud at the second stage. It may be hypothesized that the positive-pressure enhanced pulse waves at the second stage were phase-inverted through being reflected by the small microbubble cloud and converted to negative-pressure enhanced waves expanding the cloud. Because of the non-linear propagation of high intensity focused waves, it is not simple to produce highly negative focal acoustic pressure even by superimposing the second harmonic. Two ways of the second-harmonic superimposition, one by co-focal focusing as described above and the other at the sound source with wide-band transducer elements, will also be compared in experiments as well as by numerical simulation of non-linear propagation and discussed.

1p C04.

Subharmonic wave analysis in crack using the developed FEM

Tsuyoshi Mihara¹, Koji Shimaya¹, Yasushi Ikegami², Takashi Furukawa³, Ichiro Komura³

¹University of Toyama, Japan, ²ITOCHU Techno-Solutions Co., Japan, ³JAPEIC, Japan

Subharmonic wave measurement has been considered as a promising technique for the industrial NDE for the reliable detection and accurate sizing of the defects in industrial structures. However, the generating mechanism of a subharmonic wave at crack is not clear enough yet. We simulated subharmonic wave at crack using a simple analytical model considering the clapping of the crack surfaces generates subharmonic wave to obtain the similar waveform to the experimental one qualitatively. According to the basic concept of previous analysis, we tried to develop a new FEM code to simulate the subharmonic wave behaviors at crack in this research. Incidence of large amplitude ultrasound applied to the narrow opening crack and the clapping of crack surfaces made transmit the ultrasound through the gap of the crack as a first step. In addition to this, if a slight miss-clapping of crack occurred alternatively depending on the microstructure of crack, subharmonic behaviors should appear on the transited waveform. The analytical FEM code for subharmonic wave used here was newly developed basing on the commercial large-scale FEM code. The small gap of crack of nm order was represented using double contact mesh technique. After the comparison of simple analysis of transit waveform and crack length to the experimental result, we reconsidered the FEM model. Thus, residual stress at crack surface and irregularity of crack surface were considered strongly related to the clapping of crack surfaces. Then, following two parameters were added to the FEM analysis to consider to the subharmonic ultrasound behavior at industrial crack. First one was a compression residual stress at the crack surface based on the fracture mechanics considerations that the compression stress was remained in small scale yielding area at crack tip in the fatigue crack introduction process. Second one was the consideration of the geometric irregularity of crack surface. Though accurate details of the contact between crack surfaces in nm order was unknown, three dimensional complex geometries should be considered for subharmonic ultrasound generation in industrial cracks. Comparing to the simple experimental waveform of subharmonic waves, new FEM model of crack must be investigated considering the industrial crack shape to evaluate the mechanism of subharmonic ultrasound generation.

1p C05.**Two dimensional model for subharmonic generation at closed cracks with damped double nodes****Kazushi Yamanaka, Yohei Shintaku, Yoshikazu Ohara***Tohoku University, Japan*

Closed cracks are the most serious obstacle for safety of important structures such as power plants or air planes. The depth of such crack can be underestimated even by the most sensitive measurement tool, ultrasound, owing to the compression residual stress or oxide film on the crack faces. These cracks are extended by larger external stresses and cause accidents such as radiation leaks. To detect closed cracks, nonlinearity of ultrasound is regarded most promising. Among them, subharmonics is particularly useful because of their excellent selectivity for closed cracks and high temporal resolution. Subharmonic phased array for crack evaluation (SPACE) can measure depth of closed fatigue cracks and stress corrosion cracks. However, in one dimensional (1D) model, parameters relevant in real components cannot be taken into account, such as the length/depth of cracks and direction of incident wave with respect to the crack faces. Thus, detailed comparison between experiment and theory was not possible. In this study, we propose the first two dimensional (2D) model to reproduce subharmonic generation at closed cracks using damped double nodes (DDN). Numerical simulation using finite difference time domain (FDTD) method was performed using DDN and compared with experimental waveforms and time frequency analysis based on the wavelet analysis. As a result, it was found that apparently random (chaotic) high frequency vibration is excited by large amplitude input wave without the damping. However, the damping is useful in avoiding high frequency vibration and enhancing subharmonic generation efficiency by a large amplitude input wave. The displacement vibration waveforms of the incidence-side crack face, that of trasmission-side crack face and the crack opening displacement (COD) are calculated. Then is pushed up by, and the former cannot follow the return of the latter due to the inertia. In the following periods, this process is repeated with different percentages, causing doubling of period and formation of subharmonics. In conclusion, we succeeded in reproducing subharmonic generation at closed cracks in a 2-dimensional model. It will be useful in designing and evaluating testing equipment, probes and conditions for important structures with possible extension of closed cracks.

1p C06.**Formation and evaluation of closed stress corrosion cracks in Ni-based alloy weld metal for nuclear power plants****Yoshikazu Ohara, Yohei Shintaku, Satoshi Horinouchi, Kazushi Yamanaka***Tohoku University, Japan*

Although nuclear power plants have been reevaluated owing to reduction of carbon dioxide, stress corrosion cracks (SCCs) have been generated in critical structures during long-term service. To ensure the safety and reliability, the accurate measurement of crack depth is necessary. Crack depth can be measured by ultrasound if cracks are open. However, the inspection of SCCs is difficult in Ni-based alloy weld metal for dissimilar metal welding of pressurized water reactors, since the SCCs are strongly closed. Then, ultrasound can penetrate through closed cracks whose faces are in contact with each other because of compression residual stress or oxide films. This leads to the underestimation or overlook of cracks, resulting in catastrophic accidents. Thus far, we have developed a novel imaging method, subharmonic phased array for crack evaluation (SPACE) based on subharmonic waves and a phased array algorithm. We have demonstrated the performance of SPACE in closed fatigue crack specimen made of aluminum alloy and stainless steel, and in SCC specimen made of stainless steel. However, the closed SCCs have yet to be formed in Ni-based alloy weld metal in acceleration test. Here, we propose a method for forming closed SCCs in Ni-based alloy weld metal. A Ni-based alloy weld metal was partly bored, and the bored part was molded with a Ni-based alloy of high carbon content so as to form SCC in a short time. The starting notch was fabricated in the molded parts. Then, the SCC was extended from the notch in tetrathionate solution under thermal tensile stress. After forming the SCC, the specimen was immersed in high temperature pressurized water to generate oxide films between crack faces. We imaged the SCC using SPACE. Consequently, we observed subharmonic components ($f/2$) after the immersion in high temperature pressurized water, although only fundamental component (f) before the immersion. Two dimensional analysis with the damped double node (DDN) indicated that the $f/2$ component is due to contact vibration of crack faces. This result shows that the immersion in high temperature pressurized water is useful in generating oxide films, resulting in crack closure. In conclusion, we succeeded in forming closed SCCs in Ni-based alloy weld metal, and demonstrated that SPACE is useful in measuring the closed SCC. This result will significantly contribute to improve the safety and reliability of nuclear power plants.

1p C07.

Analysis of harmonic generation in Lamb waves by finite-difference time-domain method

Naoki Matsuda, Shiro Biwa

Graduate School of Engineering, Kyoto University, Japan

Nonlinear acoustic methods are attracting much attention towards early-stage evaluation of material damage and deterioration. While foregoing investigations were mostly focused on the nonlinear effects of bulk waves in damaged materials, some works have been recently carried out to utilize guided waves, such as Lamb waves in a plate, for damage evaluation of thin-walled structures. Due to the dispersive nature and the multi-mode existence, the nonlinear effects of guided waves, such as higher harmonic generation, are difficult to analyze, and the foregoing theoretical studies are limited to the perturbation analysis. In the present investigation, the nonlinear characteristics of Lamb wave propagation are analyzed numerically, by using the finite-difference time-domain (FDTD) method. The authors have extended the FDTD scheme to include the stress-strain nonlinearity (third-order elasticity) as well as the kinematical nonlinearity (Green's strain). Using this nonlinear FDTD scheme, the harmonic generation in Lamb waves is analyzed for different modes and frequencies of the primary Lamb mode. The numerical results are discussed in the light of the conditions for the cumulative harmonic generation, namely the phase and group velocity matching of the primary and the harmonic Lamb waves [1]. Furthermore, numerical simulations are carried out for the case where the plate has a locally concentrated region of enhanced material nonlinearity, and the influence of the size of this region on the harmonic generation behavior of Lamb waves is discussed. [1] N. Matsuda and S. Biwa, J. Appl. Phys. 109 (2011), 094903.

Invited Lecture**1p L2.****Sources and propagation of atmospherical acoustic shock waves****François Coulouvrat***Université Pierre et Marie Curie, UMR CNRS 7190, F-75005 Paris, France*

Sources of aerial shock waves are numerous and produce acoustical signals that propagate in the atmosphere over long ranges, with a wide frequency spectrum ranging from infrasonic to audible or even ultrasonic frequencies, and with a complex human response. They can be of natural origin, like meteors, lightning or volcanoes, or human-made as for explosions, so-called "buzz-saw noise" (BSN) from aircraft engines or sonic booms. Their description, modelling and data analysis within the viewpoint of nonlinear acoustics will be the topic of the present lecture, with focus on two main points: the challenges of the source description, and the main features of nonlinear atmospheric propagation. Inter-disciplinary aspects, with links to atmospheric and geo-sciences will be outlined. Detailed description of the source is very dependant on its nature. Mobile supersonic sources can be rotating (fan blades of aircraft engines) or in translation (meteors, sonic boom). Mach numbers range from 1 to more than 40. Detailed knowledge of geometry is critical for the processes of boom minimization and audible frequency spectrum of BSN. Sources of geophysical nature are poorly known, and various mechanisms for explaining infrasound recorded from meteors or thunderstorms have been proposed. Comparison between recorded data and modelling may be one way to discriminate between them. Moreover, the nearfield of these sources is frequently beyond the limits of acoustical approximation, or too complex for simple modelling. A proper numerical description hence requires specific matching procedures between nearfield behaviour and farfield propagation. Nonlinear propagation in the atmosphere is dominated by temperature and wind stratification. Ray theory is an efficient way to analyze observations, but is invalid in various situations. Nonlinear effects are enhanced locally at caustics, or in case of grazing propagation over a rigid surface, with specific self-similar laws. Absorption, which controls mostly the high frequency part of the spectrum contained within shocks, is controlled by humidity, cloudiness or surface properties. Variability is large at all scales, and depends simultaneously on climate, daily meteorology, and local turbulent state, especially near the ground in the planetary boundary layer. Numerous features of outdoor propagation remain to be explored in the nonlinear case, such as complex 3D atmospheric description (role of turbulence, partial reflections, gravity waves) or topography (mountains, street canyons).

1p A08.

Derivation of exact solutions of the inhomogeneous Burgers equation using the Darboux transformations

Oleg Sapozhnikov¹, Andrey Kudryavtsev²

¹*Department of Acoustics, Faculty of Physics, Moscow State University, Russia,*

²*Institute of Applied Mechanics of the Russian Academy of Sciences, Russia*

The inhomogeneous Burgers equation (BE) governs one-dimensional propagation of finite-amplitude acoustic waves in dissipative media in the presence of sources. A possible approach to analyze the solutions of such an equation is to combine two effective mathematical methods, namely the Cole-Hopf and Darboux transformations. The Cole-Hopf transformation relates solutions of the inhomogeneous BE with those of the linear diffusivity equation containing a perfusion term. The Darboux transformation relates solutions of two inhomogeneous BEs having different source functions. In this paper a method based on a combination of the Cole-Hopf and Darboux transformations is applied to the inhomogeneous Burgers equation (BE) to derive exact solutions for the upstream propagation of an acoustic wave in nozzles. Applying the first-order Darboux transformation to the homogeneous BE yields an inhomogeneous BE corresponding to near-sonic flow in a de Laval nozzle. From this transformation, the amount of nozzle narrowing is related to a specific value of medium viscosity. Based on the known exact solution of the homogeneous BE, all the possible stationary solutions are obtained for the resulting inhomogeneous BE. Transient behaviors of several typical nonsteady flows are also analyzed. In addition, an algorithm for the multi-order Darboux transformation is built that makes it possible to increase the amount of nozzle narrowing without changing the medium viscosity. It appears that such an approach gives rise to a discrete set of possible nozzle narrowings for which exact solutions of the inhomogeneous BE can be obtained. Using Crum's theorem, exact solutions of the inhomogeneous BE can be expressed based on the solutions of the classical homogeneous diffusion equation. Work supported by the RFBR.

1p A09.

On the evolution of a spherical short pulse in nonlinear acoustics

Bengt O. Enflo¹, Claes M. Hedberg²

¹*Royal Institute of Technology, Stockholm, Sweden,* ²*Blekinge Institute of Technology, Karlskrona, Sweden*

Wave propagation in nonlinear acoustics is modeled by Burgers' equation or its generalizations or modifications. In the case of a quadratic nonlinearity spherical wave propagation is modeled by a generalized Burgers' equation, in which the dissipative parameter of the plane wave Burgers' equation is replaced by an exponentially growing function of the variable symbolizing the travelled length of the wave. A procedure previously used in 1998 by B.O. Enflo on cylindrical short pulses is now used on spherical short pulses, which are originally N-waves. The procedure consists of the four steps: 1) The original N-wave implies a shock solution of the generalized Burgers' equation. The shock fades in the region where the nonlinear term in the equation can be neglected. 2) The linear equation in step 1) is rescaled and solved by an integral representation containing an unknown function. 3) The integral representation found in step 2) is evaluated by the steepest descent method in the fading shock region introduced in step 1). The unknown function introduced in step 2) is determined by comparing the result of this evaluation with the fading shock solution found in step 1). 4) The integral representation with the unknown function determined is evaluated approximately asymptotically for large values of the original length and time variables in the original Burgers' generalized equation (old-age regime). The result of this procedure is an old-age solution somewhat different from the one presented in 1979 by D.G. Crighton and J.F. Scott. The present solution is controlled by numerical calculations.

1p A10.**Whether there can be something general between methods of classical linear wave equation solving and a finding of analytical solutions of nonlinear acoustical equations?****Yury Nikolaevich Makov***Moscow State University, Department of Acoustics, Faculty of Physics, Russia*

Contrary to common opinion on "the big abyss" between methods of the solving and solutions themselves of the classical linear wave equation (it is considered that about these all is known practically) and special non-trivial methods of finding of solutions for the nonlinear acoustical equations, this report demonstrates the general (regular) technique of use of "relatively undistorted wave" anzats (R. Courant and D. Hilbert) for finding of new physically intelligent analytical solutions of all mentioned equations. It must be emphasized that this technique uses successfully for finding of new solutions of the classical linear wave equation during more than twenty years but all solutions are found only from the class of nondispersive wave solutions (in conception of Courant and Hilbert). In the report the special attention is given to use of "relatively undistorted wave" anzats for the class of dispersive wave solutions. Not only the new solutions from this class are found for linear wave equation but also "paved the way" to nonlinear acoustics. There is good physical validity for successful use of the relatively undistorted wave anzats (with little modification in its form and application method) in the finding of new exact analytical solutions for all basic model nonlinear acoustic equations in addition to the active traditional "exploitation" of this anzats for classical linear wave equation. Indeed, in nonlinear acoustics under the absence of dispersion the propagation of one-dimensional (in space) wave or a spatially localized wave structure (e.g., a beam) is accompanied by transformation of the wave profile (time profile). In the general case, this transformation has a complex character (e.g., transformation of a sinusoid into a saw-tooth profile), but there can be certain types of profiles that transform according to a simpler law reflecting only their variations in scale in the case when they retain their specific forms that describe the desired solution in the form of a relatively undistorted wave. The simplest and very well known example of this situation is a periodic saw-tooth solution to the equation of a simple wave with a profile that retains its form during propagation. However, in this case, their peak values decrease; i.e., this profile is relatively undistorted. In report this idea is evolved and some exact solutions of all types of nonlinear acoustics equations are found.

1p B08.**Nonlinear and dispersive effects in the propagation of a finite-amplitude sound wave in a waveguide****Pablo Luis Rendon***CCADET, Universidad Nacional Autonoma de Mexico, Mexico*

The problem of large-amplitude waves propagating in a waveguide with rigid walls and nonrectangular cross-section is considered. In these circumstances, dispersive behaviour of the individual modes of linear theory is expected, and can be shown to occur through the use of asymptotic expansions. The leading term of these expansions will correspond to the results of linear theory, and subsequent terms will represent finite-amplitude corrections to this term. In this paper, the method of multiple scales is used to arrive at equations which describe the joint effect of nonlinear and dispersive mechanisms at large distances for nonplanar modes of propagation. These equations can be considered as model equations which include the required effects and have the correct limiting forms. These equations are then also solved numerically in order to validate the asymptotic results.

1p B09.

Peculiarities of shocks forming in high intensity acoustic beams in the presence of soft boundary at interaction area

Dmitry A Kasyanov¹, Mikhail S Deriabin¹, Vasily V Kurin²

¹Radiophysical Research Institute, Russia, ²Nizhny Novgorod State University, Russia

Results are discussed in the paper of laboratory investigating of profile spatial changing and spectrum evolution of high intensity pump wave after reflection from soft boundary. It is considered the case of powerful acoustic beam normal incidence to water-air interface. We used piston piezoceramic acoustic radiator and pulsed regime of radiation. Power amplifier "Amplifier Research 800A3" was utilized as pumping source. Operating frequency was 1 MHz, pulse duration – 20 μ s. Experiments were conducted under changing of filling factor conditions. It needs for evaluation of soft boundary nonstationarity arising due to high-power pulse impact. Acoustic source – to – soft boundary distance approximately meets last diffraction maximum coordinate of acoustic field axial distribution at pumping frequency. Pressure amplitude of falling to boundary wave reached 2.5 MPa. Intensity of acoustic field was chosen in such a way as to continue nonlinear wave interaction after reflection. Miniature-type hydrophone (Precision acoustics, type HPM04/1) was used for nonlinear waveform recording at arbitrary point of reflected beam. Active element size of the hydrophone is 0.04mm, so it provided proper analysis about 20 harmonics of recording acoustic signal. Harmonic reflection from soft boundary approaches the antiphased reflection which results in peculiarities of further harmonics interaction. This fact exerts determinative influence on subsequent nonlinear waves forming and one can observe noticeable nonmonotony for harmonic amplitudes decrease according to its numbers. Reflected from soft boundary nonlinear wave has shock profile where negative phase considerably exceeds positive one. The amplitude of negative half-period exceeded 2 MPa in immediate proximity to reflective boundary, it is fore times more than amplitude of positive half-period approximately. Further waveform transformation in restricted beam leads to forming specific kind of shock. Formed after reflection shock is narrower than the shock in falling wave. Subsequent dynamics of waveform and spectrum of reflected nonlinear wave is also discussed in paper.

1p B10.

Nonlinear shear visco-elastic properties of liquids

Bair Damdinov, Dagzama Makarova, Tuyana Dembelova, Badma Badmaev

Buryat scientific center of RAS, Russia

The shear modules and effective viscosities of liquids were measured by acoustical resonance method at ultrasonic frequencies. Two ways of the measurement that gave the agreement results were realized. The method is based on the shifts of resonance frequency of a sensor in contact with the liquid. The sensor is the piezoelectric quartz bonded to a liquid layer covered by cover-plate. The process determines parameters of the resonance curve of piezoquartz which are changed in depending on the liquid layer thickness. The method allows to measure real and imaginary shear modules and tangent of mechanical loss angle. Experimental determination of dynamic shear properties of a series of usual and polymer liquids is presented as an example of the method. It is shown that the measured values of effective viscosity of liquids much more tabular values. We measure dependence of shear visco-elastic properties of liquids on amplitude of piezoquartz oscillation. It is shown that effective viscosity of liquids has high value at small amplitudes and decrease with amplitude increasing. We suggested that liquids have a structure at small shear deformation which breaks with deformation increasing. Supported by Russian Foundation for Basic Research (08-02-98008r_sibir_a and 09-02-00748a).

1p C08.**Nonlinearity parameter B/A and scattering of sound by sound****Kiran Shanker***Physics Dept-CMP College, University of Allahabad, India*

The nonlinearity parameter B/A plays a significant role in Nonlinear Acoustics and its determination in various liquids and organic materials is of growing interest in several fields ranging from Underwater Acoustics to Medical Ultrasonics. In the present study, the nonlinearity B/A has been determined for Eugenol and n-Butanol at 303 K under extreme conditions of pressure ranging from 0.001 to 4.983 kPa using the thermodynamic method. The values of B/A obtained in the present method have been used to obtain the scattered Beam Pressure, which are in good agreement with those obtained by Beyer and Coppens et al. In fact, the interaction between two sound waves of finite amplitude becomes a problem of considerable interest because of the failure of the superposition principle in nonlinear phenomena. Such a problem poses special difficulties on both the theoretical and experimental sides. The Pressure in the scattered field expressed in the form of an integral over the interaction region when integrated resulted in terms corresponding to the sum and difference frequencies of the original sound beam. Subsequently the scattered intensity at some distance and angle from the source was derived while an experimental verification was also carried out by Bellin and Beyer. The nonlinearity parameter B/A can also be determined from alternative methods such as the one based on Tong and Dong equation with Flory's Statistical theory or the technique used by Shigemi Saito et al. However, the Thermodynamic method used in the present work has yielded results which are in agreement with experiment. These observations suggest the use of the nonlinearity parameter B/A in tissue characterization and gives information about structure and interaction in such systems. It is shown that a high frequency oscillation is all that is needed for the determination of B/A.

1p C09.**Validation of planar wave incidence technique for measurement of transmission-loss****Koichi Mori, Yoshiaki Nakamura***Department of Aerospace Engineering, Nagoya University, Japan*

A simple technique is proposed to measure the transmission loss through single-leaf and multiple-leaf panels. The present technique uses two anechoic rooms to simulate the free acoustic field. Different from the conventional methods, the incident angle, the sound pressure distribution, and the spectral distribution of the incident sound waves can be changed arbitrarily. In the experiment, a panel is installed in between two anechoic rooms. The intensity of the transmitted waves is measured in the receiving room. The transmission loss measurements are completed for different materials. The results are used to verify the conventional analyses.

1p C10.**Acoustic micromanipulation in a microchannel****Teruyuki Kozuka¹, Kyuichi Yasui¹, Shin-ichi Hatanaka²**¹*National Institute of Advanced Industrial Science and Technology (AIST), Japan,*²*The University of Electro-Communications, Japan*

Noncontact micromanipulation technique is needed in micromachine technology, biotechnology and so on. The radiation pressure of ultrasound may be used for this purpose. In the present paper, a standing wave field is generated in a microchannel with a geometric space, it is possible to trap small objects at nodes of the sound pressure distribution in the medium. A microchannel of 1 mm x 50 mm x 1 mm was made at the center on a glass plate of 50 mm x 50 mm x 5 mm. Furthermore, a geometric space was added in the center of the microchannel. A transducer of PZT is connected on the end of the glass plate. The sound wave should be transmitted into the microchannel through the glass plate. In the experiment, when the liquid water containing alumina particles was injected into the microchannel, the particles flowed along several layers in the flat microchannel. It was shown that the traveling wave was transmitted into the microchannel and the standing wave field was formed in the microchannel. In the geometric region, the particles were agglomerated in a geometric pattern. However, when the geometric pattern was triangle, the particles moved towards the top of the triangle from the base. Moreover, when the triangle pattern was reversed, the particles moved in the reverse direction. A sound field was numerically calculated by FEM method under the experimental condition and the experimental results were discussed.

Invited Paper**2a A01.****A sonic boom propagation model including mean flow atmospheric effects****Joe Salamone, Victor Sparrow***Pennsylvania State University, United States*

This paper presents a time domain formulation of nonlinear lossy propagation in one-dimension that also includes the effects of non-collinear mean flow in the acoustic medium. The model equation utilized is an augmented Burgers equation that includes the effects of nonlinearity, geometric spreading, atmospheric stratification, and also absorption and dispersion due to thermoviscous and molecular relaxation effects. All elements of the propagation are implemented in the time domain and the effects of non-collinear mean flow are accounted for in each term of the model equation. Previous authors have presented methods limited to showing the effects of wind on ray tracing and/or using an effective speed of sound in their model equation. The present work includes the effects of mean flow for all terms included in the augmented Burgers equation with all of the calculations performed in the time-domain. The capability to include the effects of mean flow in the acoustic medium allows one to make predictions more representative of real-world atmospheric conditions. Examples are presented for nonlinear propagation of N-waves and shaped sonic booms. [Work supported by Gulfstream Aerospace Corporation.]

2a A03.**Numerical simulations for sonic boom propagation through an inhomogenous atmosphere with winds****Masafumi Yamamoto¹, Atsushi Hashimoto², Takashi Takahashi², Tomoo Kamakura³,
Takeharu Sakai⁴**¹*Research Center of Computational Mechanics, Inc., Japan,*²*Japan Aerospace Exploration Agency, Japan,* ³*University of Electro-Communications, Japan,*⁴*Nagoya University, Japan*

Noise annoyance due to sonic boom is one of the serious problems for development of next-generation supersonic transport. To decrease this sonic boom noise, the design and analysis techniques are developed at Japan Aerospace eXploration Agency (JAXA). To predict the sonic boom on the ground accurately, we have developed a numerical code (Xnoise) using the augmented Burgers equation combined with the ray tracing. In this method, effects of nonlinearity, geometrical spreading, inhomogeneity of atmosphere, thermoviscous attenuation, molecular vibration relaxation and winds are taken into account. This method gives an estimation of the rise times of ground signatures without resorting to the weak shock theory and area balancing techniques. The nonlinear term is evaluated by the finite difference scheme in this method. In ray-path calculation, an explicit updating methodology is adopted. The augmented Burgers equation is numerically solved by using the operator split method entirely in the time domain. As for the effects of nonlinearity, geometrical spreading, and atmospheric inhomogeneity, the result obtained with the augmented Burgers equation agrees well with that obtained with the waveform parameter method (Thomas' method). For the effects of absorption and dispersion, the calculation based on the augmented Burgers equation is verified by comparing with a detailed one-dimensional CFD analysis. Moreover, we show calculations which account the effect of winds on the propagation of a sonic boom. The validation of model is a future work.

2a A04.

Infrasound propagation in realistic atmosphere using nonlinear ray theory

Philippe Blanc-Benon¹, Olaf Gainville², Julian Scott¹

¹CNRS, LMFA UMR 5509, Ecole centrale de Lyon, France, ²CEA, DAM, DIF, France

Using ray theory, long range propagation of infrasound through the atmosphere is modeled in the framework of the Comprehensive Nuclear-Test-Ban Treaty. In atmospheric propagation, the high frequency hypothesis is based on the assumption that space and time scales of atmospheric properties (temperature, wind, density) are much larger than acoustic wave scales. An operational 3D nonlinear ray tracing code is developed to compute the temporal pressure signature at receivers. The global pressure signature at the receiver is the sum of eigenray contributions that link the source to the receiver. They are obtained by solving a generalized Burgers' equation along each eigenray taking into account nonlinear effects, shear and bulk viscosity absorption and molecular vibrational relaxation mechanisms. This equation is solved using a Fourier Galerkin spectral scheme. Specific developments are performed to pass through caustics and take into account ground reflection. The propagation of infrasound emitted by a motionless point source in a realistic atmosphere will illustrate the analysis. To quantify the validity limits of our approach, we investigate effects of the wind, atmospheric absorption, nonlinearities, refraction and scattering by small atmospheric scales on observed phase kinds, their travel time and their waveform. To estimate the nonlinearity effects relative to the linear dissipative effects we evaluate the Gol'dberg number. We note that nonlinear mechanisms are important to model the evolution of infrasonic waveform signatures. The 'N' and the 'U' measured waveform shape of, respectively, thermospheric and stratospheric paths are associated with nonlinear mechanisms. Nonlinearities are weak but the development of nonlinear models is necessary in order to characterize the source yield. Comparisons will be made with results available in the literature.

May 22 (Tue)

2a A05.

Numerical and asymptotic solutions of generalised Burgers equation

John Michael Schofield, Paul William Hammerton

University of East Anglia, United Kingdom

The model equation governing the balance of nonlinearity, thermoviscous diffusion and geometric spreading is related to Burgers equation. With a suitable change of variables, this can be re-expressed as the standard Burgers equation but with a range-dependent viscosity parameter. While the one-dimensional equation can be solved exactly using the Cole-Hopf transformation, no such approach exists for the two- and three-dimensional spreading that is more relevant to nonlinear atmospheric propagation. For most situations of interest, the non-dimensional viscosity parameter is small. Crighton and co-workers developed innovative asymptotic methods to describe the evolution of narrow shock regions and their eventual breakdown. Three possible breakdowns occur: (i) when the shock centre is displaced by an order one amount; (ii) when the shock region becomes relatively wide; and (iii) when the Taylor shock solution is no longer valid as the leading order description of the shock. For plane, cylindrical and spherical spreading the breakdown occurs in different ways [1]. While the long-range asymptotic form has been validated numerically using pseudo-spectral schemes, the intricate asymptotic breakdowns within the shock have not previously been investigated due to resolution problems. In the present paper, the position of the shock centre is located using weak-shock theory, then a finite-difference scheme with variable mesh is used, allowing fine resolution in the region tracking the shock. The asymptotic predictions of Crighton are validated by the numerical results. This numerical approach also provides sufficient accuracy in the shock region to compare with the analysis of Enflo, who demonstrated how the fading tail of a shock influences the main shock structure. Finally, a similar approach combining weak shock theory and numerical solution is applied to propagation involving molecular relaxation (an important mechanism in atmospheric propagation), including the effect of climatic variation and stratification. [1] Crighton & Scott (1979), Asymptotic solutions of model equations in nonlinear acoustics, Proc. Roy Soc. Lond. (A 292), pp 101-134.

2a B02.**Nonlinear modeling of 3D ultrasound fields of HIFU arrays****Petr V Yuldashev^{1,2}, Vera A Khokhlova^{1,3}**¹Moscow State University, Russia, ²Ecole Centrale de Lyon, France, ³University of Washington, United States

A current trend in HIFU technologies is to use 2D focused phased arrays that enable electronic steering of the focus, formation of patterns of multiple foci, and beam forming to avoid overheating of obstacles (such as ribs) on the way to the focus. Phased arrays can be also used to improve focusing through inhomogeneities of soft tissue using time reversal methods and to track a treatment region that moves due to respiration. In many HIFU applications, the acoustic intensity *in situ* can reach thousands of W/cm² leading to nonlinear propagation effects. At high power outputs, shock fronts develop in the focal region and significantly alter the therapeutic effect of HIFU.

Numerical modeling has been proven to be an important tool to characterize HIFU fields and to predict corresponding biological effects in tissue. Nonlinear effects including formation of shocks have been studied in detail for axially symmetric focused beams. However, no results have been reported yet for three-dimensional fields of multi-element HIFU arrays in the presence of shocks. Several difficulties are combined in this problem: the complex diffraction structure of the near field and large focusing angles require implementation of accurate diffraction models and fine spatial grid; strong nonlinear effects require a large number of harmonics included in simulations or a fine temporal grid. Simulations in a three-dimensional geometry with account for shock fronts require significant volume of RAM and computer time exceeding the capabilities of modern SMP computers.

In this paper, a novel numerical algorithm based on the Westervelt equation was developed to enable modeling of three-dimensional nonlinear fields of arrays. A varying number of harmonics was employed in the algorithm and a parallel computation model for SMP computers was implemented resulting in significant acceleration of calculations. To demonstrate the capabilities of the algorithm, simulations were performed for a 1.2 MHz array consisting of 256 elements, randomly distributed on a spherical cup of 68 mm radius and 120 mm focal distance. Acoustic intensity near the elements varied up to 10 W/cm². Waveforms in the focus and peak positive and negative pressures along propagation axis and in the focal plane were analyzed. The results showed that shock fronts were present in a focal waveform at clinically relevant outputs. [Work supported by NIH EB007643, RFBR 09-02-01530 and 10-02-91062-PICS].

2a B03.**Effective bandwidth extension by combined harmonics****Gregory Thomas Clement^{1,2}, Hideyuki Nomura², Hideo Adachi², Tomoo Kamakura²**¹Harvard Medical School, United States, ²University of Electro-Communications, Japan

Originating from signal compression techniques in radar, a wide range of ultrasound encoded excitation approaches have been developed for increasing signal strength. These techniques have been extended to nonlinear applications by isolating higher harmonic signal components, thus offering higher signal-to-noise ratios along with the harmonic's increased radial focusing abilities and a potentially broader bandwidth relative to the fundamental. Unfortunately, such techniques can suffer artifacts caused by overlap between the harmonics. We have been investigating an alternative approach to nonlinear compression that combines the fundamental and higher harmonics, effectively treating them as a single band. This extended bandwidth permits a significant increase in the ability to compress a signal. Successfully implemented, the method would permit enhanced image resolution while benefiting from the increased SNR offered by encoding. Pulse-inverted sum and difference signals are first used to isolate even and odd harmonics. Matched filters specific to the source geometry and the transmit signal are then separately applied to each harmonic band. Verification experiments are performed using up the third harmonic resulting from an underwater chirp excitation. Analysis of signal peaks after scattering indicates increased compression using the extended bandwidth as compared to standard fundamental and 2nd-harmonic chirp compression. Further optimization of the compression by altering the transmission signal is also investigated. Overall, results establish the feasibility of extended bandwidth signal compression for simultaneously increasing SNR and signal resolution.

2a B04.

Linearization strategies for the iterative nonlinear contrast source method for full-wave simulation of nonlinear ultrasound fields

Martin D Verweij, Libertario Demi, Koen WA van Dongen

Laboratory of Acoustical Imaging, Faculty of Applied Sciences, Delft University of Technology, Netherlands

Improvement of the image quality and enhancement of the possibilities of medical echography may be achieved through a better exploitation of the features of nonlinear ultrasound. As a result, research on nonlinear ultrasound has increased over the last decade and has led to the development of various methods for the simulation of nonlinear acoustic wavefields. However, the majority of these methods either cannot deal with wide-angle phenomena (grating lobes) and backscattering, or have difficulties with computational volumes that measure many wavelengths. The Iterative Nonlinear Contrast Source (INCS) method has been developed to overcome these restrictions. In its original form, it is a full-wave method that is able to accurately compute the nonlinear, wide-angle pressure field of an arbitrary transducer radiating in a large, homogeneous, three-dimensional spatial domain. The method is based on the lossless Westervelt equation. Under the assumption of weak to moderate nonlinearity, the nonlinear term is considered to represent a distributed contrast source that operates in a linear and homogeneous background medium, thereby generating the nonlinear part of the total wave field. The latter is obtained by casting the problem into an integral equation form, and solving this using the Neumann iterative solution. Each iteration step involves the spatiotemporal convolution of the background Green's function with an estimate of the contrast source. Appropriate filtering provides accurate field predictions for a discretization of only two points per smallest wavelength or period. The contrast source approach is very versatile, and recently the INCS method has been extended to include spatially dependent tissue attenuation. However, such extensions may lead to a deterioration of the convergence of the Neumann iterative solution. To improve the efficiency of the INCS method under these circumstances, we currently present some linearization strategies for this method. Linearization opens the way to employ more efficient methods (e.g. gradient methods) to solve the contrast source problem. To test the proposed strategies, a Bi-CGSTAB scheme is used for the solution of a problem involving spatially inhomogeneous attenuation. One-dimensional results have been computed, and these have been compared with the solution obtained with the original INCS method. To further show the performance of the linearized INCS method, three-dimensional results have been obtained for unsteered and steered beams in lossless and lossy media. These results show that the INCS method is steadily growing into an efficient tool for the simulation of nonlinear ultrasound fields in realistic biomedical tissues.

2a B05.

Coded excitation in detection of polymer-shelled ultrasound contrast agents: in vitro study

Veera Venkata Satya Narayana Kothapalli¹, Dmitry Grishenkov¹, Gaio Paradossi², Lars-Ake Brodin¹

¹Medical Engineering, School of Technology and Health, KTH, Alfred Nobels Allé 10, SE-14152 Huddinge, Stockholm, Sweden, ²Diapartimento di Chimica, Università di Roma Tor Vergata, 00133 Rome, Italy

A novel ultrasound contrast agent (UCA) based on air-filled polymer-shelled microbubbles, is prepared within 3MiCRON project for multimodality approach covering ultrasound, MRI and SPECT investigation. These bubbles have thick, about 30% of the radius, shell providing greater stability and longer half life in a pulmonary circulation compare to commercially available phospholipid UCAs. In addition, extensive storage capacity and possibility to incorporate drugs or pharmacological relevant materials are inherited to these bubbles.

Understanding the behavior of the UCA under ultrasound exposure is paramount to the proper and total exploitation of all unique features that these gas-filled microdevice offers. Even though, thickness of the polymeric shell is considerably higher than of commercial UCAs, the enhancement of backscattered power of about 25 dB produced from suspension insonified at low pressure (100 kPa) was observed. It should be noted that thick polymer shell could still be disrupted by high pressure (1 MPa) ultrasonic pulse. Nevertheless, diagnostic imaging typically utilizes the intermediate pressure level, where nonlinear oscillation of the microbubbles give rise to harmonic component in the received echo. It was observed that at pressure level of 400 kPa, Pulse Inversion (PI) technique fail to distinguish between the regions filled with polymer UCA and surrounding ultrasound phantom, mimicking liver tissue.

In this paper coded excitation technique is proposed to characterize the non-linear properties of the polymer-shelled microbubbles in vitro at intermediate pressure. For a decade ago, coded excitation technique has been adopted into the ultrasound scanners in order to increase the signal-to-noise ratio (SNR) and penetration depth, while matching filters compensates the decrease in axial resolution. In the proposed method, a time domain signal is modulated by a several window functions (e.g. Blackman-Harries, Hanning, Hamming, and Kaiser-Bessel) with or without linear chirp pulses constructed for experiments in vitro.

Our preliminary results suggest that coded excitation technique offers an increase of approximately 15dB in CTR and 10dB in SNR compared to the result achieved from a commercially available Pulse Inversion technique.

In conclusion, proposed polymer-shelled microbubbles provide a viable system to be used among the next generation of UCAs, and in combination with improved signal handling is superior not only in image enhancement relevant to diagnostics but also in localized and specific drug delivery for non-invasive therapy.

2a C02.**Localization and interaction of small inclusions with phase transformations in acoustic field****Vladimir A. Bulanov***V.I. Il'ichev Pacific Oceanological Institute, Far Eastern Branch of Russian Academy of Sciences, Russia*

Phase inclusions (PI) occupy various positions in a sound field depending on a relation between density and compressibility both of inclusions and fluids. The most known case is a behaviour of bubbles in the field of a standing wave. For bubbles it is important the relation between sound frequency and resonant frequency of bubbles, so a small bubbles with a resonant frequency of more than a sound frequency are localized in pressure crests while large bubbles are thrown out from fields with large pressure and they are agglomerated in pressure knots. Solid particles with a density more than a fluid density and with a small compressibility in comparison with a fluid compressibility are localized in pressure knots, i.e. behave like large above resonance bubbles. Such pattern sharply becomes complicated in the presence of phase transformations. The solution of a problem on localization PI in a sound field in the presence of phase transformations is obtained. It is shown, that the change of localization place in ultrasonic wave depends on radius PI and sound frequency. The matter is that in the presence of phase transformations along with the contribution to effective compressibility of purely mechanical effects it is important as well a mass transfer leading to additional compressibility which sharply changes a habitual pattern of PI behaviour in external field of pressure. For small PI such additional compressibility can exceed the adiabatic compressibility PI considerably. It is shown that this circumstance can lead to change of a place of PI arrangement by ultrasonic field depending on their size and sound frequency. Essential dependence of a localization place on the size of crystallization centers can be taken as a base of guidance for decomposition of structure of solid crystallizing in an ultrasonic field. In addition it is shown, that forces of interaction between crystallization centers (Bjerkness forces) sharply increase in comparison with a case of solid particles without phase transformations. It is necessary to pay attention that due to phase transformations the existence of the negative sign of real part for complex value of compressibility leads to appearance of repulsion forces between PI of various sizes instead of usual attractive forces characteristic for PI without mass transfer.

2a C03.**Ultrafast solitons measurement in crystalline semiconductor wafers by femtosecond laser ultrasonics****Nicolas Chuecos, Émmanuel Péronne, Bernard Perrin***Institut des NanoSciences de Paris, CNRS UMR 7588 - Université Pierre et Marie Curie, France*

Nonlinear acoustics manifestations occur daily in a wide range of natural, industrial and research contexts. At high frequencies, it allows reliable Non-Destructive Testing, making it a well-spread tool, especially in medical diagnosis or material sciences, for the characterization of various types of materials. In most cases, resolution is limited by the diffraction, i.e. the wavelength used for the measure. Consequently, if one wants to image nanostructures in semiconductors for example, one needs to generate frequencies close to 1 terahertz, which is well above any transducer's reach. In this experiment, we show how the absorption of a femtosecond laser pulse in a thin metallic film acting as a transducer can generate a short longitudinal strain pulse which propagates with strong nonlinearity at high enough laser fluence. Such propagation is well described in crystals by a Kadomtsev–Petviashvili (KP) equation, which simplifies into the Korteweg-de-Vries (KdV) equation when diffraction is negligible. This equation is well known for having solitons as solutions, which exhibit very particular properties well described by the inverse scattering approach. The strength of this time-resolved pump-probe set-up relies in its sensitivity to frequencies up to the terahertz and capability to study properties of ultra-thin layers of various materials on a wide range of temperatures and input fluences. This versatility is illustrated by showing how we can independently tune the different terms in the KP equation such that non-linearity, absorption or diffraction can be neglected. We report how the nonlinearity and dispersion interaction modifies the initial acoustic spectrum and how solitons appear after propagation through the sample. We checked experimentally that, when KdV equation holds, the initial conditions (initial strain pulse, transducer nature, laser pulse properties, etc.) greatly influence the solitons distribution in the same way as bound states determine a potential quantum well. Specifically, how the transducer's nature influences the solitons properties after propagation through a thick crystalline substrate (0.350 to 1 mm) and what it tells about nonlinear strain generation. In a nonlinear acoustics experiment where inverse propagation simulation is tedious, we extract by mean of a pump-probe set-up reliable data on these initial conditions. In other words, the unique properties of solitons and the analysis of their distribution lead to the experimental determination of the pump-generated strain profile.

2a C04.

Low-frequency intrinsic localized modes in a spatially periodic and articulated structure of rigid members with elastic supports

Yosuke Watanabe, Sojiro Awata, Nobumasa Sugimoto

Osaka University, Japan

This paper examines localized, flexural oscillations of an articulated structure consisting of identical, rigid members connected with neighboring ones through a coupler giving nonlinear restoring moment. The structure is elastically supported by springs at the center of mass of each member which is straight and uniform in density. Each member is subject to displacement in a plane from the straight position. It is supposed that the coupler gives a restoring torque proportional to a cubic function of difference in angle between two adjacent members on top of the linear torque, while the elastic support gives a restoring force linearly to yield a passing band in frequency. Numerical solutions are sought to the governing equations with free boundary conditions at both ends of the structure and appropriate initial conditions. They show existence of time-periodic localized oscillations, intrinsic localized modes (ILMs), which emerge due to the nonlinearity and spatial discreteness of the system. It is revealed that the ILMs oscillating at a frequency occur lower than the passing band in contrast to the quasi-periodic ones appearing above the band. It is also revealed that for a hard resorting torque, excitations of the ILMs are restricted within a narrow range in a parameter plane between nonlinearity and stiffness of the support.

May 22 (Tue)

2a C05.

A study on bifurcations and structure of phase space concerning intrinsic localized modes in a nonlinear magneto-mechanical lattice

Masayuki Kimura¹, Takashi Hikihara²

¹The University of Shiga Prefecture, Japan, ²Kyoto University, Japan

Intrinsic localized mode (ILM) is a kind of spatially localized waves in nonlinear lattice. Since ILM has theoretically been discovered by A. J. Sievers and S. Takeno in 1988, ILM is investigated theoretically as well as numerically for many of nonlinear lattices. In this decade, several experimental systems in which ILM can exist and even travel have been reported, for instance, Josephson-junction arrays, optic wave guides, micro-mechanical cantilever array and electronic circuits. Those experimental results allow us to expect applications of ILM for practical engineering. However there remain numerous questions associated with how ILM travels in lattice. The aim of this research is to clarify the mechanism of the traveling and to establish the control scheme for ILM. The nonlinear magneto-mechanical lattice proposed in this paper is also an experimental system for investigating the dynamics of ILM. The lattice consists of nonlinear magneto-mechanical oscillators, an elastic coupling rod, and an exciter vibrating the whole system. In the system, ILM was successfully observed. Due to sensors attached to oscillators, the displacement of each oscillator can individually be measured. This allows us to obtain the complete waveform of ILM and to compare precisely with numerical simulations. In addition, the strength of nonlinearity for each site is designed to adjustable in time. An excited ILM can move to the neighboring site by varying the nonlinearity at the site. The proposed system thus enables us to investigate experimentally the dynamics of ILM. The motion of nonlinear oscillators is described by a coupled ordinary differential equation. Because each oscillator consists of an elastic beam and magnets, the Euler-Bernoulli beam theory and static magnetism are applied for modeling the system. By numerically integrating the equation, ILM is obtained as a temporally periodic solution in the same conditions as the experiment. The obtained ILM has almost the same waveform as the experimentally observed ILM. It implies that the obtained model is precise enough to discuss ILM by numerical simulations. By using the mathematical model, bifurcations and the phase structure around ILM are numerically investigated. In particular, the relationship between invariant manifolds of unstable ILMs and the behavior of traveling ILMs is clarified. That is, it is revealed that the phase structure around unstable ILMs governs the onset of traveling ILMs. We will discuss the details of the phase structure concerning traveling ILM and will mention bifurcations of coexisting ILMs.

Invited Lecture**2a L3.****Nonlinear aspects of modern ultrasound applications in medicine****Vera A. Khokhlova**^{1,2}¹*Dept. of Acoustics, Faculty of Physics, M.V. Lomonosov Moscow State University, Moscow 119991, Russia,*²*Center for Industrial and Medical Ultrasound, Applied Physics Laboratory, University of Washington, 1013 NE 40th Street, Seattle, WA 98105, USA*

Medical ultrasound is an exciting example of modern science and technology where fundamental nonlinear phenomena have found successful applications and continue to play a critical role in development of novel diagnostic and therapeutic methods. In this paper, an overview of current nonlinear-based medical technologies is presented. The benefits of utilizing nonlinear effects, physical mechanisms of the interaction of ultrasound and shock waves with biological tissues, and the results of recent experimental and numerical studies are discussed.

In diagnostics, the methods based on nonlinear wave propagation (THI - tissue harmonic imaging), nonlinear scattering (CHI - contrast harmonic imaging), and energy transfer to different acoustic modes (SWEI - shear wave elasticity imaging) have substantially improved the capabilities of diagnostic imaging. In extracorporeal shock wave lithotripsy (ESWL), a method to comminute kidney stones by focused shock waves, nonlinear propagation effects determine pressure waveform in the focal region and thus mechanical effect on the stones, cavitation, and tissue injury around the stone. Shock waves are currently used in newer therapies to treat sites of chronic pain, bone fractures and non-unions, and to accelerate chronic wound healing.

High Intensity Focused Ultrasound (HIFU) is used to locally deposit the acoustic energy within the body, which can cause thermal necrosis of tissue (tumor treatment), stop bleeding (acoustic hemostasis), or enhance drug delivery. Nonlinear propagation effects during HIFU exposures can lead to formation of shocked waveforms at the focus. Extremely high heat deposition due to absorption at the shocks results in rapid initiation of localized boiling in tissues that dramatically changes the treatments. There has been also a significant interest to use HIFU to generate purely mechanical disruption of tissue without thermal coagulation. In this approach, called "histotripsy", high amplitude microsecond-long pulses of shocks generate a cavitation bubble cloud in tissue. The exposures are at low duty cycles to sustain the cloud but to avoid thermal effects. Recently it has been shown that a different approach using longer, millisecond bursts of ultrasound shock waves and repeated localized boiling can be used to induce similar mechanical ablation of soft tissue.

Although ESWL and HIFU methods have been proven to be successful in clinical practice, the physical and biological mechanisms of nonlinear wave interaction with concretions, bones, and soft tissues still remain unclear. An improved understanding of nonlinear wave propagation and interaction with tissue is essential to further advance medical ultrasound.

2p A06.**Sound propagation in saturated gas-vapor-droplet mixtures with evaporation and nonlinear particle relaxation****Max Kandula***ESC - Team QNA, United States*

The effect of nonlinear particle relaxation on sound propagation (attenuation and dispersion) in evaporating gas-vapor-droplet mixtures initially in equilibrium (saturated) has been theoretically investigated. The analysis is based on an extension of the linear theory of Davidson (J. Atm. Sci., 1975) to accommodate the effects of nonlinear particle relaxation processes of mass, momentum and energy transfer on sound attenuation and dispersion. The nonlinear particle relaxation theory is based on the author's recent work (Kandula; JASA, 2008, 2010). It is shown that nonlinear relaxation has an appreciable effect on sound absorption and dispersion for both low and high droplet mass concentrations.

The results suggest that with nonlinear relaxation the peak frequency (for attenuation per unit frequency) is reduced relative to that indicated by the linear theory. The shift in peak frequency due to nonlinearity seems to be reduced with an increase in the droplet mass concentration. The spectrum width of attenuation per unit frequency is reduced relative to that predicted by the linear theory. In the high frequency range (beyond the peak frequency), the reduction in the linear absorption coefficient predicted by the nonlinear theory relative to that predicted by the linear theory is seen to increase with increasing droplet concentration. The nonlinear effects become important for frequency range where viscous and heat conduction effects become predominant. In this frequency range, the dispersion coefficient according to the nonlinear theory is smaller than that provided by the linear relaxation. The results indicate for low droplet mass concentrations the existence of a spectral broadening effect in the dimensionless linear attenuation coefficient with a decrease in droplet mass concentration. It is also found that at large values of the droplet mass concentration, the dimensionless linear attenuation spectrum exhibits a universal shape independent of the droplet mass concentration.

2p A07.**Instability and breakup of a gas-cored viscous annular jet****Takao Yoshinaga***Osaka University, Japan*

A gas-cored annular liquid jet is of particular use for the formation of hollow microsphere capsules having the advantage of low effective density and high specific surface. This paper analytically deals with the encapsulation process of the jet due to the surface tension instability. Applying long wave approximations to the basic and boundary conditions for a viscous annular liquid phase and an inviscid core gas phase, a set of reduced nonlinear equations is derived for large deformations of the jet. Breakup of the jet is numerically examined in the equations assuming a semi-infinite jet when sinusoidal disturbances are given at a nozzle exit. For small or medium Weber numbers based on the annular phase, it is shown that the jet breaks up by closing the annular phase, which leads to the encapsulation of the core gas. For large Weber numbers, however, the jet breaks up by disintegration of the annular phase and, so that, fails to encapsulate the core gas. It is found that there exist the most unstable frequencies of input disturbances giving the shortest breakup time (or length) and such frequencies determine natural capsule formation periods and capsule sizes. It is also found that these periods and sizes increase with the increase of the velocity ratio of the core to the annular phases. This enables us to control the produced capsule sizes, without using the forcing at the nozzle exit which sometimes makes the capsule size nonuniform because of the intrinsically strong instability of the jet itself. The numerical results are shown to well agree with the previous experiment and the existing phenomenological model with respect to the capsule producing periods and sizes. Boundaries of the parameters for successful encapsulation are also shown for the Weber numbers and velocity ratios.

2p A08.**Focused ultrasound induced free-surface breakup and damage in acrylic plates****Yukio Tomita, Shigenori Tanaka***Hokkaido University of Education, Hakodate, Japan*

This paper provides some experimental results associated with the water-surface breakup, spray formation and material damage caused by focused ultrasound. Ultrasonic waves of both continuous and burst waves with the frequency of 1 MHz were focused at the free surface by employing a concave ultrasound probe (US probe) made of PZT ceramics whose vibrating chord length was 40 mm and geometric radius of curvature was 80 mm. Two types of experiments were carried out. One is an experiment for investigating the dynamics of water-surface, especially surface elevation, surface breakup and spray formation. The other is concerned with a damage experiment using a 3 mm thick acrylic plate as a test piece. Visualization of the phenomena was made by means of high-speed photography with the maximum rate of 50,000 frames/sec, together by taking snap shots. When ultrasonic waves were focused at the water-surface without an acrylic plate, a variety of surface responses took place depending on the acoustic properties of focused ultrasound. For example, a stable cusp was produced when ultrasonic energy was small. As increasing it, the free-surface grew to form an ejecting jet with its surface being fluctuating, showing a sequence of drop-like shapes. Afterwards spray formation and multiple breakups occurred. On the other hand, a damage experiment was conducted by using acrylic plates with four different positions setting both in air and in water layers. It was found that wave interaction played an important role to cumulated damage in acrylic plates. When an acrylic plate was set underwater with its upper surface being at the position equivalent to the acrylic plate thickness, the both surfaces of an acrylic plate were damaged one of which marked on the lower surface seemed to come from the focusing effect of ultrasound.

2p A09.**Bubble dynamics and decompression wave structure in a magmatic melt: diffusion effects****Valeriy Kirillovich Kedrinskiy***Lavrentyev Institute of Hydrodynamics, SB Russian Academy of Sciences, Russia*

One of the main problems arising at a simulation of unsteady high-speed flows of a magma is the understanding process kinetics (phase transitions, diffusion, viscosity effect) developing in an over-compressed magmatic melt under an explosive character decompression. The researches of magma state dynamics carried out within the frame work of the math-model [1] have shown that exactly a cavitation development plays key role both in the formation of a wave field structure and in multi-phase flow disintegration during an eruption. It turned out that the behavior of dynamic characteristics which determine a magma state is the self-coordinated one and can not be considered individually. It means that the dynamics of "average" bubble in a cavitation zone must be considered as a whole in the dependence on the dynamics of magma state behind a wave decompression front. The paper presents the results of numerical analysis of dissolved gas diffusion influence on the wave field structure and the bubble dynamics in "lagrange cross – section" of magma flow behind a zone saturation front. The state dynamics of a heavy magma under a decompression wave (170 MPa pressure in a volcanic chamber, $z = 1000$ m magma column height) is analyzed for two cases: when the diffusion fluxes into bubbles are strongly restricted and when natural diffusion provides the mass gas increasing in bubbles. It was shown than in the first case the profiles of decompression wave and mass velocity have the classical shapes. In the saturation zone the nuclei density N_b reaches value 10^{10} m^{-3} and the bubble radii distribution has an essential gradient in the vicinity of magma free surface. When the restrictions mentioned are removed the profile of decompression wave is fundamentally changed at the transition through the saturation front. In the vicinity of free surface of magma column ($z \geq 950$ m) the distributions of mass velocity $U(z)$ and pressure $P(z)$ are changed by leaps and bounds. It was found that during long time the gas pressure $P_g(t)$ in cavitation bubbles turned out to be stabilized in spite of an increase both bubble radius $R_b(t)$ and gas concentration $C_g(t)$ inside bubbles in a result of intense diffusion. The researches were carried out under financial support of RFBI (project 09-01-00500a), and, partly, of SB RAS IP 59 and of Presidium RAS IP (project 2.12).

1.Kedrinskii V.K., Davydov M.N., Chernov A.A., Takayama K. Initial stage of volcanic explosive eruption: dynamics of magma state under rarefaction waves. Doklady Acad. Sci. 2006. V. 407, № 2. P. 190-193.

Invited Paper**2p B06.****Principles of shear wave elastography: challenges and opportunities****Jacques Souquet, Jeremy Bercoff, Claude Cohen-Bacrie***SuperSonic Imagine, France*

Today there is an intrinsic limitation regarding frame rate acquisition of ultrasound information coming from the body. This limitation is due in part to the speed at which ultrasound wave propagates in the tissue, but also to the architecture of every system on the market whereby the somewhat sequential nature for data acquisition limits the speed at which images can be displayed. The new paradigm consists in the creation of a new ultrasound system architecture with heavily parallelized acquisition where the receive beamformer is achieved in software. With such a unique architecture we have demonstrated acquisition frame rate of more than 5000 frames/sec. Such an architecture is an enabler of new approaches to ultrasound: speed of sound optimization, transmit synthetic flat focus... Some of those advantages will be demonstrated, however one of the most interesting approach is to leverage such frame rate for transient elastography. Transient elastography is a unique patented approach to elastography (assessment of tissue elasticity) totally user skill independent and quantifiable. The new approach consists in sending a shear wave in tissue and assessing the speed at which the shear wave propagates. Shear wave velocity is directly proportional to the square root of the Young's modulus, therefore by inverse problem knowing the shear wave velocity we can derive the elastic properties of tissues. We will demonstrate how one can generate shear wave propagation in tissues, why ultra fast frame rate acquisition is a must and demonstrate the capability of such system to assess tissue elasticity.

May 22 (Tue)

2p B08.**Endoscopic optical coherence elastography using acoustic radiation force and a vibrating fiber scanner****Ryoichi Isago, Daisuke Koyama, Kentaro Nakamura***Precision and Intelligence Laboratory, Tokyo Institute of Technology, Japan*

High-speed measurement of biomechanical property such as elastic and viscoelastic constants in tissue is required. We try to combine endoscopic optical coherence tomography (OCT) which has a depth resolution of less than 10 μm with ultrasonic radiation force.

Two-dimensional lateral scanning of the measurement light of OCT is accomplished by the vibration of an optical fiber in an OCT probe. A cylindrical piezoelectric actuator is mounted at the fiber's neck to excite a circular or linear vibration at the fiber end, where the outer electrodes of the piezoelectric element is divided into four parts, and the voltages with a phase shift are applied between the adjacent electrodes. The optical fiber is vibrated in the bending cantilever mode at its resonant frequency, and the output light from the fiber end is collimated by a lens. The depth scanning in the tissue sample is carried out by the wavelength-swept method of the frequency domain OCT. The prototype probe is 1 mm in diameter and 20 mm in length.

Stress is caused in a sample tissue due to acoustic radiation force which is induced by the difference of acoustic energy density at the interface of the propagating media using a perforated focused transducer. The focused transducer is driven by sinusoidal burst waves of 10,000 cycles at 2.2 MHz. The deformation is slowly relaxed after removal of the force, and its behavior is measured by the prototype endoscope. The displacement and the strain are calculated with the cross-correlation between the images before and after applying the force.

Finger pad as a sample tissue is set at the focal position of the transducer. In this experiment, a two-dimensional tomographic image was plotted with scanning lines of 400 and the frame rate of 50 fps. We demonstrated the measurement and the imaging of strain distribution of the finger pad at the stationary condition and during deformation. The elastic image taken by the proposed setup provided several different information from the ordinary OCT images.

2p B09.**Ultrasonic actuation of biological tissues using dual acoustic radiation force for assessment of elastic properties****Hideyuki Hasegawa, Jun Yamaguchi, Hiroshi Kanai***Tohoku University, Japan*

Many studies have been conducted to measure mechanical properties of tissues using ultrasound-induced acoustic radiation force. To assess mechanical properties, strain must be generated in an object. However, a single radiation force is not effective because it mainly generates translational motion when the object is much harder than the surrounding medium. In this study, two cyclic radiation forces are simultaneously applied to a muscle phantom from two opposite horizontal directions so that the object is cyclically compressed in the horizontal direction. By the horizontal compression, the object is expanded vertically based on its incompressibility. The resultant vertical displacement is measured using another ultrasound pulse. Two ultrasonic transducers for actuation were both driven by the sum of two continuous sinusoidal signals at two slightly different frequencies [1 MHz and (1 M + 5) Hz]. The displacement of several micrometers in amplitude, which fluctuated at 5 Hz, was measured by the ultrasonic phased tracking method. Increase in thickness inside the object in the vertical direction was observed at the time of increasing acoustic radiation forces. Such changes in thickness corresponded to vertical expansion due to horizontal compression and show that the proposed method successfully generated strains inside the object. By evaluating the magnitude of strain, it would be possible to assess the change in elastic property of tissue due to diseases or therapies. Furthermore, in an in vitro experiment using a porcine liver, a shear wave propagating from the actuated region to the outside was observed. Its propagation speed was found to be 1.3 m/s corresponding to shear modulus of 1.7 kPa at a density of 10^3 kg/m^3 . This result was in good agreement with shear moduli of liver tissues in literature.

2p C06.**Molecular dynamics study of sound propagation in a gas****Takeru Yano***Osaka University, Japan*

Large scale molecular dynamics simulations have been performed to clarify the nonlinear and non-equilibrium processes of large-amplitude and high-frequency sound waves in a gas. To reduce statistical errors in calculating macroscopic variables, we put more than 0.3 million molecules in a simulation box with the length of several micrometers in the direction of wave propagation, because the number density of molecules in a gas is considerably small compared with those in liquids and the wavelengths of sound is very large compared with molecular scales even for high-frequency (gigahertz) sound. The one-dimensional sound wave is generated by a harmonic oscillation of sound source with the Lennard-Jones intermolecular potential, which is the same as that of gas molecules. As a result, we find that the large-amplitude and high-frequency sound propagates with strong attenuation, in some cases, exhibiting a stream-like profile accompanied with mass, momentum, and energy transports. This leads to a completely different picture and a different dispersion relation from a classical theory of high-frequency sound based on the linear standing wave analysis.

2p C07.

Resonant gas oscillation with evaporation and condensation

Masashi Inaba¹, Takeru Yano², Masao Watanabe¹, Kazumichi Kobayashi¹, Shigeo Fujikawa¹

¹Hokkaido University, Japan, ²Osaka University, Japan

Resonant gas oscillations in a tube filled with a polyatomic vapor, e.g. water vapor, is theoretically analyzed. The wave motion is induced by an oscillating plate mounted on an end of the tube, the other end of which is closed by a rigid wall and a thin liquid film of the vapor formed on it. The evaporation and condensation are induced by the wave motions in vapor and liquid phases. The one-dimensional wave motion in the gas phase is mathematically formulated as a boundary value problem of the Gaussian-BGK Boltzmann equation for polyatomic gases with the diffuse-reflection boundary condition at the plate and the kinetic boundary condition including the evaporation coefficient at the vapor-liquid interface. The formulation of the problem is valid for the entire range of the Knudsen number (defined by the ratio of the mean free path of vapor molecules and a typical wavelength), and contains the problem of a monatomic molecule as a special case of the Gaussian-BGK Boltzmann equation for polyatomic gases. Our main interest here is the effect of the evaporation and condensation at the vapor-liquid interface on the behavior of the one-dimensional resonant gas oscillation for the case of small Knudsen numbers, where the mass, momentum, and energy conservation equations in fluid dynamics are retrieved from an asymptotic analysis of the Gaussian-BGK Boltzmann equation. The boundary conditions at the interface for the conservation equations in fluid dynamics can also be derived, into which the evaporation coefficient in the kinetic boundary condition at the interface can be consistently incorporated. As a result, the nonlinear differential equation for the wave profile derived by Chester (1964) in a closed-tube problem is extended to the problem accompanied with the evaporation and condensation. A critical Mach number for shock formation can be deduced as a function of the evaporation coefficient, from which we can discuss the effect of the evaporation and condensation at the interface on the nonlinear resonant gas oscillation.

May 22 (Tue)

2p C08.

Numerical simulation of non linear acoustic streaming in a standing wave resonator

Virginie Daru^{1,3}, Diana Baltean-Carlès^{1,2}, Catherine Weisman^{1,2}

¹LIMSI-CNRS, France, ²Université Pierre et Marie Curie, France, ³Arts et Métiers ParisTech, France

Among nonlinear phenomena that appear in thermoacoustic systems, acoustic streaming is a continuous secondary flow, superimposed on the dominant acoustic oscillations, which affects the systems' efficiency. In this paper, acoustic streaming generated by standing waves inside a two-dimensional rectangular resonator filled with a compressible viscous fluid is simulated and the nonlinear regime is investigated, up to nonlinear Reynolds number Re_{nl} values of 70. The standing wave is excited by imposing a sinusoidal vibration of all resonator walls along the main axis, at frequency corresponding to the lowest resonant acoustic mode of the waveguide. Navier-Stokes compressible equations for perfect gas are solved using a high resolution finite difference scheme recently developed, that proved to be accurate for highly compressible flows as well as for acoustic propagation problems [V. Daru, X. Gloerfelt, AIAA Journal, 45 (10), 2007]. This allows the investigation of the effects of nonlinearities created by high intensity acoustic excitations. The wave amplification and its saturation are computed for different excitations and different resonator widths. Simulations are performed for different values of the Mach number up to 0.3 where shocks occur. The mean field is computed by time-averaging over the main acoustic period. Rayleigh outer vortices as well as boundary layer inner vortices are described. The results show good adequacy with several published experimental studies, although significantly different from numerical simulations previously performed in similar configurations. As the Reynolds number Re_{nl} is increased, the vortex pattern becomes unsymmetrical. The center of the outer vortices is displaced towards the resonator ends. Then two additional vortices per quarter-wavelength are generated at the channel centerline. These results are in agreement with recent experimental measurements performed in the nonlinear regime of fast streaming [Moreau et al, JASA 123(2), 2008; Nabavi et al., Wave Motion 46, 2009]. Current simulations are performed for rather small values of the resonator length, leading to high frequency waves. In order to predict the behavior of acoustic streaming for thermoacoustic systems with longer resonators, the effect of the resonator's length is also investigated.

2p C09.**Experimental study of acoustic streaming in a high level standing wave guide: influence of mean temperature and higher harmonics distribution****Ida Rey¹, Solenn Moreau^{1,2}, H el ene Bailliet¹, Jean-Christophe Vali ere¹**¹*Institut Pprime, CNRS - Universit e de Poitiers - ENSMA, D epartement Fluides - Thermique - Combustion, France,*²*Laboratoire Roberval UMR UTC-CNRS No. 6253 - Universit e de Technologie de Compi egne, France*

Particle velocity in an acoustic standing waveguide is measured using Laser Doppler Velocimetry (LDV). The experimental apparatus consists in a cylindrical standing wave resonator filled with air at atmospheric pressure, having an acoustic driver at each end for high intensity sound levels excitation at the lambda mode of the system that corresponds to a 240 Hz frequency. Measurements are performed for non-linear Reynolds numbers from 1 to 150 ($Re_{NL} = (\frac{U}{c})^2 (\frac{R}{\delta_v})^2$ with U the acoustic velocity amplitude at the velocity node, c the speed of sound, R the tube radius and δ_v the acoustic boundary layer thickness). The guide is surrounded simply by air so that a temperature gradient sets up between acoustic velocity nodes and antinodes, which goes up to 8K for higher acoustic levels. Thanks to thermocouples, the temperature is measured at different locations along the wave guide. As expected, the axial streaming velocity in the center of the guide measured along the axis agrees reasonably well with the slow streaming theory for small Re_{NL} but deviates significantly from such predictions for fast streaming ($Re_{NL} \geq 1$). As the Reynolds number increases, the centerline axial streaming velocity goes to zero except near the acoustic velocity nodes. For high amplitudes, the structure of the streaming vortices is more complex but maintains a certain consistency, symmetry and keeps stable. Different factors that can be causing such mutation of the measured velocity compared with the theory are discussed such as the effects of the temperature gradient and the non-linear propagation in the guide.

2p A10.**Theoretical study on the shape instability of an encapsulated bubble in an ultrasound field****Yunqiao Liu, Kazuyasu Sugiyama, Shu Takagi, Yoichiro Matsumoto***The University of Tokyo, Japan*

A theoretical study on the shape instability of a slightly deformed bubble encapsulated by a hyperelastic membrane in an ultrasound field is performed. To describe the dynamic balance on the bubble surface, the membrane effects of the in-plane stress and the bending moment are incorporated into the equation set for the perturbed spherical flow of viscous incompressible fluid (Prosperetti (1977) *Quart. Appl. Math.*, 35, 339). The spherical motion of the bubble is numerically obtained by solving the Rayleigh-Plesset equation with the elastic stress. The deflection therefrom is linearized and expanded with respect to the Legendre polynomial. Two amplitudes for each shape mode are introduced because the membrane has mobility not only in the radial direction but also in the tangential direction. The derived system is applied to the temporal evolution of the higher-order shape mode. Stability diagrams for the higher-order shape mode are mapped out in the phase space of driving amplitude versus driving frequency over a range of elastic modulus of the membrane. The most unstable driving frequency is found to satisfy an integer multiple relationship with twice of the higher-order natural frequency: $2\omega_k / \omega_d = n$. This finding is justified by a fact that the system with a boundary layer approximation is simplified into the Mathieu's equation, of which the instability is known to be described by such a relationship. A simple expression for the natural frequency of shape mode is also derived, which is validated by that obtained by numerical simulation.

2p A11.

Pattern formation on the wall of acoustically driven gas bubble

Alexey Maksimov¹, Timothy Leighton²

¹*Pacific Oceanological Institute FEBRAS, Russia,*

²*Institute of Sound and Vibration Research, University of Southampton, United Kingdom*

The final stable shape taken by a fluid–fluid interface when it experiences a growing instability can be important in determining features as diverse as weather patterns in the atmosphere and oceans, the growth of cell structures and viruses, and the dynamics of planets and stars. An example which is accessible to laboratory study is that of an air bubble driven by ultrasound when it becomes shape-unstable through a parametric instability. Above the critical driving pressure threshold for shape oscillations, which is minimal at the resonance of the breathing mode, regular patterns of surface waves are observed on the bubble wall. The existing theoretical models, which take account only of the interaction between the breathing and distortion modes, cannot explain the selection of the regular pattern on the bubble wall and the conditions for the realization of different shape structures (see, for example, <http://www.isvr.soton.ac.uk/fdag/Faraday.htm>). This paper proposes an explanation which is based on the consideration of a three-wave resonant interaction between the distortion modes. Using a Hamiltonian approach to nonlinear bubble oscillation, corrections to the dynamical equations governing the evolution of the amplitudes of interacting surface modes have been derived. Steady-state solutions of these equations describe the formation of a regular structure. A basic feature of pattern formation, which is applicable for the interpretation of preferred patterns of parametrically unstable Faraday ripples on the sphere, is that these structures have symmetry of point subgroups including the symmetries of Platonic solids. Our predictions are confirmed by images of patterns observed on the bubble wall.

May 22 (Tue)

2p A12.

Direct numerical simulations of nonspherical bubble collapse with nonequilibrium phase transition by the improved ghost fluid method

Yoshinori Jinbo, Hiroyuki Takahira

Osaka Prefecture University, Japan

The extremely high pressure and temperature fields generated by the bubble collapse provide a new environment for chemical reactions and medical applications. The detailed understanding of the violent collapse of nonspherical bubbles is needed to clarify such fields. The nonequilibrium phase transition through bubble interfaces is a key factor in determining the bubble collapse. Although a lot of theoretical or numerical studies were done for the collapse of spherical or nonspherical bubbles, the nonequilibrium phase transition of collapsing nonspherical bubbles is still open. The objective of the present study is to develop a numerical method that can be applied to the violent collapse of nonspherical bubbles with nonequilibrium phase transition due to evaporation and condensation. In the present study, the ghost fluid method [Fedkiw, et al., *J. Comput. Phys.* 152 (1999) 457-492] is improved so as to consider the heat and mass fluxes through the interfaces of collapsing nonspherical bubbles in a compressible liquid. The multi-grids method with adaptive mesh refinement and the level set method are utilized in the method. The definition of ghost fluids is improved to reduce the artificial diffusion in the thermal boundary layers for phase transition. The nonequilibrium condensation and evaporation are implemented successfully in the method. First, the present method is applied to the collapse of a spherical vapor bubble, and the numerical results are compared with the experiments by Akhatov et al. [*Phys. Fluids* 13 (2001) 2805-2819]. It is shown that the present method can predict successfully the violent collapse of a spherical bubble even though the Eulerian grid is employed. Second, the present method is utilized to simulate the collapse of an axi-symmetric nonspherical vapor bubble induced by the interaction of an incident shock wave with the bubble. The liquid-jet formation and the generation of shock waves from the collapsing nonspherical bubble, which cause the local high pressure and temperature, are also simulated successfully by taking the nonequilibrium condensation and evaporation of vapor into account. The thermal boundary layers inside and outside the bubble are captured with the present method. It is also shown that the phase transition causes the decrease of the internal pressure leading to more violent collapse.

2p B10.**Acoustic radiation force on a gas bubble in tissue****Yurii A. Ilinskii, Evgenia A. Zabolotskaya, Mark F. Hamilton***University of Texas at Austin, United States*

The motion and deformation of a gas bubble subjected to acoustic excitation in a soft elastic medium such as tissue was analyzed previously assuming the radiation force acting on the bubble is the same as in liquid [Ilinskii et al., J. Acoust. Soc. Am. 117, 2338 (2005)]. In the present work we discuss corrections to the acoustic radiation force for finite values of the shear modulus. The analysis is based on the Piola-Kirchhoff equation in Lagrangian coordinates, in which only the stress tensor is nonlinear, and the equation is solved by perturbation. In the linear approximation an analytical solution is obtained for the scattered acoustic wave. The nonlinear stress and full radiation force are calculated at the next order of approximation. For negligible shear modulus the result for a liquid is recovered. For finite shear modulus but still several orders of magnitude smaller than the bulk modulus, the resulting force differs from that for a liquid by a factor that depends on $k_t R$, where R is bubble radius, $k_t = \omega/c_t$ the wave number, ω the angular frequency and c_t the shear wave propagation speed. For $k_t R > 10$ the radiation force is practically the same as in liquid, but for $k_t R < 10$ its value can be significantly different. At this order of approximation, for small but finite shear modulus it is also found that radiation force depends on only one elastic constant, the shear modulus. It does not depend on the bulk modulus or any of the third-order elastic constants for an isotropic medium. [Work supported by NIH grants DK070618 and EB011603.]

2p B11.**Experimental study on temperature rise of acoustic radiation force elastography****Marie Tabaru, Hideki Yoshikawa, Takashi Azuma, Rei Asami, Kunio Hashiba***CRL, Hitachi Ltd., Japan*

Acoustic radiation force elastography (ARFE) is potentially useful for creating images of the elasticity variation in human tissue. A "push wave" is used to apply radiation force, and the elasticity is estimated by measuring the tissue displacement induced by the propagation of the shear wave. The push wave is a long burst wave comparable to the imaging usually used in the clinical field. Therefore, detailed safety research, especially that focusing on the temperature rise in the tissue, is needed. The typical push wave conditions for elasticity imaging are estimated in this report, and the temperature rises between soft tissue and bone are also compared. A push wave at a frequency of 2 MHz for a time duration of 1 msec and at an intensity of 1 kW/cm² was applied to a pig liver sample. Then, we measured the displacement in the liver at several different distances from the push point using a commercial ultrasonic scanner. With these conditions, we found that an imaging area could be created from up to 4 mm from the push point, which is minimally needed for imaging a tumor. In addition, the temperature rise in the push area was measured by using a K-type thermocouple. A plane wave at a frequency of 2 MHz for a time duration of 20 sec was exposed to a tissue mimicking phantom and a piece of bone of pig rib, and the relation between the temperature rise and the exposed intensity was then examined. As a result, we found that the temperature rise was linearly increased with higher intensity, and the temperature rises on the surface of the bone was 12 times higher than that of the phantom. When the push wave at a time duration of 1 msec and an intensity of 1 kW/cm² is repeatedly applied to the bone 10 times at 1-second intervals, the total temperature rise estimated to be 2.3°C due to heat accumulation. In conclusion, the thermosensitivity of the bone is 12 times higher than that of the soft tissue, and repeated push wave poses the potential risk of exceeding the allowable maximum temperature rise, which is 1°C, on the surface of the bone. In order to safely use ARFE, the imaging area, including the path of the push wave, should be carefully checked and the time interval for consecutive use should be adjusted to prevent thermal risk on the surface of the bone.

2p B12.

Temperature elevation of biological tissue model exposed by focused ultrasound with acoustic radiation force

Naotaka Nitta¹, Nobuki Kudo², Iwaki Akiyama³

¹Human Technology Research Institute, National Institute of Advanced Industrial Science and Technology (AIST), Japan,

²Laboratory of Biomedical Engineering, Graduate School of Information Science and Technology, Hokkaido University, Japan,

³Department of Human and Environmental Science, Shonan Institute of Technology, Japan

Purpose: Focused ultrasound with acoustic radiation force (ARF) is beginning to be used for imaging and measuring tissue elasticity. The ARF technology uses periodic burst waves with long pulse duration and low duty factor. On the other hand, it was suggested that the temperature elevation near focus at bone might be significant within the limits of acoustic output regulation in diagnostic ultrasound devices (Herman; 2002). In this study, with the aim of obtaining the relation between temperature elevations and parameters of ultrasound exposure with ARF, temperature elevations in two kinds of tissue models with and without bone is numerically evaluated. Methods: The tissue model without bone (Model A) was a 3-D cylindrical body, and includes skin, fat, muscle and viscera layers whose attenuation coefficients were uniformly 0.3dB/cm/MHz. Another tissue model with bone (Model B) includes additional bone layer with attenuation coefficients of 10 to 30 dB/cm/MHz, and the focal point was set on the surface of bone. The focused transducer (2.5 MHz, focal depth = 35 mm, f-number = 2) was put on the upper surface of each model. On the same scan line, focused ultrasound with ARF was irradiated periodically with a pulse duration (PD) of 0.3 to 100ms, a pulse repetition time (PRT) of 2 to 20s and a positive pressure up to 10 MPa. Heat generation rate of bioheat transfer equation is determined by intensity in these acoustic field and attenuation in tissue model. By solving bioheat transfer equations with the thermophysical and blood perfusion constants (NCRP No.113), time-dependent temperature elevations at the focal point were calculated during 200 second. Results: In all cases, temperature elevations during ultrasound exposure time and temperature decreases during rest time were repeated, and resultant maximum temperature elevation increased according to number of irradiation during 200 second. The maximum temperature elevation increased in proportion to the acoustic intensity. The higher instantaneous acoustic intensity and longer PD induced higher temperature elevation, and the longer PRT suppressed significant temperature elevation. In comparison with Model A and B, the temperature elevations near focus at bone in Model B were higher than those at focus in Model A. The temperature elevations near focus at bone increased according to attenuation coefficient of bone. Conclusion: In this study, the relation between temperature elevations and parameters of ultrasound exposure with ARF was obtained in two kinds of tissue models with and without bone.

2p C10.

Existence and stability of localized modes in one-dimensional nonlinear lattices

Kazuyuki Yoshimura

NTT Communication Science Laboratories, Japan

It is well known that spatially localized modes emerge in a variety of space-discrete nonlinear systems. Experimental evidence for the existence of such localized modes has been reported for various systems so far. The localized modes are called discrete breathers (DBs) or intrinsic localized modes (ILMs). A space-discrete nonlinear system can be modeled by a nonlinear lattice. From a mathematical point of view, DBs are time-periodic and spatially localized solutions of the equations of motion. Fundamental and important issues, associated with DB, are the existence and stability of DB solutions. We studied these issues for one-dimensional diatomic Fermi–Pasta–Ulam (FPU) type lattices. The diatomic FPU type lattice is a chain of alternating light and heavy particles coupled by nonlinear interaction potentials. In this lattice model, the limit of zero mass ratio is called the anti-continuous limit. There exist a large number of localized periodic solutions, i.e., the trivial DB solutions, in this limit. A trivial DB solution consists of a finite number of in-phase or anti-phase excited light particles, separated by particles at rest. We have proved the existence of DB solutions for small mass ratio by continuation of the trivial DB solutions from the anti-continuous limit. Then we have proved the stability criterion for these DB solutions. The stability criterion is that the DB solutions are all linearly unstable near the anti-continuous limit, except for those continued from trivial solutions consisting of alternating anti-phase excited particles. This prediction of the stability criterion is clearly observed in numerical simulations.

2p C11.**Modulational instability and chaotic breathers in two dimensional Fermi-Pasta-Ulam lattices****Yusuke Doi, Akihiro Nakatani***Department of Adaptive Machine Systems, Graduate School of Engineering, Osaka University, Japan*

Modulational instability of zone boundary modes (ZBMs) and band edge modes (BEMs) in two dimensional diatomic Fermi-Pasta-Ulam (FPU)- β lattices is analyzed rigorously. Discrete breathers (DBs) or intrinsic localized modes (ILMs) in the higher dimensional lattice systems have attracted great interests in various fields recently. Modulational instability of the ZBMs and BEMs is one of the most important problems in excitation of DB in the system, since chaotic breather (CB) which is interaction process of DB, is observed. We consider the two dimensional lattices in which a lattice point interacts their nearest neighbor and second nearest neighbor lattice points. First we derive the nonlinear periodic solutions which correspond to the linear ZBMs and BEMs of the system. Then the stability of the perturbation to the periodic solutions is investigated based on characteristics of the monodromy of Gauss's hypergeometric equation, since the perturbation equations can be transformed into Gauss's hypergeometric equation which have the explicit form of the monodromy. We find the stability of the ZBMs and BEMs depend on the mass ratio of the system and the strength of interactions between lattice points. Moreover we present some results of numerical simulations of temporal evolution of the ZBMs and BEMs with small perturbations. The numerical results show the dynamics after the system becomes unstable, which cannot be tracked by the linear analysis.

2p C12.**Controlled translation of an intrinsic localized mode****Masayuki Sato¹, Naoki Fujita¹, Souichi Nishimura¹, Yuichi Takao¹, Yurina Sada¹, Weihua Shi¹, A. J. Sievers²**¹*Graduate School of Natural Science and Technology, Kanazawa University, Japan,*²*Laboratory of Atomic and Solid State Physics, Cornell University, United States*

As mechanical arrays continue to decrease in size it becomes important to characterize their nonlinear vibrational dynamics. One feature for a micro or nano-mechanical array is that a localized nonlinear excitation called an intrinsic localized mode (ILM) can be generated even in a perfect array. Some ideas and applications for vibrational localization in small scale arrays have already been proposed. Experimental and simulation studies with micromechanical arrays, mainly of the di-element type, have shown that in the nonlinear regime a steady state ILM can be produced by chirping the frequency of the uniform driver beyond the plane wave spectrum and then locking its amplitude with a cw oscillator. The resulting locked ILM is stable at a lattice site. It can be moved incrementally from one place to another by introducing a mobile impurity in the array that, when nearby, shifts the ILM location. Depending on the details of the nonlinear lattice either attraction or repulsion of the ILM can occur. By studying vibrational impurity mode-ILM dynamics a number of different processes have been uncovered such as seeding, and annihilation. In addition, a time-varying impurity mode has been used to invert the existence or absence of an ILM. Such a process can be applied to information processing, a smart sensor, or an actuator. In this paper, we numerically demonstrate, without the use of an impurity, the translation over large distances of a driver locked ILM that is close in frequency to the band mode spectrum. The new technique is to apply to an ILM locked at frequency ω a second somewhat weaker driver that is tuned to ω' , below the ILM frequency but near the top of the band mode spectrum. By tuning ω' we find a resonant process in which, on resonance, the ILM moves through the lattice as long as the additional excitation exists. This new traveling ILM state is synchronous with the beating perturbation made from the two drivers and moves with speed v , where d is the unit cell size. The observed translation appears to be the physical manifestation of the nonlinear locked excitation tunneling back and forth between its localized vibrational state and a nearby extended-wave vibrational state with the coupling made possible by the second driver.

2p P01.**The nonlinear multifrequency sonars for underwater navigation****Vadim Yur'evich Voloshchenko***Department of Engineering Drawing and Computer Design, Taganrog Institute of Technology, South Federal University (TIT SFedU), Russia*

The paper presents an original hydroacoustic navigation sonar's improvement trend – the extension of operating frequency band without complication of hydroacoustic antenna's design by means of reception and processing of echo-signal's amplitude, phase and frequency characteristics of generated in nonlinear water medium phase coupled multiple high harmonic components $2f, 3f, \dots, nf$ of finite amplitude pump waves with fundamental frequency f . The hydroacoustic antenna's directional radiation patterns and calculated curves for several sonar equations at multiple high harmonic components of fish-finding echo sounders "Sargan", "Taimen" are discussed. The extension of frequency band by additional registration of higher harmonic's echo-signals allows to realize original broadband echo-ranging systems with different antenna's angular resolution. The patented block diagrams and operation principles of the multifrequency correlation and Doppler logs, the impulse parametric upward-beamed fathometer for providing of autonomous vessel's safety underwater (under the ice cover) navigation are considered. The application of these devices enable to increase the accuracy of vessel's velocity measurements on the reverberation signals from sea bottom and moving water masses, gauging the ice thickness above the vessel and detection of suitable for vessel's emersion paths of ice-free water in ice-fields (the shore-lead sonar's mode of operation), etc.

May 22 (Tue)

2p P02.**A novel method for detecting second harmonic ultrasonic components generated from fastened bolts****Makoto Fukuda, Kazuhiko Imano***Department of Electrical and Electronic Engineering, Graduate School of Engineering and Resource Science, Akita University, Japan*

Bolts and nuts are a standard fastener used in the assembly of mechanical structures. Because broken, slack, or over-tightened bolts can lead to serious accidents, quality control is an important issue. Current inspection methods for measuring bolt axial force include ultrasonic, strain-gauge, and load-cell techniques. However, complex corrections of the measured values are required to obtain accurate measurements of the bolt axial force when using these methods. Therefore, there is demand for simple quality-control techniques. Recently, the measurement of nonlinear ultrasonics, including second harmonic (SH) components, has been applied for nondestructive evaluation. The SH components are generated by the nonlinear response of plastic deformation, closed cracks and the contact acoustic nonlinearity (CAN). When a structure is fastened using a bolt, an axial force is applied to the bolt. The bolt will be plastically deformed and may develop fractures included closed cracks when the axial force exceeds the bolt's elastic yield point. Moreover, in the interface of the screw threads of the bolt and the nut, the SH ultrasonic waves will be generated by CAN. In this study, a novel method for detecting the SH components, from a bolt fastened with a nut, using the ultrasonic-transmission method is proposed. To drive the system, 20 cycles of a 1-MHz burst sinusoidal waveform, which was generated using an arbitrary waveform generator, were amplified to 100 V (peak-to-peak) with a high-frequency power amplifier. The amplified signal was used to drive a 1-MHz-resonant transmitting transducer, which transmitted the ultrasonic pulses through the bolt. A SH component of 2 MHz was generated by the fastened bolts, and was received by a 2-MHz-resonance receiver transducer. An oscilloscope captured the receiving pulses. A hexagon head iron bolt (12-mm diameter and 25-mm long) was used in the experiments. The bolt was fastened using a digital torque wrench. The SH component increased by approximately 20 dB before and after fastening bolts. The sources of SH components were CAN in the bolt-nut interface and the plastic deformation with fastening bolts. Consequently, usefulness of the novel method for detecting SH ultrasonic components generated from fastened bolts was confirmed.

2p P03.**Droplet propulsion on non-piezoelectric substrates induced by Lamb waves****Wei Liang***ISAT, Coburg University of Applied Sciences, Germany*

1. Background, Motivation and Objective Droplet propulsion on piezoelectric substrates was intensively investigated for lab-on-a-chip applications in the last few years [1-2]. However piezoelectric lab-on-a-chip devices suffer from fabrication problems, costs, maintenance and cleaning [3-4]. These are the reasons why current research is focusing on exciting surface acoustic waves on non-piezoelectric substrates by a plate / matching layer / piezoelectric substrate configuration [3-4]. Recently, we demonstrated the propulsion of droplets of μl size on non-piezoelectric substrates by Lamb wave. Lamb waves are excited by a structured piezoelectric block attached to the underside of the plate, which is not in contact with the liquid droplet [5]. 2. Statement of Contribution/Methods In this contribution the propulsion of microliter droplets with different volumes are investigated both theoretically and experimentally. The ratio of absorbed power to incident power of droplet propulsion on glass plate is calculated. The electrical input power and the distance, in which the droplet can be moved, are investigated in respect to droplet volume, the optimized propulsion frequency in respect to droplet volume. For all experiments antisymmetrical zero order Lamb waves are produced on a 1 mm glass plate with an interdigital transducer of 1 MHz center frequency. The glass plate is coated with a hydrophobic coating of 2-propanol. 3. Results The propulsion of droplet with different μl volumes is investigated. When the volume of the droplet is changed from 10 μl , 20 μl , 30 μl , 40 μl , 50 μl , to 60 μl , the droplet displacement changes, from 1.9 mm, 4.6 mm, 4.9 mm, 5 mm, 5.1 mm, 5.4 mm, by electrical input power of 6.66 W, 4.6 W, 5.19 W, 4.35 W, 4.28 W, 4.94 W, which are matched up to the theoretical result. Moreover, with increasing droplet volume (10 μl , 20 μl , 50 μl) the excitation frequency (1.03 MHz, 1.04 MHz, 1.06 MHz) must be slightly increased too, for optimization of the propulsion process. 4. Discussion and conclusion The propulsion of μl droplets on non-piezoelectric substrates depends on droplet size, electrical input power and excitation frequency. With a detailed investigation on the relevant propulsion parameter the propulsion effect can be optimized. With this knowledge droplet removal by Lamb waves on technical objects, such as windows, mirrors or lenses may be realized.

Reference [1] Wixforth, A.,(2003) 389 – 396. [2] L. Y. Yeo, and J. R. Friend, (2009). [3] R.P. Hodgson, M. Tan, L. Yeo, and J. Friend, Journal 2009, pp. 3-5. [4] T. Sugita, and J. Kondoh, Proc. IEEE Sensors 2010, pp. 253-256. [5] M. Schmitt, G. Lindner, S. Krempel, H. Faustmann, and F. Singer, Proceedings IEEE Ultrasonics Symposium, 2009, pp. 1640-1643.

2p P04.**Finite difference calculation of acoustic streaming including the boundary layer phenomena in an ultrasonic air pump on graphics processing unit array****Yuji Wada, Daisuke Koyama, Kentaro Nakamura***Precision and Intelligence Laboratory, Tokyo Institute of Technology, Japan*

Finite difference fluid simulation of acoustic streaming on the actual fine-meshed three-dimensional analysis model using graphics processing unit (GPU)-oriented calculation array is discussed. Airflows due to the acoustic traveling wave are induced when an intense sound field is generated in a gap between a bending transducer and a reflector. This phenomenon can be applied to an ultrasonic air pump, which supplies gas into narrow space in which conventional fans or pumps cannot be embedded. Efficient simulation of acoustic streaming enables the optimization of the pump design. However, until now, derivation of acoustic streaming considering boundary layers from time-averaging process is almost impossible because of huge calculation costs and convergence problem. We found that high performance computing utilizing GPU can be a solution to this problem. A bending transducer composed of an aluminum plate (20x30x2 mm) and a PZT element (20x10x0.4 mm) is used for the air pump. The fundamental bending vibration mode at 26.2 kHz is excited on the transducer, while an acrylic resin plate is located over the transducer with a gap of approximately 1 mm to act as a reflector. Then, in order to obtain the directional flow, the reflector is tilted by 4 degrees along the length direction. The computation of the compressive three-dimensional Navier-Stokes equation by finite difference method is executed for the calculation region (60x75x18 mm) where the device is located in the middle of the region. Mesh sizes of the calculation model are 0.05 mm in the height direction in the air gap, and 0.25 mm in the length and the width directions, and height direction outside the air gap. Calculation region is divided into 80 calculation units whose dimension is 15x15x1.5 mm and number of node is 75,000 points, so that each GPU processes every corresponding calculation unit. To connect the calculation units, the edge region of the unit is transferred to the other region using Message-Passing Interface. Total number of calculation node is the 6,000,000 points. Calculation results showed good agreement with the measurements in the pressure distribution. In addition to that, several flow-vortices were observed near the boundary of the reflector and the transducer, which have been often discussed in acoustic tube near the boundary, and have never been observed in the conventional calculation in the ultrasonic air pumps of this type.

2p P05.

Spectral hole burning in piezoelectric resonators

Fujio Tsuruoka

Kurume university, Japan

Spectral hole burning phenomena have been well studied in the field of light energy absorption. The requirements for their observation are, 1. the absorption frequencies are different from each other, 2. the absorption spectrum spread wide and moderately, 3. the absorption characteristics of some absorbers are changed by absorbing large amplitude energy to show hole(s). These conditions might be satisfied by piezoelectric resonant oscillators, of which dimensions and resonant frequencies are slightly different from each other. The third conditions were found to be fulfilled by applying large amplitude RF electric field and certain particles changed their oscillation characteristics to form hole(s). We prepared commercial grade piezoelectric powders, KBrO₃, destroyed with pestle and mortar, and sieved with standard meshes, for example, 105 and 125 μm . They were set in a parallel plate condenser with surface of $8 \times 12 \text{ cm}^2$ and plate distance of 1 mm. Though their crystallographic angles were at random and their oscillation modes were not identified, their resonant oscillations were well excited by pulsed electric fields. Holes were introduced by applying pulsed RF electric field. The pulse amplitude was up to 400 V/mm, the pulse width from 1 to 100 μs , the total pulse number up to 10^4 . The holes were detected with the AC impedance meter and by the magic-T method. We observed spectral holes in the spectrum of their complex impedance. The hole mechanism was attributed to the introduction of crystal deformations, which introduced changes into the damping constant of their free oscillation and their elastic constants. We found the hole profiles were well described with the absolute values of the Fourier components of applied pulses. Furthermore, we applied multiple sequent pulses with pulse separation of 1 to 20 μs and the number of the sequent pulses up to 20. The resultant profiles in electric impedance spectrum were well described with the absolute values of the Fourier components of the sequent pulses. In conclusion, we observed spectral hole burning phenomena in piezoelectric resonators and enlarged the notion of hole burning phenomena.

May 22 (Tue)

2p P06.

Measurement of temperature gradient in a stack of a prime mover in a loop-tube-type thermoacoustic cooling system

Shin-ichi Sakamoto¹, Ryoichi Isago¹, Yoshitaka Inui¹, Yoshiaki Watanabe²

¹University of Shiga Prefecture, Japan, ²Doshisha University, Japan

In this paper, the main focus is on spatial and temporal variation of temperature gradient in a stack of a prime mover in a loop-tube-type thermoacoustic cooling system. Spatial and temporal variation in temperature gradient was measured for various stack lengths. Measurement was also conducted in both cases with and without self-sustained sound. Since the thicknesses of thermal and viscous boundary-layers depend on the temperature, knowledge of detailed spatial and temporal variation of temperature gradient in the stack will be important to design a stack, especially stack channel radius. Since little has been reported about temperature gradient formed in the stack, the results obtained in the experiments will contribute to raise the cooling effect of the thermoacoustic cooling system.

From the observation of the temperature variation in both cases with and without self-sustained sound in the loop-tube, it is confirmed that with self-sustained sound, temperature gradient is linearly formed along the stack. This resulted from the heat flow caused by the thermoacoustic effect.

2p P07.**Consideration of nonlinear vibration characteristic of object for irradiating high-intensity ultrasonic waves by a point-convergence-type aerial ultrasonic source****Ayumu Osumi, Youichi Ito***Nihon University, Japan*

Recently, technologies employing aerial ultrasonic waves have been developed. Ultrasonic inspection can be performed in a noncontact manner using an aerial ultrasonic probe. Methods using such a probe are based on the detection of waves reflected from an object and waves transmitted through it. However, ultrasonic inspection using an aerial ultrasonic probe requires a short measurement distance and a stringent condition of incidence in setting a suitable incidence angle of the transmitted waves. Previously, we proposed an entirely different method that uses high-intensity aerial ultrasonic waves, generated using a point-converging acoustic source with a stripe-mode vibration plate, to detect defects in materials. We considered a noncontact method that can detect defects in materials by analyzing frequency information obtained from the vibration of an object excited with high-intensity ultrasonic waves of finite amplitude, that has a measurement distance several times longer than that of ultrasonic inspection using an aerial ultrasonic probe, and a condition of incidence relative ease in setting the angle of incidence. However, to achieve such a method, it is important to generate high-intensity ultrasonic waves of finite amplitude and to elucidate the mechanism of ultrasonic irradiation onto materials. In this study, we examine the sound pressure and vibration characteristics of the surface of materials for irradiation with high-intensity ultrasonic waves of finite amplitude. From our results, it is found that the sound pressure characteristics at the fundamental frequency and the harmonic frequency characteristics of the surface are difficult to determine from its free field. It is also found that the object vibrates at the fundamental and harmonic frequencies corresponding to those of ultrasonic waves of finite amplitude, and that sound pressure and vibration on the surface are strongly affected by the relationship between the acoustic resonant systems of the sound source and object. In addition, it is found that the vibration at the fundamental and harmonic frequencies on the surface is strongly influenced by that relationship.

2p P08.**On the two-dimensional patterning of inorganic particles in resin using ultrasound****Toru Tuziuti***National Institute of Advanced Industrial Science and Technology (AIST), Japan*

The ultrasonic manipulation technique is applicable to opaque particle suspensions and has merits in comparison with the other methods such as radiation force by a laser that needs media transparency and electrostatic force that requires attention to be paid to electrolysis [A. Ashkin: Phys. Rev. Lett. 24 (1970) 156]. Goddard and Kaduchak [G. Goddard and G. Kaduchak: J. Acoust. Soc. Am. 117 (2005) 3440] demonstrated the concentration of polystyrene particles using a line-driven cylindrical glass tube. Oberti et al. [S. Oberti, A. Neild and J. Dual: J. Acoust. Soc. Am. 121 (2007) 778] directly excited ultrasonic transducers attached to a glass plate on a fluidic system to cause propagation of surface wave emitting a sound wave into an adjacent fluid. They achieved particle concentration in parallel lines in the case of one transducer while in the case of two transducers an oval-shaped two-dimensional pattern of particle concentration was obtained. The present study deals with for the first time the formation of a two-dimensional pattern of concentrated particles with indirect irradiation of ultrasound from one transducer. A two-dimensional millimeter-sized pattern of micrometer-sized titanium dioxide particles in UV-reactive acrylic resin using 1.93 MHz ultrasound is fabricated. A mixture of particles and resin is set in a thin layer between square glass plates of which one plate is irradiated with ultrasound. Both vibration normal to the plate and the wave propagating in the mixture form standing waves to provide a two-dimensional pattern of the particles. The two-dimensional pattern was hardened with UV irradiation. It is confirmed that the two-dimensional pattern keeps a similar structure before and after UV hardening. The present technique will be promising for novel material fabrication by controlling the boundary condition for the mixture of the particle and resin or vibration mode of the glass.

2p P09.

Dynamics of second harmonics in nonlinear surface acoustic waves and a proposal of its device application

Koji Aizawa, Yoshiaki Tokunaga

Kanazawa Institute of Technology, Japan

Dynamic behavior of nonlinear surface acoustic waves (NLSAWs) generated on a piezoelectric single crystal has been much interested in application to new engineering fields from a viewpoint of complex system. In this study, characterization of fundamental (FUN) and second-harmonic (2nd HMC) components in NLSAW propagating on a LiNbO₃ single crystal were investigated, and we proposed a novel photonic signal control device (PSCD) using a dynamic behavior of NLSAW. 128°-rotated Y-cut X-propagating LiNbO₃ single crystal was used as substrate in this experiment. The interdigital transducer (IDT) with a center frequency of 50 MHz was formed on the surface of LiNbO₃ substrate. The RF burst signal was introduced to its IDT through RF connector, in which its duration time and duty cycle was 250 ns and 0.05 %, respectively. Additionally, a gold (Au) film (10x10 mm²) was also formed on the center of substrate due to enhancement of velocity dispersion. The probing beam with 300 μm in diameter using He-Ne laser was irradiated to an Au film, and then the time dependence of diffracted light intensity from NLSAW was measured using digital oscilloscope through a photomultiplier tube. Either FUN or 2nd HMC was chosen by changing a diffraction angle. A pulse-like FUN (or 2nd HMC) propagated from IDT(I) comes into collision with another one from IDT(II) at the center of a Au film, in which the distance between two IDTs is fixed at 20mm. It was found that diffracted light intensity from 2nd HMC at collision point was larger than algebraic sum of two pulses before and after collision, whereas its value of FUN was smaller than that of peak intensity. This extraordinary variation of diffracted light intensity at collision point must be occurred by a nonlinear effect such as enhancement of coupling efficiency between FUN and 2nd HMC and energy conversion from FUN to 2nd HMC. To demonstrate an operation as PSCD, we measured the diffracted light intensities of FUN and 2nd HMC components at collision point when 4-digit pulse signals corresponding to 1010 and 1111 were applied as input signal to the IDT(I) and IDT(II), respectively. The measured pulse pattern was independent on the input signals applied to their IDTs when FUN component was used, whereas its pattern using 2nd HMC component showed an AND operation between two input signals. PSCD using this phenomenon may be one of promising candidates for application to information security device.

2p P10.

Acoustic harmonic generation in a multilayered structure with nonlinear interfaces

Yosuke Ishii, Shiro Biwa

Kyoto University, Japan

Many types of interfacial imperfections can be found in various multilayered structures, such as thin interphase layers, weak bonds, and delaminated but contacting surfaces. Foregoing studies have revealed that such imperfect interfaces can be modeled as spring-type interfaces with finite interfacial stiffness. When these multilayered structures are insonified by finite-amplitude elastic waves, these interfaces become a source of nonlinear acoustic phenomena such as higher harmonic generation. Understanding nonlinear acoustic properties of multilayered structures is important from a practical point of view when, for example, composite laminates are to be evaluated by nonlinear acoustic methods. In this study, the second-harmonic generation phenomenon is studied numerically and theoretically for a multilayered structure having nonlinear interlayer interfaces. First, the dynamic finite element analysis is performed to compute the elastic wave propagation in the layered structure in the normal direction, and the computed transmitted or reflected waveforms are investigated by the spectral analysis based on the short-time Fourier transform. The results show a complex behavior that the amplitude of the generated second harmonics is influenced not only by the interfacial nonlinear properties but also by the layered structure. To examine this behavior from a theoretical point of view, the perturbation analysis by Biwa et al. [1] for a single nonlinear interface between semi-infinite elastic media is extended to study wave propagation across multiple nonlinear interfaces. The transfer matrix method is employed to formulate the problem for a multilayered structure subjected to a harmonic wave excitation. By aid of the perturbation analysis, the problem is decomposed into one for the linear propagation of the fundamental wave and one for the occurrence of the second harmonics due to the interfacial nonlinearity. Some explicit results are obtained based on this formulation, and the results are compared to the dynamic finite element analysis. References [1] S. Biwa, S. Nakajima and N. Ohno, *Trans. ASME J. Appl. Mech.*, 71 (2004), pp. 508-515.

2p P11.**Laser induced stress waves emerged by laser-target interaction****Yoshiaki Tokunaga, Motoaki Nishiwaki, Mieko Kogi, Koji Aizawa***Kanazawa Institute of Technology, Japan*

Recently, a method of laser induced stress waves (LISWs) mediated drug delivery or gene transfection into human cells is paid remarkable attention since it is a nonchemical, nonviral, and noninvasive method for transport of drugs and genes into the cells. LISWs can be emerged by the following complicated mechanisms: Optical breakdown, ablation and plasma formations, and shock wave with recoil momentum. The characteristics such as peak pressure, rise-time, full width at half maximum of LISWs are not dependent only the laser parameters such as wavelength, pulse width, but also fluence and the optical and mechanical characteristics of the irradiated target. Unfortunately, discussions from physical standpoints of these processes on generation and dynamics of LISWs have never been done in detail up to now. Although it is very difficult to analyze these complicated nonlinear phenomena, quantitative explanation of these processes may be necessary as entrance for getting further and fruitful results in medical applications. In this paper, we describe a physical model of emergence process of LISWs and also transfection of pEGFP plasmid DNA into HeLa cells by LISWs. Nd:YAG laser (Spectra Physics: LAB-130, USA) was used with 15ns duration with energies up to 200mJ/pulse at 532nm (second harmonics) at one shot as an energy source. A natural rubber (Sound Lab.Co.Ltd. Japan) was used as an endothermic surface absorbing target, and a polyethylene terephthalate, as a transparent overlay, was also used for growing of impulse peak and pulse duration of LISW due to detonation and blast waves. The stress pressure was measured by PVDF transducer with about 110 μ m thickness. The PVDF output voltage was statistically processed by 1.5GHz digital oscilloscope (LeCroy: LC684DXL, USA). Obtained results were as follows: HeLa cells viability were 80 percent at 2.4J/cm² of irradiation fluence. The peeling rate of the cell was approximately 20 percent. The gene transfection efficiency was of approximately 3 percent in our experimental condition. We also describe an acoustic profile of LISWs for getting better results on gene transfection into cells

2p P12.**The numerical simulation of evolution of finite-amplitude noise pulses****Igor Yu. Demin, Sergey N. Gurbatov, Nikolay V. Pronchatov-Rubtsov***Nizhny Novgorod State University, Russia*

The propagation of finite amplitude sound waves is of fundamental interest in nonlinear acoustics. In the simplest model of propagation in fluids these waves are described by the well-known Burgers' equation (plane waves) [1, 2]. In studies of nonlinear wave propagation an important problem is to find the waveform of the asymptotic wave at long time after the preparation of the initial wave or at long distance from the source emitting the wave. In case of noise-type initial disturbance, the analytical calculation the velocity field is very complicated mathematical problem. The Fast Legendre Transform Algorithm (FLTA) [3] should be applied to solve the problem. FLTA allows to reduce the number of the mathematical operations, that is necessary to be done to obtain the BE solution. As the result of time reducing for each realization processing, more realization can be analyzed and the statistic data accuracy is increasing.

In the present paper we consider the numerical simulation of evolution of complex pulses which are characterized by two scales (l - the inner scale of the carrier, L - the scale of the modulation, and the condition $L \gg l$). For such signals the generation of a low-frequency component or a non-zero mean field takes place. It has also been shown that, for a pulse with random carrier, the parameters of the asymptotic waveform depend weakly on the fine structure of the initial pulse, but that the old-age behaviour is very sensitive to the properties of the carrier.

This work was supported by RFBR (11-02-00774) and by the Federal Program "Scientific and Scientific-educational brainpower of innovative Russia" for 2009-2013 (Contract N 02.740.11.0565).

[1] O.V. Rudenko and S. I. Soluyan, *Theoretical Foundations of Nonlinear Acoustics* (Nauka, Moscow, 1975; Consultants Bureau, New York, 1977).

[2] S.N. Gurbatov, A.N. Malakhov, A.I. Saichev. *Nonlinear random waves and turbulence in nondispersive media: waves, rays, particles*. Manchester: Manchester University Press, 1991.

[3] A.Noullez and M.Vergassola. A Fast Legendre Transform Algorithm and Applications to the Adhesion Model, *Journal of Scientific Computing*, 1994, v.9, 259-281.

3a A01.**Stability thresholds for multi-bubble systems****David Sinden, Eleanor Stride, Nader Saffari***Dept Mechanical Engineering, University College London, United Kingdom*

High-intensity focused ultrasound (HIFU) aims to destroy pathogenic tissue by converting energy from ultrasound into heat. Under certain conditions, cavitation activity has been shown to greatly enhance the local rate of heat deposition and also provide a significant aid to treatment monitoring. However, cavitation occurring pre-focally or growing unstably around the focal region is known to impede safe and effective treatment delivery. There is thus a significant need for better understanding of the generation of cavitation during HIFU treatments and its influence on wave propagation and beam focusing. It is shown that at therapeutically relevant acoustic pressures and frequencies, the threshold for inertial cavitation is typically independent of the number of bubbles present. This is because the re-radiated pressure field from any one bubble only has a significant influence upon the oscillations of the surrounding bubbles if it collapses inertially. When this occurs the inertial collapse of a large bubble may initiate the collapse of smaller bubbles nearby and lead to a synchronised collapse. Furthermore, if a bubble begins to oscillate irregularly, the surrounding bubbles will experience an irregular re-radiated pressure field from the interaction and appear to oscillate in an irregular manner. The calculated Lyapunov dimension of a chaotic attractor for a multi-bubble system is essentially equal to that of a single bubble system. The computation of Lyapunov exponents leads to a threshold for chaotic oscillations, that is which exhibit extreme sensitivity to initial conditions, and revised stability thresholds for multi-bubble systems are calculated. In a unique case of a regular array of equally sized bubbles a nonlinear normal form about the Blake critical radius can be derived. Consequently Mel'nikov analysis then provides an analytical expression for a lower bound for the onset of chaotic oscillations of the multibubble system. The effects of fluid viscosity and compressibility, due to delays in the interactions, on the stability of the oscillations of multi-bubble systems is then investigated. For a pair of linearly oscillating interacting bubbles it is shown that typically the system undergoes a Hopf bifurcation and reaches a stable limit cycle. From this a revised Bjerknæs force between a pair of bubbles is derived. It is then shown that the effects of compressibility, through time delays in the interaction, raises the thresholds for instabilities due to radial and non-spherical oscillations. The effect of translational motion on the stability of the radial oscillations through the delays is formulated. The physical implications of these findings for cavitating liquids in general, and for clinical practice are then discussed.

3a A02.**Derivation of nonlinear wave equations for ultrasound beam in nonuniform bubbly liquids****Tetsuya Kanagawa¹, Takeru Yano², Junya Kawahara³, Kazumichi Kobayashi³, Masao Watanabe³, Shigeo Fujikawa³***¹The University of Tokyo, Japan, ²Osaka University, Japan, ³Hokkaido University, Japan*

We theoretically investigate nonlinear propagation of weakly diffracted ultrasound beams in an initially quiescent liquid containing many spherical gas bubbles distributed with a weak nonuniformity. We assume that the spatial distribution of the initial number density of bubbles is a slowly varying function of space coordinates and the amplitude of its variation is small compared with a mean number density. For simplicity, the viscosity of gas inside the bubble, heat conduction, and phase change across the bubble-liquid interface, are neglected. The system of basic equations for bubbly flows consists of the conservation equations of mass and momentum for gas and liquid in a two-fluid model, Keller equation for the bubble-wall motion, state equations for gas and liquid, and so on. Nonlinear wave equations for long range propagation of beams are derived from the basic equations based on appropriate choices of scaling relations of a set of physical parameters composed of the wavelength, frequency, propagation speed, diameter of the beam, and small wave amplitude. The scaling of parameters prescribes the magnitudes of dissipation, dispersion, and diffraction effects relative to that of the nonlinear effect in the weakly nonlinear propagation of the beams concerned. With the aid of the method of multiple scales, we can derive two-types of equations, i.e., a KZK (Khokhlov-Zabolotskaya-Kuznetsov) equation with dispersion and nonuniform effects [or a KP (Kadomtsev-Petviashvili) equation with dissipation and nonuniform effects] for a long wave in a low frequency case, and an NLS (nonlinear Schrödinger) equation with dissipation, diffraction, and nonuniform effects for an envelope of a carrier wave in a high frequency case.

3a A03.

A model for coupled bubble dynamics between thin elastic tissue layers

Todd A. Hay, Yurii A. Ilinskii, Evgenia A. Zabolotskaya, Mark F. Hamilton

Applied Research Laboratories, The University of Texas at Austin, Austin, TX 78713-8029, United States

Photographs of acoustically-excited ultrasound contrast agent microbubbles in *ex vivo* blood vessels have revealed that the bubbles translate and form jets toward the center of the vessel and that the associated vessel displacement is often asymmetric [Chen et al., J. Acoust. Soc. Am. 126, 2175 (2009)]. There is also interest in exploiting bubble-bubble interaction to aid sonoporation of an adjacent cell membrane [Sankin et al., Phys. Rev. Lett. 105, 078101 (2010)]. These observations have motivated the development of a model for a pair of coupled aspherical, translating bubbles in an incompressible liquid between parallel elastic tissue layers. The bubbles are assumed to lie along the axis perpendicular to the parallel tissue layers. Deformation of the bubble surfaces, leading to the onset of jetting, is taken into account by including spherical harmonics in the boundary conditions on the bubbles, and translation is included through the dipole mode. The effect of the tissue layers is taken into account through the potential energy of the system. Lagrange's equations yield a system of eight coupled second-order ordinary differential equations for the shapes and positions of the bubbles. Numerical integration of an expression for the liquid velocity at the tissue interfaces yields an estimate of tissue displacement. Simulations reveal behavior which is consistent with laboratory observations. For example, during inertial growth and collapse of a single bubble the amount of vessel wall distention is predicted to be less than the associated invagination, and the bubble is predicted to translate away from the nearest vessel wall while forming a jet directed away from that wall. [Work supported by NIH grant nos. DK070618 and EB011603.]

3a A04.

Nonlinear interaction among oscillating non-spherical bubbles

Eru Kurihara

Oita University, Japan

Multiphase flow is one of the most important problem not only in the field of fluid mechanics but also for industrial applications. For cavitation flow, high-speed photographs have shown that mutually interacting bubbles experience shape deformation and even form intense liquid jets. Such liquid jets are considered to be one of the mechanisms of collateral damage to tissue during the medical procedure like shock wave lithotripsy. Similarly, cavitation erosion may be induced by the liquid jet or shock wave associated with violent bubble collapse. Regardless of the importance of the problem, purely numerical simulations for cavitation flow is quite difficult because such calculations require enormous computer resources. In this study, therefore, the dynamical equations for interacting non-spherical bubbles are derived theoretically in the framework of Lagrangian formalism with multipole expansion of the bubble boundaries. Boundaries of the bubbles are expanded with spherical harmonics so that deformation and translation of the bubbles can be treated. In order to compose the Lagrangian of the system, corresponding amplitudes of the spherical harmonics are chosen as the generalized coordinate. The study takes account of the order of the spherical harmonics up to 3 (octupole mode) because octupole mode is the lowest mode oscillation contributing asymmetrical deformation of the bubble. Derived equations can represent motion of interacting non-spherical bubbles, which agree qualitatively with experimental results including onset of jetting. As well as the general n-body problem, it should be noted that chaotic behavior may be observed in the system of three or more bubbles.

3a A05.**Orbital motions of bubbles in an acoustic field****Minori Shirota, Kou Yamashita, Takao Inamura***Faculty of Science and Technology, Hirosaki University, Japan*

This experimental study aims to clarify the mechanism of orbital motion of two oscillating bubbles in an acoustic field. Trajectory of the orbital motion in a standard round-bottom flask type levitator used in a single bubble sonoluminescence experiment was observed using a high-speed video camera. Because of a good repeatability in volume oscillation of bubbles, we were also able to observe the radial motion driven at 24 kHz by stroboscopic like imaging; the cyclic bubble oscillation was appeared to slow down by capturing images at the framing rate close to the forcing frequency. The orbital motions of bubbles ranging from 0.13 to 0.18 mm were examined with different forcing amplitude and in different viscous oils. As a result, we found that pairs of bubbles revolve along an elliptic orbit around the center of mass of the orbiting two bubbles. We also found that the two bubbles perform anti-phase radial oscillation. Although this radial oscillation should result in a repulsive secondary Bjerknes force, the bubbles kept a constant separate distance of about 1 mm, which indicates the existence of centripetal primary Bjerknes force. The angular velocity of orbital revolution increases linearly with the increase in Bjerknes force. Coupled dynamics among radial pulsation, translational oscillation and orbital revolution of bubbles are discussed based on the experimental results.

Invited Paper**3a B01.****Nonlinear spectroscopy of closed delaminations and surface breaking cracks: finite element simulations of clapping and nonlinear air-coupled emission****Steven Delrue, Koen Van Den Abeele***K.U.Leuven Campus Kortrijk, Belgium*

Kissing bonds and clapping contacts inherently demand a nonlinear diagnostic method, applying a finite excitation amplitude that is able to overcome an activation threshold to open and close the contact. In order to obtain a better understanding and analysis of the macroscopic nonlinear behavior, we developed and investigated the results of a finite element model that makes use of local node splitting and implements the non-linear constitutive behavior by means of spring-damper elements with local activation thresholds at the delamination interface. Numerical experiments show that subharmonics and harmonics of the excitation frequency are generated by the clapping delamination if the excitation amplitude is large enough to overcome the local activation threshold. The results of an intensive parametric study also show that the shape, position, depth and orientation of one or multiple delaminations can be determined by studying the excited subharmonic and harmonic frequencies and the corresponding amplitude patterns. To increase the signal-to-noise ratio of the detected nonlinear contributions, sweep signals can be used in combination with the scaling subtraction method. For surface breaking cracks, the model also confirms the emission radiation patterns of harmonic energy in the surrounding air, as experimentally observed in NACE experiments (Nonlinear Air-coupled Emission).

3a B03.

Nonlinear resonant ultrasound spectroscopy (NRUS) applied to fatigue damage evaluation in a pure copper

Toshihiro Ohtani, Yutaka Ishii

Shonan Institute of Technology, Japan

In this paper, we describe a monitoring technique of fatigue damage in 99.9 % pure copper plates under a cyclic 0-to-tension loading by the nonlinear resonant ultrasound spectroscopy (NRUS), which is a resonance-based technique exploiting the significant nonlinear behavior of damaged materials. In NRUS, the resonant frequency of an object is studied as a function of the excitation level. As the excitation level increases, the elastic nonlinearity is manifest by a shift in the resonance frequency. NRUS exhibits high sensitivity to microstructural change of damaged materials. We use an electromagnetic acoustic transducer (EMAT) to monitor NRUS of bulk shear wave propagating in the thickness direction of the sample. The EMAT operates with the Lorentz-force mechanism and is the key to establish a monitoring for microstructural change during fatigue with high sensitivity. Furthermore, use of EMAT makes contactless transduction possibility. We also monitor the change of linear ultrasonic characterizations, shear-wave attenuation and velocity. NRUS exhibits much larger sensitivity to the damage accumulation than the velocity. It rapidly increases from 70 % of fatigue life to the fracture. The attenuation shows the peak at 80 % of the life. These are independence on the stress amplitude. The NRUS evolution as creep progress is related to the microstructure change, especially, dislocation mobility. This is supported by TEM observation for dislocation structure. This noncontact resonance-EMAT measurement can monitor the evolution of NRUS throughout the fatigue life and has a potential to assess the damage advance and to predict the fatigue life of metals.

3a B04.

A quantitative imaging of bonding strength at the bonded solid-solid interface obtained by nonlinear test

Jianjun Chen, De Zhang, Yiwei Mao

The Institute of Acoustics, Nanjing University, China

As well known, when a longitudinal wave propagates through an interface between solids, the contact acoustic nonlinearity (CAN) will be generated dramatically due to micro-cracks, micro-defects existing at interface and the nonlinear parameter can be used to contour the bonding state of the interface. However the contour can only show the relative state of bonding strength and can not be used to judge whether the multilayered composite materials in use is safe because the safe judgment is not by the relative state while by the absolute value of the bonding strength. For example, the difference of bonding state is small in the relative contour; it only indicates a uniform bonding state, but does not indicate whether the bonding strength is strong or weak. Therefore characterization of quantitative bonding strength at the interface is very important for judging a multilayered material in safe use. In this paper, how to get the quantitative bonding strength from the CAN parameter is studied. After the vibration amplitude of incident focusing wave at the bonded interface was calculated, the standard bonding strength with complete bonding state was established by tension test and CAN parameter is calibrated, the quantitative imaging of the bonding strength is obtained by CAN microscope in experiments. From the imaging, the positions with weak bonding strength could be easily located, which can be used to decide whether the material could be employed continuously. This abstract is submitted to the organized session "Acoustic/elastic nonlinearity in media with complex structures".

3a B05.**Evaluation of the concrete structure integrity via nonlinear ultrasonic measurements****Marta Korenska, Monika Manychova, Michal Matysik***Brno University of Technology, Faculty of Civil Engineering, Czech Republic*

The paper deals with nonlinear interaction between elastic wave and structural defects in concrete specimens. Our research has addressed three groups of specimens which differed from each other in the structure quality. After the concrete hardening had been completed the specimens were divided into three groups. The first specimen group was kept, in accordance with standard conditions, in water for the entire ripening period. The second specimen group was kept in air in laboratory environment conditions and the third specimen group was placed for twelve days of the ripening process into a dryer in which the air temperature was 60°C in order to increase the specimen load and obtain more serious structure deterioration. Non-standard concrete ageing conditions resulted in the development of micro-cracks in the specimen structure. In the first stage of the experiment we aimed at identifying the effect of non-standard conditions of the concrete mix ripening on the structure integrity. A single harmonic ultrasonic signal method was applied to the specimens and evaluating of the second and third harmonic components as a quantity of nonlinearity was reviewed. After the first measurements the specimens were undergone freeze-thaw cycles. In the second stage of the experiment our objective consisted of determining how the freeze-thaw cycle application induced degradation that depends on the input structure initial quality. Verification measurements which have been carried out in parallel with the nonlinear ultrasonic ones, give evidence of the specimen structure integrity deteriorations and confirm the correlation between the non-linear effects on the transfer characteristics with the existence of defects in the specimen internal structure.

3a C01.**Improvement of energy conversion efficiency of thermoacoustic engine by a multistage stack with multiple pore radii****Kohei Yanagimoto¹, Shin-ichi Sakamoto², Kentaro Kuroda¹, Yosuke Nakano³, Yoshiaki Watanabe¹**¹*Faculty of Life and Medical Sciences, Doshisha University, Japan,*²*Department of Electronic Systems Engineering, University of Shiga Prefecture, Japan,*³*Faculty of Science and Engineering, Doshisha University, Japan*

In the conventional thermoacoustic engine, the pore radius of stack is almost constant in the axial direction. Therefore, we aim at the improvement of energy conversion efficiency of thermoacoustic engine by proposing a new type of multistage stack with multiple pore radii. The stack is composed of several stages, each of which is a bundle of a number of narrow tubes with specified pore radii. The pore radius is determined so that its ratio to the thickness of acoustic boundary layer on the tube wall may be a suitable value for the enhancement of the thermoacoustic oscillation in the tube. Owing to the temperature gradient along the axis of the stack, however, the thickness of the acoustic boundary layer changes along the axis and hence the suitable pore radius also changes in the axial direction. We therefore introduce a multistage stack with multiple pore radii, thereby realizing a desired ratio of pore radius and boundary layer thickness everywhere in the stack. The energy conversion efficiency of the multistage stack is experimentally studied on a straight tube type thermoacoustic engine and compared with that of a conventional single-stage stack. In the experiments, in spite that a sufficiently large temperature difference from ambient temperature near low-temperature heat exchanger was not attained, we have been able to confirm a slight improvement of energy conversion efficiency. Furthermore, we used a numerical method with transmittance matrix to include the effect of multistage stack, and obtained a good agreement between the experimental and numerical results. They show the future possibilities of the stack design aiming at the higher efficiency of the thermoacoustic engine.

3a C02.

Thermoacoustics design using stems of goose down stack

Irna - Farikhah

IKIP PGRI Semarang, Indonesia

Use of CFC-contained systems has caused severe environmental hazard that has caused researchers to look for alternatives. Previous studies have shown that thermoacoustics technology is a candidate for conventional vapor compression cooling systems in particular for special uses¹. Many variables influence thermoacoustics design. One of them is the conductivity of the material of the stack. The stack material must have a low thermal conductivity and a heat capacity c_s larger than the heat capacity of the working gas, in order that the temperature of the stack plates is steady². In this research we used organic stack made of goose down. It has superior thermal insulating and a heat capacity c_s larger than the heat capacity of the working gas³. It means that they have the lowest thermal conductivity and the temperature of the stack plates is steady. In this research we just used stems of goose down because it is easier for the design of the stack. The system uses no refrigerant or compressor, and the only mechanical moving part is the loudspeaker connected to a signal generator that produces the acoustics. The working fluid is air and the material of the resonator is PVC. A series of tests in the laboratory found that there is a thermoacoustics effect produced by the thermoacoustics design using stems of goose down stack. **Keyword :** thermoacoustics design, stems of goose down stack

References:

- 1) Mohd Ghazali Normah, Abd Aziz Azhar, Rajoo Sritar, Che Sidek Nor Aswadi, Environmentally friendly refrigeration with thermoacoustics, Research Report, Faculty of Mechanical Engineering, University Technology Malaysia, 2006
- 2) Tijani MEH, Zeegers JCH, deWaele ATAM, Design of Thermoacoustics refrigerator. Cryogenic 2002
- 3) Gao Jing, Yu Weidong and Pan Ning, Structures and Properties of the Goose Down as a Material for Thermal Insulation, Textile Research Journal 2007; 77; 617

3a C03.

Amplitude dependence of thermoacoustic properties of stacked wire meshes

Atsushi Obayashi, Tetsushi Biwa

Tohoku University, Japan

We studied two types of regenerators experimentally through measurements of acoustic powers entering and leaving the regenerator. The type I regenerator has uniform flow channels and is made of ceramic honeycomb catalyst or stacked etching meshes. The type II has complicated flow channels because it is comprised of stacked wire meshes. The regenerator was installed in a tube containing air at atmospheric pressure. The acoustic power was determined from pressure measurements by using a two-sensor method, when acoustic drivers forced the gas oscillation at 44 Hz. From experiments without the axial temperature difference along the regenerator, we determined the resistance per unit length for the regenerator. It was found to be independent of volumetric acoustic velocity for the type I, as expected from linear theory. On the other hand, the resistance increased in proportion to the velocity for the type II. An empirical equation of the resistance was obtained for the type II by using two dimensionless parameters of acoustic Reynolds number and $\omega\tau_v$, where ω is the angular frequency and τ_v is the viscous relaxation time of the gas. In the presence of a positive temperature difference, acoustic power production was measured as the difference between the acoustic powers at hot and cold ends of the regenerator. The contribution of the temperature gradient was extracted by taking into account the acoustic power damping by the resistance. The acoustic power production due to the temperature gradient was proportional to the square of velocity amplitude in the type I. On the other hand, it was expressed by the sum of cubic and square terms in the type II. Appearance of a cubic term is not expected within a framework of the thermoacoustic theory, whereas the result obtained for the type I gave support to the thermoacoustic theory.

3a C04.**Investigation of the acoustic field in a standing wave thermoacoustic refrigerator using time-resolved particle image velocimetry****Philippe Blanc-Benon¹, Gaëlle Poignand², Emmanuel Jondeau¹**¹LMFA UMR CNRS 5509, France, ²LAUM UMR CNRS 6613, France

In thermoacoustic devices, the full understanding of the heat transfer between the stack and the heat exchangers is a key issue to improve the global efficiency of these devices. Thermoacoustic refrigerators are systems which convert acoustic energy into thermal energy. More precisely, a standing-wave thermoacoustic refrigerator consists of a stack of plates placed in an acoustic resonator. The thermoacoustic effect takes place in the thermal and viscous boundary layers along each plate of the stack. It results in a thermoacoustic heat transport along the plates and in a temperature difference between the two stack ends. Two heat exchangers are located at each stack extremity. They play an important role since they allow the heat transfer from the stack to the surroundings. The heat transfer between the heat exchangers and the stack of plates is a complex process because of the oscillating flow in the device. This heat transfer, which is directly related to the efficiency of the systems, is still not completely understood. Moreover, to achieve significant efficiency a high pressure level is required. For this high pressure level, non linearities can occur at the extremities of the stack. They result in thermal wave harmonics and in vortex shedding at the extremity of the stack, which can disturb the heat transfer and thus reduce the global efficiency of the device. For instance, non periodicity of the flow behind the stack has been observed, at high pressure level, numerically and experimentally. This unsteady behaviour, is accompanied by the appearance of a large-amplitude wavy motion which have an effect on the cooling load. Recently, classical PIV technique has been used to investigate the vortex phenomenon behind a single stack. The influence of some dimensionless parameters on the vortex wake patterns have been studied. However, in these previous studies, velocity fields have been obtained without heat exchanger as it will be in a realistic device. In addition, instantaneous velocity fields are averaged to obtain the velocity field which can affect the estimation of the heat transfer, if the cycle-to-cycle variations of the flow is important.

3a C05.**High-amplitude acoustic oscillations externally induced in a thermoacoustic engine****Hideki Seki, Masataka Sakamoto, Yuki Ueda***Tokyo University of A&T, Japan*

The acoustic intensity is the rate of the energy transmission due to an acoustical gas oscillation through a unit area and increases with the square of the increasing pressure amplitude. This provides motivation to design a thermoacoustic engine operating at higher pressure amplitude. On the other hand, the increasing of pressure amplitude causes the problems due to the nonlinearity of acoustic wave. One of the most important nonlinearities would be the generation of shock wave. However, very few studies have investigated the generation of the shock wave in a thermoacoustic engine. In this work, we constructed a standing wave thermoacoustic engine having the piston that allowed us to input an external oscillation. The constructed thermoacoustic engine was composed of a 4 m length tube and a stack of flat plates. One end of the tube was closed and the other was attached to the piston via bellows. Using the piston, we controlled the pressure oscillation induced in the engine and determined the critical pressure amplitude at which the shock wave was generated as a function of the temperature ratio across the stack. It was found that the critical pressure amplitude was about 10% of mean pressure when the temperature ratio was unity, and however, it decreased with the increasing in the temperature ratio.

Invited Lecture

3a L4.

Understanding of thermoacoustic phenomena and their applications

Tetsushi Biwa

Tohoku University, Japan

We will present the physical mechanism of thermoacoustic phenomena from experimental point of view, and introduce some applications of them as acoustic heat engines. Problem of acoustic wave propagation in a tube gives a starting point for the study of thermoacoustic phenomena. We show measurements of propagation constant in a tube for a wide range of $\omega\tau$, where ω is the angular frequency of acoustic waves, and τ is a thermal relaxation time for the gas to equilibrate with tube walls. Comparison with theoretical solution for wide tube approximation ($\omega\tau \gg 1$) and that for narrow tube approximation ($\omega\tau \ll 1$) show the presence of intermediate $\omega\tau$ region where thermal interaction between the gas and the solid walls is sufficiently strong whereas the viscous interaction is moderate. As Ceperley predicted theoretically, when an acoustic traveling wave goes through differentially heated porous media with such $\omega\tau$ values, acoustic power amplification becomes possible because of a thermodynamic cycle that the gas executes. Experiments of the acoustic power at the ends of a stack of plates with $0.1 < \omega\tau < 20$ is shown to verify his proposal. The concept of acoustic Stirling heat engine has promoted the recent developments of various energy conversion devices with extremely simple structures. For example, the acoustic Stirling heat engine has achieved a thermal efficiency comparable to conventional heat engine technologies. Also, thermoacoustics has made it possible to make a pistonless cooler in which an acoustic wave generated from heat pumps heat from the cold end. Operation of these devices will be shown based on energy flow diagrams.

3p A06.**Studying acoustic and shock wave effects accompanying the optical breakdown of water and some alcohols by 1,064 nm nanosecond radiations****Grigory Toker***Research Prof., Chemical Dept., Technion, Israel*

Specific effects accompanied the optical breakdown in water and alcohols (methanol, ethanol, butanol and heptanol) initiated by 1,064 nm focused laser radiation were investigated by applying high spatial resolution nanosecond optical diagnostic techniques: dark field Schlieren, shadow and Mach-Zehnder interferometry. As a probing beam was used collimated 532nm radiation of second Nd:YAG laser synchronized with the first laser. The testing the laser breakdown region was realized in 900 geometry setup. The dynamics of a laser spark column was studied in wide range of time delays of probing beam relative to breakdown pulse: from shortest (few ns) as well as for relatively long time delays ~ 1 μ s. The shortest time delays are characterized by generation of powerful micro spherical shock waves over inclusions which getting a strong acoustic wave after 100-200 ns. Structural characteristics of a laser spark column in the liquids were visualized by imaging the breakdown region on the sensitive area of a CMOS camera or a photo film by an optical collimator. The discrete structure of a plasma column leads to the effect of interference of the strong acoustic waves. The mechanism of optical breakdown is discussed. Dynamics of micro-spherical shock waves and bubbles over inclusions was studied. As a result of laser radiation absorption the warming liquids in the focal volume was observed and different character of thermo-relaxation is visualized in water and alcohols. Self-focusing and canalization of the heating laser beam was observed in the alcohols. At the same time water behaviors itself as a linear liquid.

3p A07.**Peak gas density during shock driven cavity collapse****Nicholas Hawker, Yiannis Ventikos***Dept of Engineering Science, University of Oxford, United Kingdom*

This paper examines the peak gas densities achieved during collapse of a gas cavity in a liquid medium by a shockwave. Study of this phenomenon has relevance to shockwave lithotripsy, sensitization of explosives and cavitation damage. It is also of interest in a more fundamental sense, due to the complexity of the fluid dynamic mechanisms and the level of energy focusing that such a collapse demonstrates. We use the high resolution front tracking code *FrontTier* to numerically explore the collapse process. *FrontTier* uses an overlaid lower dimensional Lagrangian grid to represent discontinuities in flow on top of a uniform Cartesian grid for solving the basic conservation equations. The Lagrangian grid-front is advanced each timestep based on physical rules and yields excellent resolution of the gas-liquid contact, completely free from numerical smearing.

Recent work by the authors began with a detailed analysis and classification of the dynamics of shock driven cavity collapse. It continued with a parametric study varying the incident shock strength from 100MPa to 100GPa. Within this we uncovered a novel and counter-intuitive result; as the shock strength is increased (over the range indicated) the peak gas density monotonically decreases. A feature of shock driven cavity collapse is the formation of a high speed transverse jet which impacts the leeward cavity wall; it is at this point of impact that the highest gas densities occur. The unusual trend can be explained by observing the bow shock that forms in front of this jet. Before impact the bow shock reflects from the leeward wall. This reflected bow shock recompresses the gas and then interacts with the fast approaching jet to form a re-reflected bow shock. A weaker shock gives a slower jet; hence there is a greater amount of time available for these reflections and as many as four can be seen. For higher pressure incident shocks the jet moves faster and even a single reflection can become difficult to resolve. The nature of shock compression means that, whilst the pressures and temperatures are higher, the density is less for a stronger shock. This paper presents these results and then concludes by investigating the effect of different gas properties on these dynamics. We conduct a dimensional analysis to interpret our results and then utilize this understanding to speculate a comparison between gas and vapor cavities.

Invited Paper

3p A08.

News from bubble dynamics: high static pressures, shock waves and interior dynamics

Werner Lauterborn, Thomas Kurz, Philipp Koch, Mohsen Alizadeh, Hendrik Söhnholz, Daniel Schanz

Drittes Physikalisches Institut, Universität Göttingen, Germany

Three topics from the vast area of bubble dynamics are addressed: (i) the influence of high static pressure on the oscillation of a spherical bubble in a sound field (calculations), (ii) the response of a bubble to a shock wave (experiments), and (iii) the interior dynamics as seen by molecular dynamics calculations. The influence of high static pressures on bubble dynamics is explored in the context of a single spherical noble gas bubble in a sound field for the further parameters bubble radius at rest, sound field frequency, sound pressure amplitude and gas concentration. The notion of a bubble habitat is used for positionally and spherically stable, not dissolving bubbles in some two-dimensional space of parameters (mainly bubble radius at rest and sound pressure amplitude) for presenting the results. An elevated static pressure substantially enlarges the bubble habitat and thus the range, where bubbles can be stably trapped. Shock wave - bubble interaction is investigated in the context of laser induced bubbles collapsing in the neighborhood of a solid, plane boundary. Jet development as influenced by both the boundary and by a shock wave propagating parallel to the boundary is studied by high speed photography. The jet direction is dependent on bubble distance and shock wave strength, becoming more oblique with shock wave strength. The interior of a bubble is explored by molecular dynamics for testing homogeneity assumptions for physical quantities during bubble oscillation. Temperature and density are calculated for different species in the bubble, as there are noble gases, water vapor and its decomposition products.

Invited Paper

3p B06.

Nonlinear dynamical processes in media with relaxation

Lev A. Ostrovsky^{1,2}, Andrey V. Lebedev²

¹Zel Technologies and University of Colorado, United States, ²Institute of Applied Physics, Russia

By present, a rich experimental material has been collected demonstrating that in media with complex structure such as rock and non-consolidated soils, the elastic response is characterized by a relaxation (slow time), so that after the action of a strong, short-time force, the medium elastic properties need many minutes, or even some hours, to return to their initial state. Also some physical models explaining such a phenomenon (based on water content, thermal, kinetic, and diffusion effects) have been suggested. However, there is apparently almost no works concerning modeling the effects of medium relaxation on wave propagation and oscillations. This presentation is intended to partially fill this gap. Among the problems discussed are:

1. A brief overview of experiments and models.
2. Analysis of wave propagation in several models with slow time, including those with hysteresis.
3. Field experiments on propagation of Rayleigh waves in a non-consolidated soil during the restoration of the material parameters after a short-time impact.

In conclusion, some unsolved issues and relevant future work are outlined.

3p B08.**Localization of a nonlinear source in the bulk of a solid****Pierre-Yves Le Bas¹, Timothy J Ulrich¹, Paul A Johnson¹, Brian E Anderson²**¹*Los Alamos National Laboratory, United States, ²Brigham Young University, United States*

Time Reversal (TR) has the potential to become a powerful tool in non-destructive evaluation. Coupled with nonlinear properties of cracks in a group of techniques known as Time Reverse Nonlinear Elastic Wave Spectroscopy (TRNEWS), it provides the means to detect and image mechanical damage in complex solids. Although this has been quite well studied for surface cracks, buried features have been only considered in modeling situation. In this prototype experimental study we show that we can excite a buried nonlinear feature applying TR. The feature scatters energy that is detected on the sample perimeter. The time signals are filtered about the nonlinear-generated components and are broadcast back, focusing on their source, the buried nonlinear feature. The current challenge is introducing sufficient energy in order to excite the buried feature and produce nonlinear scattering that can be detected on the edges of the sample. This was achieved using a 30 channel system. Two features were localized: a part of the interface between two blocks submitted to a high amplitude signal, and a defect on the same interface (a cured drop of glue creating hard contact between the two solids, thus distorting waves travelling at this point and generating nonlinear signals). Results are visualized using the energy flux quantity to find the location where the wave field coalesces.

3p C06.**Account of heat convection by Rayleigh streaming in the description of wave amplitude growth and stabilization in a standing wave thermoacoustic prime-mover****Guillaume Penelet¹, Matthieu Guedra¹, Vitalyi Gusev²**¹*Laboratoire d'Acoustique de l'Universite du Maine, France, ²Laboratoire de Physique de l'Etat Condense, France*

This study focuses on the transient regime of wave amplitude growth and stabilization occurring into a standing wave thermoacoustic engine. Experiments are performed on a standing wave thermoacoustic oscillator, which show that the transient regime leading to steady state sound exhibits complicated dynamics, like the systematic overshoot of wave amplitude before its final stabilization, and the spontaneous and periodic switch on/off of the thermoacoustic instability at constant heat power supply. A simplified model is presented which describes wave amplitude growth from the coupled equations describing thermoacoustic amplification and unsteady heat transfer. In this model, the assumption of a one-dimensional temperature profile is retained and the equations describing heat transfer through the thermoacoustic core are coupled to that describing wave amplitude growth. These equations include the simplified description of the processes saturating wave amplitude growth (minor losses, additional losses due to nonlinear propagation, heat pumping by acoustic waves), among which the heat convection by Rayleigh streaming is included in a very simplified way. It is notably shown that accounting for the effect of acoustic streaming allows to reproduce qualitatively the overshoot process.

3p C07.

Numerical analysis of thermoacoustic spontaneous oscillations in a 2D rectangular and an axisymmetric closed tube

Masahiro Ishigaki¹, Koichiro Shirai², Shizuko Adachi³, Katsuya Ishii^{2,4}

¹Japan Atomic Energy Agency, Japan,

²Department of Computational Science and Engineering, Graduate School of Engineering, Nagoya University, Japan,

³School of Business and Commerce, Tokyo International University, Japan,

⁴Information Technology Center, Nagoya University, Japan

For understanding fundamental dynamics of thermoacoustic oscillations, we analyze the stability of thermoacoustic spontaneous oscillations of helium gas (Taconis oscillation) using the numerical simulation. Taconis oscillations are observed in a helium-filled tube with a liquid helium reservoir. The flow fields in a 2D rectangular closed tube and an axisymmetric cylindrical closed tube are simulated by solving the 2D or axisymmetric compressible Navier-Stokes equations, respectively. Both ends of the tube are hot, and the center part is cold. In order to obtain various thicknesses of the boundary layers in the tube, we use various values of the initial pressure of the helium gas. Taconis oscillations are simulated in a 2D rectangular tube with the length ratio of the hot part and cold part $\xi = 1$ for various temperature ratios θ of the hot part and the cold part. The steady oscillations of the fundamental mode of a standing wave are observed when θ exceeds a critical value. The hysteresis phenomena are observed when the boundary layers are thin. However, the hysteresis phenomenon is not observed when the boundary layer is thick. The critical temperature ratios for each initial pressure almost agree with those by theoretical analysis by Rott. On the other hand, we analyze the Taconis oscillations in an axisymmetric tube with $\xi = 1$ and 0.3. In both cases of $\xi = 1.0$ and 0.3, steady oscillations of the fundamental mode of a standing wave are obtained, and the critical temperature ratios agree with the theoretical prediction by Rott. In the case of $\xi = 0.3$ the second mode of the oscillation and an acoustic wave with discontinuity are observed as well as the fundamental mode. Most of the temperature ratios for these oscillation states (the fundamental mode, the second mode and the oscillations with a shock wave) are included in the unstable region of the stability curve by plotting the data points against the ratio of the tube radius to the thickness of the viscous boundary layers at the cold part. We analyze the Taconis oscillations in a 2D rectangular and an axisymmetric closed tube numerically, and show the stabilities of each type of the oscillations.

3p C08.

Numerical simulations of thermoacoustic oscillations in a looped tube

Dai Shimizu, Kohei Nishikawa, Nobumasa Sugimoto

Department of Mechanical Science, Graduate School of Engineering Science, University of Osaka, Japan

This paper attempts to simulate, by using a boundary-layer theory, emergence of thermoacoustic oscillations in an air-filled, looped tube with a so-called stack inserted and subjected to a temperature gradient. Although the theory can describe the emergence of self-excited Taconis oscillations in a helium-filled, quarter-wavelength tube, it is open whether or not the theory is applicable to the case of the looped tube because the stack consists of many narrow tubes. According to the marginal conditions derived by Ueda & Kato (*J. Acoust. Soc. Am.*, 124(2), pp.851-858 (2008)) for linear instability, the marginal curves for the temperature ratio versus the tube radius in the stack are shown to consist of right and left branches with respect to the minimum temperature ratio. As far as the right branch is concerned, there must be a situation to which the boundary-layer theory is still applicable. With expectation of this, the theory is applied not only to the gas in the wide tube outside of the stack but also to the one in the narrow tube in the stack. In doing this, discontinuities in temperature gradient, the tube's cross-sectional area and wetted perimeter at its both ends are taken into account. Assuming geometrical configuration studied by Ueda & Kato, an initial-value problem is solved numerically by imposing a disturbance in the axial velocity impulsively along the loop with no pressure disturbance. From the marginal curves obtained, it is found that the temperature ratios for the marginal oscillations are slightly lower than the experimental results by Ueda & Kato. It is also seen that the temperature distribution along the thermal buffer tube affects the marginal conditions. By pursuing evolution of physical variables, it is unveiled that traveling waves tend to emerge in the course of time.

Invited Lecture**3p L5.****Nonlinear acoustic/seismic waves in earthquake processes****Paul A. Johnson***Geophysics Group, Los Alamos National Laboratory, Los Alamos, New Mexico 87544, USA*

Nonlinear dynamics due to seismic sources is common in Earth. Observations range from seismic strong ground motion (the most damaging aspect of earthquakes), intense near-source effects, and distant nonlinear effects that have important consequences. The distant effects include dynamic earthquake triggering—one of the most fascinating topics in seismology today—which appears to be elastically nonlinearly driven. Dynamic earthquake triggering is the phenomenon whereby seismic waves generated from one earthquake trigger slip events on a nearby or distant fault. Dynamic triggering may take place at distances thousands of kilometers from the triggering earthquake, and includes triggering of the entire spectrum of slip behaviors currently identified. These include triggered earthquakes and a noise-like, long-duration signal termed tremor, as well as triggered slow, silent-slip during which no seismic energy is radiated. It appears that the elastic nonlinear dynamics of the fault gouge—the granular material located between the fault blocks—is key to the triggering phenomenon.

In this presentation I will provide an overview of different nonlinear phenomena in Earth for non-geoscientists, with a primary focus on dynamic wave triggering. The triggering portion will include Earth observations, laboratory experiments and numerical modeling.

May 23 (Wed)

Invited Paper**3p A10.****Observing multi-bubble sonoluminescence in phosphoric acid**

Kai Yang¹, Maimaititusong Maimaitiming^{1,2}, Cui Ying Zhang^{1,3}, Qi Rong Zhu¹, Yu An¹

¹*Department of Physics, Tsinghua University, China,* ²*Hetian Institute of Education, China,*

³*College of Physics and Electronic Information, Hulunbeir University, China*

We observe multi-bubble sonoluminescence at an intense acoustic standing wave field in phosphoric acid. Rotating the liquid column in a cylindrical flask, we find the rotating velocity is inversely proportional to the distance from the central axis. According to Bernoulli's principle, there forms pressure gradient and Bjerknes force assembles those widely spread cavitation air bubbles to the vicinity of the axis. Then, there appears a twister tail type luminescent region at the centre of flask from where a continuum of visible and near-infrared spectrum is measured. Using a photomultiplier tube, we observe that the flash is not exactly periodic, and the times of flash from those bubbles are some different. These phenomena may be interpreted qualitatively by numerically solving the cavitation dynamic equation together with the bubble motion equation. In fact, each vibrating bubble produces radiation pressure onto the other bubbles which is the bubble-bubble interaction. This interaction may be described by a nonlinear sound wave equation in bubbly liquid, which is the cavitation dynamic equation. Our calculation reveals how the bubble-bubble interaction affects the sound wave intensity and bubble motion in cavitation cloud. In addition, we also observe phenomena which are uninterpretable in the present paper: solving sodium phosphate into phosphoric acid, we find the multi-bubble sonoluminescence dramatically weakens; in a few millimeters thin layer of phosphoric acid, we observe multi-bubble sonoluminescence, too, and find the luminescent intensity sensitively depends on the layer thickness of the liquid.

3p A12.**Two components of Na atom emission from collapsing bubbles in surfactant solutions**

Yuichi Hayashi, Pak-Kon Choi

Meiji University, Japan

Sonoluminescence from alkali-metal atoms has been studied intensively in recent years because its emission mechanism is still under debate. In a surfactant solution containing Na⁺ ion, such as sodium dodecyle sulfate (SDS), the intensity of Na emission is known to be enhanced because of the high local concentration of Na⁺ ions around bubble surfaces which are adsorbed by surfactant molecules. We observed multi-bubble sonoluminescence spectra from SDS solutions saturated with Ar gas at the frequencies of 148 kHz and 1 MHz. The results showed that the Na emission at 148 kHz consists of broadened lines which are shifted from original D lines and unshifted narrow lines. Sonication-time dependence of the Na emission was also measured with every 3 minutes for the total sonication time of 30 minutes. The unshifted narrow line gradually disappeared with sonication time, and the only shifted broadened line remained after 12 minutes. The spectra obtained at 1 MHz showed only unshifted narrow lines and no shifted broad lines. The unshifted narrow lines are easily affected by decomposition gases derived from SDS molecules inside bubbles. Previous study of saturation-gas dependence of Na emission spectra has suggested that the shifted broadened lines come from the gas phase inside bubbles. The present results suggest that the narrow lines also originate from gas phase although the emitting environment of two components will be different.

3p B10.**Dilatance and acoustic non linearity of dry and saturated marine sand****Nora A. Vilchinska***LAA-Latvian Acoustics Association, Latvia*

In practice the mechanism of volume change-dilatation is the reason of the sharp nonlinear response of pure quartz sea sand (granulated material) on dynamic and static loading. It is shown in jumping change of velocity of propagation, in short-term sands liquefaction. Dilatance in laboratory and in -situ were observed. Experiments were carried out on the dense water-saturated quartz marine sand on Riga-er bay beaches, Latvia, in situ and in laboratory on samples of the same sand. Were studied the of surface waves propagation velocity from impact (the weight of 16 kg, falling from 5cm till 200cm) and from micro explosion. Loading regimes from quasi static till strong motions are realized. It is shown, that propagation velocity and resonant frequencies of marine sands depend from energy in shock. The low velocity zone is the dilatance zone. The same is observed at laboratory experiments at the tree axial test device with sounding: falling compression wave velocity caused by dilatance. Experiments on vibro table of water-saturated sand confirm existence of a threshold of accelerations, causing dilatance. Is measured dilatance propagation velocity in-situ. The role of dilatance in formation short-term liquefaction in water-saturated marine soils around the objects on bottom is discussed. Dilatance occurrence in sandy marine soils is accompanied by signals of acoustic emission.

3p B11.**Comparative study of two wideband nonlinear methods applied to an experimental model of prostheses osseointegration****Jacques Riviere¹, Sylvain Haupert¹, Pascal Laugier¹, Paul Johnson²**¹*UPMC Univ Paris 6 & CNRS, Laboratoire d'Imagerie Paramétrique, France,*²*EES-17, Los Alamos National Laboratory, United States*

This work is part of the long-term perspective to implement in vivo some new non-invasive methods to monitor the bone prostheses sealing or osseointegration (dental implants, hip prostheses). Although the most widely used clinically, X-ray radiography suffers from low sensitivity, limiting for instance its ability to detect early loosening of a prosthesis. The potential of methods developed over the past twenty years and based on elasticity measurements has been shown in vitro, but their in vivo effectiveness is still questionable. In this study, we compare two nonlinear wideband methods, suited to the highly dissipative conditions. The first one is the so-called scaling subtractive method, and the second one is based on the analysis of intercorrelation functions. Associated with an instrumentation close from an in vivo case, an experimental model is studied, comprised of an interface between a dental implant and either a mock cortical bone or a bovine bone. This approach allows the extraction of the most promising nonlinear parameters for this application. Thus, we show that one nonlinear parameter extracted from the analysis of intercorrelation functions has a higher sensitivity than any other one. Also, its sensitivity is compared to that of a commercial parameter based on linear elasticity. Results show that this work will have to be carried on in the future by complementary experiments, including manifold types of prostheses (material, geometry, surface roughness) and bone quality, to compare in a more detailed and absolute manner the sensitivity of both approaches. In addition, we propose some new perspectives to increase the sensitivity of the nonlinear method.

3p B12.**Imaging of partial plastic deformation in thin steel plate by immersion nonlinear ultrasonic resonance****Koichiro Kawashima¹, Ryusuke Imanishi¹, Fumio Fujita², Takumi Aida²**¹Nonlinear Ultrasonic Lab. Ltd., Japan, ²Insight k.k., Japan

Classic ultrasonic materials evaluation is based on sound velocity and/or attenuation measurement. However they are not sensitive to detect the changes of microstructures such as dislocation density, microvoids and microcracks, which appear in the early stage of material degradation. On the contrary, higher harmonic amplitudes show good correlation with densities of dislocations and precipitations and microcracks. However, the higher harmonic imaging of such material degradation has not been reported. The present paper describes a novel nonlinear ultrasonic imaging technique using immersion local resonance and the application to partial plastic deformation in a perforated steel plate and a plastic zone ahead of a low cycle fatigue crack in a plate of 7075 aluminum alloy. By using a focused immersion transducer, local resonance in thickness is excited in a thin metal plate and higher harmonics are extracted from received waves by high pass filters. The higher harmonic amplitude and time delay to the peak amplitude are mapped to the scanned area. The technique is applied for imaging partial plastic deformation in a SUS 304 strip with a hole and a 7075 aluminum alloy plate subjected to low cycle fatigue. The higher harmonic amplitude image of the plastic deformation well corresponds to micro Vickers hardness number and electron backscatter diffraction images. The delay time image clearly delineated the plastic zone ahead of a low cycle fatigue crack. This imaging technique could be applied for nondestructive evaluation of material properties and degradation such as densities of dislocation, inclusions, microvoids, and microcracks in metal and those of reinforced particles and short fibers in composites.

3p C10.**Asymptotic analysis of thermoacoustic effects near the critical point****Pierre Carles^{1,2}**¹Université Pierre et Marie Curie (Paris 06), France, ²Case Western Reserve University, Cleveland, Ohio, United States

This work examines the rapid thermal relaxation of a fixed-volume cell filled with a fluid near its liquid-vapor critical point. On the acoustic time-scale, a local heat flux (emitted from a boundary or from an immersed heating device) creates a very thin thermal boundary layer, which expands strongly due to the fluid's enormous compressibility. As a result, a set of thermoacoustic waves propagate in the bulk fluid, slowly building up pressure and increasing the average temperature. On the long term, this process leads to the now well-known Piston Effect, speeding up temperature relaxation near the liquid-vapor critical point. On the acoustic time-scale, it demonstrates an extreme case of "thermal noise", where a local heat input inside a compressible fluid leads to the generation of strong (and sometimes non linear) thermoacoustic waves.

Although this near-critical thermoacoustic phenomenon had been the object of earlier theoretical works (*Zappoli and Carlès, Eur. J. Mech./B Fluids 14, 1 (1995)*), it was not experimentally observed until the recent work of Miura et al. in Japan (*Miura et al., Phys. Rev. E 74, 010101(R) (2006)*). This first experiment triggered a renewed interest in a more detailed modeling of the problem, both theoretically (*Carlès, Phys. Fluids 18, 126102 (2006)*, *Onuki, Phys. Rev. E 76, 061126 (2007)*) and numerically (*Zhang and Shen, Phys. Rev. 79, 060103 (2009)*).

In this work, we develop our initial 2006 asymptotic model in order to explore new case studies, like resonance effects and active wave cancellation. We also perform direct comparisons with recent numerical results which, added to the earlier experimental comparisons, confirm that asymptotic models such as ours can be a powerful tool for analyzing near-critical thermoacoustic phenomena.

3p C11.**Nonlinearity analysis of model-scale jet noise****Kent L. Gee¹, Anthony A. Atchley², Lauren E. Falco², Micah R. Shepherd³**¹*Dept. of Physics and Astronomy, Brigham Young University, United States,*²*Graduate Program in Acoustics, The Pennsylvania State University, United States,*³*Applied Research Laboratory, The Pennsylvania State University, United States*

In the analysis of high-amplitude jet noise for nonlinear acoustic propagation, limitations in measurement bandwidth and propagation range can create difficulties in identifying nonlinear propagation effects via power spectral comparisons. This can be of particular importance in anechoic, model-scale jet noise measurements, where many frequencies of interest are above the audio range and maximum propagation range is limited by chamber size. Hence, the ability to extract evidence of nonlinearity directly from time waveform analysis can be important. This paper describes the use of a spectrally-based "nonlinearity indicator" to complement ordinary spectral analysis of jet noise propagation data. This indicator stems directly from ensemble averaging the generalized Burgers equation and involves the cross spectrum between the temporal acoustic pressure and the square of the acoustic pressure. This spectral quantity is applied to unheated model-scale jet noise from subsonic and supersonic nozzles. The results demonstrate how the indicator can be used to interpret the evolution of power spectra in the transition from the geometric near to far field. Geometric near-field and nonlinear effects can be distinguished from one another, thus lending additional physical insight into the propagation.

3p C12.**Numerical study of a silencer****Mikael A Langthjem¹, Masami Nakano²**¹*Yamagata University, Japan,* ²*Tohoku University, Japan*

The present study is concerned with the sound generated by the flow through an axisymmetric duct, consisting of an expansion chamber followed by a tailpipe. The system can be viewed as a model of a simple automotive silencer. The aim of the silencer is to attenuate pulsating combustion noise; but in certain parameter ranges the silencer may act as a sound generator as well. Self-sustained fluid oscillations may exist in the expansion chamber due to the impingement of the jet shear layer onto the cavity end wall. (This kind of mechanism is utilized in the common teapot whistle.) If the cavity 'roof' is removed the phenomenon is known as the hole-tone feedback cycle. In case of the silencer configuration considered here, the self-sustained flow oscillations may interact with the acoustic modes of the cavity and the tailpipe. The aim of the study is to acquire a good understanding of how such interactions can occur. At this time the analysis is limited to axisymmetric modes only. The theory is formulated in terms of cylindrical polar coordinates. The background flow is simulated via a discrete vortex method which represents the unstable shear layer as a 'necklace' of axisymmetric vortex rings. The aeroacoustic source modeling is based on Howe's theory of vortex sound for low Mach number flows. The scattering of sound due the expansion chamber and the tailpipe is included via a time-domain boundary element model. The nonlinear flow-acoustic interaction is accounted for by evaluating the acoustic velocity field (from the computed pressure field) and imposing it to the free vortex rings, as a feedback. In this way the flow oscillations are modulated and may 'lock-in' to the resonance frequencies of the cavity and the tail pipe.

4a A01.**Tissue lesion created by HIFU in continuous scanning mode****Dong Zhang, TingBo Fan***Institute of Acoustics, Nanjing Univ, China, China*

The lesion formation were numerically and experimentally investigated by the continuous scanning mode. Simulations were presented based on the combination of Khokhlov-Zabolotskaya-Kuznetov (KZK) equation and bio-heat equation. Measurements performed on porcine liver tissues using a 1.12 MHz single-element focused transducer at various acoustic powers, confirmed the predicted results. Controlling of the peak temperature and lesion by the scanning speed may be exploited for improvement of efficiency in HIFU therapy. This work was supported by the National Basic Research Program 973 (Grant No. 2011CB707900) from Ministry of Science and Technology, China, National Natural Science Foundation of China (10974093 and 11011130201), and the Fundamental Research Funds for the Central Universities (Grant Nos. 1103020402 and 1112020401).

4a A02.**Real-time sonoporation through HeLa cells****Anthony Delalande¹, Spiros Kotopoulos¹, Chantal Pichon², Michiel Postema¹***¹University of Bergen, Norway, ²University of Orléans, France*

The purpose of this study was to investigate the physical mechanisms of sonoporation, to understand and ameliorate ultrasound-assisted drug and gene delivery. Sonoporation is the transient permeabilisation of a cell membrane with help of ultrasound and/or an ultrasound contrast agent, allowing for the trans-membrane delivery and cellular uptake of macromolecules between 10 kDa and 3 MDa. We studied the behaviour of ultrasound contrast agent microbubbles near cancer cells at low acoustic amplitudes. After administering an ultrasound contrast agent, HeLa cells were subjected to 6.6-MHz ultrasound with a mechanical index of 0.2 and observed with a high-speed camera. Microbubbles were seen to enter cells and rapidly dissolve. The quick dissolution after entering suggests that the microbubbles lose (part of) their shell whilst entering. We have demonstrated that lipid-shelled microbubbles can be forced to enter cells at a low mechanical index. Hence, if a therapeutic load is added to the bubble, ultrasound-guided delivery could be facilitated at diagnostic settings. However, these results may have implications for the safety regulations on the use of ultrasound contrast agents for diagnostic imaging.

4a A03.

Sonoluminescence, sonochemistry and bubble dynamics of single bubble cavitation

Shin-ichi Hatanaka

Department of Engineering Science, University of Electro-Communications, Japan

The amount of hydroxyl radicals produced from a single cavitation bubble was quantified by terephthalate dosimetry at various frequencies and pressure amplitudes, while the dynamics of the single bubble was observed by stroboscopic and light-scattering methods. Also, sonoluminescence (SL), sonochemiluminescence (SCL) of luminol, and sodium atom emission (Na^*) in the cavitation field were observed. The amount of hydroxyl radicals per cycle as well as the intensity of SL was proportional to pressure amplitude at every frequency performed, and it decreased with increasing frequency. When the single bubble was dancing with a decrease in pressure amplitude, however, the amount of hydroxyl radicals was greater than that for the stable bubble at the higher pressure amplitude and did not significantly decrease with frequency. Furthermore, SCL and Na^* were detected only under unstable bubble conditions. These results imply that the instability of bubbles significantly enhances sonochemical efficiency for non-volatile substances in liquid phase.

Invited Paper

4a A04.

Generation and aggregation of BaTiO₃ nanoparticles under ultrasound

Kyuichi Yasui, Toru Tuziuti, Kazumi Kato

National Institute of Advanced Industrial Science and Technology (AIST), Japan

According to Gedanken [Ultrason.Sonochem. 11, 47 (2004)], nanomaterials were obtained in almost all the sonochemical reactions leading to inorganic products. However, there has been no numerical study on sonochemical production of nanoparticles. Furthermore, the detailed mechanism of sonochemical production of nanoparticles is still unclear. In the present study, numerical simulations of sonochemical production of nanoparticles are performed for the first time under the condition of the experiment by Dang et al. [Jpn.J.Appl.Phys. 48, 09KC02 (2009)]. In the experiment of Dang et al., an aqueous solution of BaCl₂ and TiCl₄ with the same molar concentration was irradiated by 20 kHz ultrasound. After 20 min. irradiation at 80 °C, BaTiO₃ nanoparticles were produced. The mean diameter of the particles was 150 nm for the initial BaCl₂ concentration of 0.2 mol/L. The mean diameter is larger for lower initial BaCl₂ concentration. Surprisingly, the particles were mesocrystals which are agglomerates of nanocrystals with their crystal axes aligned. The numerical simulations consist of the three steps. One is the chemical reaction leading to the generation of BaTiO₃. The second is the nucleation of BaTiO₃ nanocrystals. The last is the aggregation of nanocrystals. With regard to the aggregation of nanocrystals, two different models have been studied in the present paper. One is the model widely used in aerosol dynamics that any particles aggregate when they collide each other with some probability. The other is a new model that only primary particles (nuclei) aggregate with other particles. The results of the numerical simulations have indicated that the latter model is more adequate. It has also been shown that larger aggregates are produced for lower initial concentration of BaCl₂ due to longer reaction time and lower viscosity which results in higher rate of aggregation. The mechanism of mesocrystal formation is also discussed.

4a A06.**Autoreduction of tetrachloride gold(III) ions and spontaneous formation of gold nanoparticles in sonicated water****Toshio Sakai, Shoichi Miwa, Tomohiko Okada, Shoji Mishima***Shinshu University, Japan*

Gold nanoparticles (AuNPs) were spontaneously formed through autoreduction of tetrachloride gold(III) ions ($[\text{AuCl}_4]^-$) in sonicated water. The $[\text{AuCl}_4]^-$ reduction and the resulting AuNP formation were observed after mixing of an aqueous $[\text{AuCl}_4]^-$ solution with an argon (Ar)-purged ultrapure water sonicated with 950 kHz both-type ultrasonicator at 20 °C for 8 min in the absence of any added reducing agents. This indicates that $[\text{AuCl}_4]^-$ are reduced by some products generated from the sonolysis of water. Activity of the products generated from sonolysis of water for $[\text{AuCl}_4]^-$ reduction remained for 1 day after sonication of water. Rates of the $[\text{AuCl}_4]^-$ reduction and AuNP formation became faster with higher temperature. In order to evaluate the mechanism on the autoreduction of $[\text{AuCl}_4]^-$ and the resulting AuNP formation in the sonicated water, we checked the effects of hydrogen peroxide (H_2O_2) and nitric acid (HNO_3) on the $[\text{AuCl}_4]^-$ reduction and AuNP formation because H_2O_2 and HNO_3 are produced via rebinding of radicals generated from the sonolysis of water. We revealed no significant $[\text{AuCl}_4]^-$ reduction and AuNP formation in aqueous H_2O_2 and HNO_3 solutions. This suggests that the $[\text{AuCl}_4]^-$ reduction and the resulting AuNP formation are caused by some products other than H_2O_2 and HNO_3 in the sonicated water.

4a B02.**An analysis on the second-order nonlinear effect of focused acoustic wave around a scatterer in an ideal fluid****Gang Liu¹, Boo Cheong Khoo^{1,2}, Pahala Gedara Jayathilake^{1,2}***¹National University of Singapore, Singapore, ²Singapore-MIT Alliance, Singapore*

Two nonlinear models were proposed and analyzed to investigate the effect of multiple incident acoustic waves focused on certain domain where the nonlinear effect are important. Firstly, the general solution for the one dimensional Westervelt equation with different coordinates (planar, cylindrical and spherical) was obtained based on the perturbation method with the second order nonlinear terms. Then, by introducing the small parameter (Mach number), we applied the compressible potential flow theory and proposed a novel asymptotic perturbation expansion for the velocity potential and enthalpy in a nonlinear acoustic model. Our model permits the decoupling between the velocity potential and enthalpy to second order, with the first potential solutions satisfying the linear wave equation (Helmholtz equation), whereas the second order solutions are associated with the linear non-homogeneous equation. Based on the model, we study the multiple incident acoustic waves focused on certain area in which the findings may have important implications for bubble cavitation/initiation via focused ultrasound called HIFU. Finally, the one-dimensional analytical validation for planar, cylindrical and spherical wave together with the numerical calculation of the models were presented to discuss the influence and validity of the second order nonlinear effects for the acoustic wave interaction. We found that for domain encompassing less than ten times of the radius of the scatterer, the non-linear effect exert a significant influence on the focused high intensity acoustic wave. Moreover, at the comparatively higher frequencies, for the model of spherical wave, a lower Mach number may result in stronger nonlinear effects.

4a B03.

Slow variations of mechanical and electrical properties of dielectrics at high-intensity ultrasonic irradiation

Claes M. Hedberg, Oleg V. Rudenko

Blekinge Institute of Technology, Sweden

Mesoscopic solids like polycrystals, granular media, defective materials, soils and rocks are widespread in nature, science and engineering. Acoustic nonlinearity of such media can be 2-4 order higher than “physical” or “geometrical” nonlinearity of perfect media. The huge nonlinearity is caused by Hertzian contact between grains and micro-asperities of rough grain surfaces, by cracks, or weak bonds between stiffer sections in the medium. Another important property is the interconnection between variations of elasticity and dielectric permittivity under exposure to high-intensity ultrasound. This phenomenon is experimentally observed, and a phenomenological theory generalizing the Debye approach for polar fluids is developed to explain the measured data. A substitution of acoustic measurements by dielectric ones not only improves the accuracy, but also offers new ways to remotely evaluate mechanical properties of materials and natural media. The dependence of dielectric properties of materials on their mesoscopic structure makes it possible to detect internal defects or inclusions of different phases, or to evaluate the material strength. Former dielectric measurements were not accompanied by mechanical ones, but it is just the mechanical properties of frozen soil that are of prime interest for construction of roads, buildings and pipelines in the north, and these data have to be obtained by processing of electro-magnetic data. In addition, the microwave satellite measurements requires this nonsteady-state theory to describe the frequency dispersion.

4a B04.

Shear waves in a cubic nonlinear inhomogeneous resonator

Timofey Borisovich Krit, Valery Georgievich Andreev, Oleg Anatol'evich Sapozhnikov

Department of Acoustics, Faculty of Physics, MSU, Russia

Sound waves could be used to obtain viscoelastic constants of material. Such constants provide one with necessary information about the material condition. Nonlinear shear constants, that carry extra diagnostic information, could be measured by means of finite amplitude shear waves. Resonator seems to be the most convenient and novel device for shear waves amplification. One-dimensional resonator is considered. It is represented by layer of a rubber-like medium with a rigid plate of finite mass on the top surface of the layer. The bottom surface of the layer oscillates harmonically with a given acceleration. Amplitude and form of shear waves were calculated numerically by means of both finite difference method for the displaced grids and finite elements method. Resonance curves were obtained at different acceleration amplitudes of the bottom surface of the layer. Measurements were performed with a resonator filled with 15-mm layer of rubber-like polymer plastisol. Shear modulus for small displacements and nonlinear coefficient of the medium were obtained from measured dependence of mechanical stress versus shear deformation. Relaxation properties and viscosity were measured from amplitude-frequency response in linear mode. Oscillation amplitudes in nonlinear mode reached values that correspond to maximum deformations 0.4 – 0.6 in the layer, so that nonlinear effects could be observed. Measured dependencies of resonance frequency versus oscillation amplitude corresponded ones, calculated in case of lower value of nonlinear coefficient. It was shown that as amplitude of oscillations in the resonator increases, resonance frequency increases, and form of resonance curve becomes asymmetrical. When amplitudes are large enough, region of bistability could be observed. Oscillations of the top surface of the layer were investigated. Acceleration profile was both calculated and measured. Its Fourier-transform was performed. Profile distortion was shown theoretically and experimentally. The growth of third harmonic was shown at high amplitudes of driving force. Nonlinear effects dependency on the location of inhomogeneities was found out. Nonlinear effects become more pronounced in pored layer when pores are located near the bottom surface and less pronounced in case when pores are near the top surface.

4a B05.**Simulation of multi-cracks in solid using harmonics filtering with a time reversal process****Xiaozhou Liu, Ying Zhang, Jinlin Zhu, Xiufen Gong***Institute of Acoustics, Nanjing University, China*

Nonlinear elastic wave spectroscopy has been shown as an effective method to use in the non-classical nonlinear medium. However, it is still difficult to determine the position of defects in solid using this method. And previous studies testified that with the help of the TR process, people can overcome the disadvantages of time-delay techniques and finally get good results of the position of the defect. In this study, based on a two-dimensional pseudo-spectral, a numerical study is used here to validate the NEWS-TR method as a potential technique for the location of one and two defects in an attenuated medium. We consider the linearly elastic sample containing crack zones of non-classical nonlinear without classical nonlinear as the whole. The modified PM model is introduced to simulate the non-classical nonlinear behavior of the damaged zones. The TR steps correspond to those described in the literature: firstly transmit a signal into the sample, then filter nonlinear components of received signals, reverse the filtered signals and retransmit into the sample to observe the final image. The simulations prove that it is valid to use a tone burst pressure field to execute a TR imaging for judging the positions of defects in an attenuated medium. This project is supported by the financial support of the National Natural Science Foundation of China (Grant No.11074122)

Invited Paper**4a C01.****Actively created quiet zones by parametric loudspeaker as control sources in the sound field****Chao Ye, Ming Wu, Jun Yang***Institute of Acoustics, Chinese Academy of Sciences, China*

In active noise control system, omnidirectional loudspeakers are utilized as control sources to suppress the noise in the targeted area. However, the sound pressure levels of noise outside the target region may actually increase. Based on the nonlinear interaction of ultrasonic waves in air, the parametric loudspeaker generates highly directional audible sound by the self-demodulation of amplitude modulated sound waves. As a result, taking the advantage of the high directivity, the parametric loudspeakers can be used as a control source to reduce the sound pressure levels in the control points without noise increase in other areas. In this study, the application of parametric loudspeaker as a secondary source in active noise control system is discussed. The power outputs of both primary and secondary sources are analyzed by the impedance-based approach. It is found that when the total power output of the two sources is minimized, the secondary source absorbs the acoustic power of the primary source because of the weak coupling between the two sources. Therefore, the minimization of the power output of the primary source is the same as the maximization of the power absorption of the secondary source. Furthermore, the quiet zone generated by the control system in a pure tone sound field is examined as well. Numerical and Experimental results show that there is a quiet zone along the axial direction of the secondary source, when the two sources are arranged in a line. There is negligible increase of sound pressure in the sound field and the total acoustic power is reduced after control. In addition, the disadvantages of the exploitation of the parametric loudspeaker as a control source are discussed as well. It is hard to control the parametric loudspeaker to suppress broadband noise due to the nonlinearity mechanism of directional sound production and the nonuniform of the ultrasonic transducers of parametric loudspeaker. The harmonic distortion and the uneven frequency response especially in low frequency of the parametric loudspeaker may deteriorate the control effect.

4a C03.

Estimation of parametric sound field controlled by source amplitudes and phases using numerical simulation

Hideyuki Nomura¹, Claes M. Hedberg², Tomoo Kamakura¹

¹The University of Electro-Communications, Japan, ²Blekinge Institute of Technology, Sweden

The parametric array is formed by two finite-amplitude ultrasound beams with neighboring frequencies. The nonlinear interaction of the beams generates a highly directive audible sound at the difference frequency. Up to now, we have analyzed theoretically parametric sound fields in a free space. This study proposes a numerical simulation method of nonlinear ultrasound propagation to estimate the parametric sound field in the time domain. Using the finite-difference time-domain method based on the Yee algorithm with operator splitting, axisymmetric nonlinear propagation was simulated on the basis of equations for a compressible viscous fluid. As model application, a length-limited parametric sound beam, which is formed by four finite-amplitude ultrasound beams with different frequencies and controlled by phases and amplitudes of sound sources and has a truncated array length [C.M. Hedberg et al., *Acoust. Phys.* 56, 637–639 (2010)], was numerically simulated. The simulation showed a spatially restricted and very narrow difference frequency sound beam similar to their experiment. In addition, to investigate the dependence of amplitude and phase on the length-limited beam profiles, parametric sound fields were numerically estimated by varying the amplitude and phase slightly from the condition of the length-limited beam. Numerical results indicated that the changes of the amplitude and phase affected the beam length and width, in particular, amplitude changes drastically deformed the beam shape from that of the length-limited beam. This result suggests that precisely controlled sound sources are necessary to obtain the best length-limited sound beam.

4a C04.

Modeling the directivity of parametric loudspeaker

Chuang Shi, Woon-Seng Gan

Nanyang Technological University, Singapore

Due to the new deployment of a parametric loudspeaker in applications, such as active noise control of moving targets and 3D sound reproduction, accurate directivity control of the parametric loudspeaker is desired. It has been previously proven by experiment that the directivity pattern of the difference frequency can be controlled with certain degree of errors using a delay-and-sum beamforming structure applied to both primary input frequencies of the parametric loudspeaker. However, accurate prediction of the main beam and its sidelobes of the difference frequency (i.e. the desired audible frequency) remain a challenging problem. This problem is mainly due to the approximated relationship between the directivities of the primary frequencies and the difference frequency. Furthermore, the mismatch observed between the theoretical beampatterns and the directivities measured in the experiment are caused by the system errors incurred at different stages of implementation. In practical applications of the parametric loudspeaker, these system errors change with environments, which in turn make it harder to design an accurate beamsteering system. In this paper, we propose directivity models to describe beampatterns of the parametric loudspeaker at both the primary frequencies and the difference frequency. This directivity models can be used to predict the directivity pattern of arbitrary steering angles. The primary frequency model consists of two tuning vectors corresponding to two typical system errors, namely, the weight error and the spacing error. The difference frequency model consists of a modified form of the product directivity principle to further enhance the modeling accuracy of the difference frequency. The experimental results show that the proposed models can be used to predict the directivities at both the primary frequencies and the difference frequency, and assist in designing a better beam-control parametric loudspeaker.

4a C05.**Inverse system design based on the Volterra modeling of a parametric loudspeaker system****Wei Ji, Woon-Seng Gan***Nanyang Technological University, Singapore*

Parametric loudspeaker systems have been widely used for projecting audible sound beam with high directivity. However, the nonlinear interaction among primary waves also generates harmonics, which distort the desired signal and degrade the sound quality. In order to investigate this inherent nonlinear mechanism, a baseband distortion model is developed from nonlinear system identification using an adaptive Volterra filter structure.

For the conventional double-sideband amplitude modulation technique, it is found that the harmonic distortion is largely attributed to the second harmonic. An adaptive Volterra filter with reduced complexity to the second-order kernel is employed to model the reproduced baseband signal and second harmonic present in the demodulated signal. The adaptation results derived from both simulation and measurement indicate that the first few coefficients of the second-order kernel are dominant.

Based on the Volterra model, a p -th order inverse system is designed to compensate the harmonic distortions present in the demodulated signal. Simulation and measurement results demonstrate that the harmonic distortion can be greatly reduced to an acceptable level when the inverse system is introduced with a suitable recursive order. Besides, the performances of the inverse system and the square-root amplitude modulation (SRAM) technique are also compared for different modulation indices with the emitter's effect taken into account.

4a C06.**3D Simulation of parametric ultrasound fields****Fabrice Prieur***University of Oslo, Norway*

Parametric sonar is widely used for sea-floor characterization, sub-bottom object detection, or underwater communication. It takes advantage of the interaction between two primary beams transmitted at slightly different frequencies. Due to nonlinear propagation, two secondary beams at the sum and difference frequency are generated. The radiation at the difference frequency combines sub-bottom penetration due to low attenuation, and high resolution due to an acoustic beam with a narrow mainlobe and negligible sidelobes. It allows to generate directive low frequency beams with transducers of reasonable size. A method that estimates the pressure level and the beam profile of the radiation at the sum and difference frequencies is presented. It solves the Westervelt equation in the frequency domain under the quasi-linear approximation. A full three dimensional estimate of the radiated fields can be computed at any depth without the need for stepwise propagation from the source plane. The method applies to two dimensional transducers of arbitrary geometry and distribution. It does not rely on the parabolic approximation and is not limited to monochromatic radiations, thus allowing to model pulses with wide bandwidth. The limits of the method come from the assumptions of a homogeneous medium and input pressure levels sufficiently low to satisfy the quasi-linear approximation. The obtained results in the case of a flat piston transducer compare favorably to previous measurements and numerical estimates from proven methods.

Closing Lecture**4a L6.****Conditions inside a collapsing bubble****Kenneth S. Suslick***University of Illinois, United States*

Extreme temperatures and pressures are produced through acoustic cavitation: the formation, growth and collapse of bubbles in a liquid irradiated with high intensity ultrasound. Single bubbles have generally been assumed to give higher temperature conditions than bubble clouds, but confirmation from the single bubble sonoluminescence (SBSL) emission spectra have been problematic because SBSL typically produces featureless emission spectra that reveal little about the intra-cavity physical conditions or chemical processes. Here we present definitive evidence of the existence of a hot, highly energetic plasma core during SBSL. From a luminescing bubble in sulfuric acid, excited state to excited state emission lines are observed both from noble gas ions (Ar^+ , Kr^+ , and Xe^+) and from neutral atoms (Ne, Ar, Kr, and Xe). The excited states responsible for these emission lines range from 8.3 eV (for Xe) to 37.1 eV (for Ar^+) above the ground state. Observation of emission lines allows for identification of intra-cavity species responsible for light emission; the energy levels of the emitters indicate the plasma generated during cavitation is comprised of highly energetic atomic and ionic species. Effective emission temperatures of >18000 K, pressures of ~ 1 kBar and ion densities with $N_e > 10^{21} \text{ cm}^{-3}$ have been experimentally determined.

Author Index

A

Adachi, Hideo 2a B03.
 Adachi, Shizuko 3p C07.
 Aida, Takumi 3p B12.
 Aizawa, Koji **2p P09.**
 2p P11.
 Akiyama, Iwaki 2p B12.
 Alizadeh, Mohsen 3p A08.
 An, Yu **3p A10.**
 Anderson, Brian E 3p B08.
 Andreev, Valery Georgievich 4a B04.
 Asami, Rei 2p B11.
 Assink, Jelle 1p A04.
 Atchley, Anthony A. **3p C11.**
 Awata, Sojiro 2a C04.
 Azuma, Takashi 2p B11.

B

Badmaev, Badma 1p B10.
 Bailliet, Hélène 2p C09.
 Baltean-Carlès, Diana **2p C08.**
 Bas, Pierre-Yves Le **3p B08.**
 Bercoff, Jeremy 2p B06.
 Biwa, Shiro 1p C07.
 2p P10.
 Biwa, Tetsushi 3a C03.
3a L4.
 Blanc-Benon, Philippe 2a A04.
3a C04.
 Brodin, Lars-Ake 2a B05.
 Bulanov, Alexey V. **1a B01.**
 Bulanov, Vladimir A. **2a C02.**

C

Carles, Pierre **3p C10.**
 Chen, Jianjun **3a B04.**
 Chen, Rui 1p B05.
 Choi, Pak-Kon 3p A12.
 Chuecos, Nicolas **2a C03.**
 Chunchuzov, Igor **1p A04.**
 Clement, Gregory Thomas **2a B03.**
 Cohen-Bacrie, Claude 2p B06.
 Coulouvrat, François **1a A01.**
 1p A05.
1p L2.

D

Damdinov, Bair **1p B10.**
 Daru, Virginie 2p C08.
 Delalande, Anthony 4a A02.
 Delorme, Philippe 1a A01.
 Delrue, Steven 3a B01.

Dembelova, Tuyana 1p B10.
 Demi, Libertario 2a B04.
 Demin, Igor Yu. **2p P12.**
 Deriabina, Mikhail S 1p B09.
 Doi, Yusuke **2p C11.**

E

Enflo, Bengt O. **1p A09.**

F

Falco, Lauren E. 3p C11.
 Fan, TingBo 4a A01.
 Farikhah, Irna - **3a C02.**
 Fujikawa, Shigeo 2p C07.
 3a A02.
 Fujita, Fumio 3p B12.
 Fujita, Naoki 2p C12.
 Fukuda, Makoto **2p P02.**
 Furukawa, Takashi 1p C04.

G

Gainville, Olaf 1a A01.
2a A04.
 Gallin, Louis-Jonardan 1p A05.
 Gan, Woon-Seng 4a C04.
4a C05.
 Gaudard, Eric 1p A05.
 Gee, Kent L. 3p C11.
 Gong, Xiufen 4a B05.
 Grishenkov, Dmitry 2a B05.
 Guedra, Matthieu 3p C06.
 Gurbatov, Sergey N. 2p P12.
 Gusev, Vitaliy 3p C06.

H

Hamilton, Mark F. **2p B10.**
 3a A03.
 Hammerton, Paul William 2a A05.
 Hasegawa, Hideyuki **2p B09.**
 Hashiba, Kunio 2p B11.
 Hashimoto, Atsushi 2a A03.
 Hatanaka, Shin-ichi 1p C10.
4a A03.
 Hauptert, Sylvain 3p B11.
 Hawker, Nicholas **3p A07.**
 Hay, Todd A. **3a A03.**
 Hayashi, Yuichi **3p A12.**
 Hedberg, Claes M. 1p A09.
4a B03.
 4a C03.
 Hennenon, Martin 1a A01.
 Hikiyama, Takashi 2a C05.

Hiziroglu, Huseyin R 1a C02.
 Horie, Sachiko 1p B05.
 Horinouchi, Satoshi 1p C06.

I

Ichihara, Mie **1a A03.**
 Ikegami, Yasushi 1p C04.
 Ilinskii, Yurii A. 2p B10.
 3a A03.
 Imanishi, Ryusuke 3p B12.
 Imano, Kazuhiko 2p P02.
 Inaba, Masashi **2p C07.**
 Inamura, Takao 3a A05.
 Inui, Yoshitaka 2p P06.
 Isago, Ryoichi 1a B02.
 2p B08.
 2p P06.
 Ishigaki, Masahiro **3p C07.**
 Ishii, Katsuya 3p C07.
 Ishii, Yosuke **2p P10.**
 Ishii, Yutaka **3a B03.**
 Ito, Youichi 2p P07.

J

Jayathilake, Pahala Gedara 4a B02.
 Ji, Wei 4a C05.
 Jinbo, Yoshinori 2p A12.
 Johnson, Paul 3p B11.
 Johnson, Paul A 3p B08.
3p L5.
 Jondeau, Emmanuel 3a C04.

K

Kamakura, Tomoo 2a A03.
 2a B03.
 4a C03.
 Kanagawa, Tetsuya **3a A02.**
 Kanai, Hiroshi 2p B09.
 Kandula, Max **2p A06.**
 Kari, Leif **1a C03.**
 Kasyanov, Dmitry A **1p B09.**
 Kato, Kazumi 4a A04.
 Kawahara, Junya 3a A02.
 Kawashima, Koichiro **3p B12.**
 Kedrinskiy, Valeriy Kirillovich **2p A09.**
 Khokhlova, Vera A **2a B02.**
2a L3.
 Khoo, Boo Cheong 4a B02.
 Kimura, Masayuki **2a C05.**
 Kobayashi, Kazumichi 2p C07.
 3a A02.
 Koch, Philipp 3p A08.

Kochi, Takashi 1p B05.
Kodama, Tetsuya 1p B05.
Kogi, Mieko 2p P11.
Komura, Ichiro 1p C04.
Kondoh, Jun **1a B03**.
Korenska, Marta **3a B05**.
Kothapalli, Veera Venkata Satya
Narayana **2a B05**.
Kotopoulos, Spiros **4a A02**.
Koyama, Daisuke **1a B02**.
2p B08.
2p P04.
Kozuka, Teruyuki **1p C10**.
Krit, Timofey Borisovich **4a B04**.
Kudo, Nobuki 2p B12.
Kudryavtsev, Andrey 1p A08.
Kulichkov, Sergey 1p A04.
Kurihara, Eru **3a A04**.
Kurin, Vasily V 1p B09.
Kuroda, Kentaro 3a C01.
Kurz, Thomas 3p A08.

L

Langthjem, Mikael A **3p C12**.
Laugier, Pascal 3p B11.
Lauterborn, Werner **3p A08**.
Lebedev, Andrey V. 3p B06.
Leighton, Timothy 2p A11.
Li, Li 1p B05.
Li, Shenwei 1p B05.
Liang, Wei **2p P03**.
Liu, Gang **4a B02**.
Liu, Xiaozhou **4a B05**.
Liu, Yunqiao 2p A10.
Lyons, John 1a A03.

M

Maimaitiming, Maimaititusong
..... 3p A10.
Makarenko, Nikolay Ivanovich 1a A02.
Makarova, Dagzama 1p B10.
Makov, Yury Nikolaevich **1p A10**.
Maksimov, Alexey **2p A11**.
Maltseva, Janna Lvovna **1a A02**.
Manychova, Monika 3a B05.
Mao, Yiwei 3a B04.
Marchiano, Régis **1p A05**.
Matsuda, Naoki **1p C07**.
Matsumoto, Yoichiro 2p A10.
Matysik, Michal 3a B05.
Mihara, Tsuyoshi **1p C04**.
Mishima, Shoji 4a A06.
Miwa, Shoichi 4a A06.
Moreau, Solenn 2p C09.
Mori, Koichi **1p C09**.

Mori, Shiro 1p B05.
Morimoto, Kenshi 1p B06.

N

Nakamura, Kentaro 1a B02.
2p B08.
2p P04.
Nakamura, Yoshiaki 1p C09.
Nakano, Masami 3p C12.
Nakano, Yosuke 3a C01.
Nakatani, Akihiro 2p C11.
Nishikawa, Kohei 3p C08.
Nishimura, Souichi 2p C12.
Nishiwaki, Motoaki **2p P11**.
Nitta, Naotaka **2p B12**.
Nomura, Hideyuki 2a B03.
4a C03.

O

Obayashi, Atsushi **3a C03**.
Obayashi, Shigeru 1p A06.
Ohara, Yoshikazu 1p C05.
1p C06.
Ohtani, Toshihiro 3a B03.
Oikawa, Jun 1a A03.
Okada, Tomohiko 4a A06.
Ostrovsky, Lev A. **3p B06**.
Osumi, Ayumu **2p P07**.

P

Péronne, Émmanuel 2a C03.
Paradossi, Gaio 2a B05.
Penelet, Guillaume **3p C06**.
Perrin, Bernard 2a C03.
Pichon, Chantal 4a A02.
Poignand, Gaëlle 3a C04.
Popov, Oleg 1p A04.
Postema, Michiel 4a A02.
Prieur, Fabrice **4a C06**.
Pronchatov-Rubtsov, Nikolay V.
..... 2p P12.

R

Rénier, Mathieu 1p A05.
Raju, Krishna Murti **1a C01**.
Rendon, Pablo Luis **1p B08**.
Reyt, Ida **2p C09**.
Riviere, Jacques **3p B11**.
Rudenko, Oleg V. 4a B03.

S

Söhnholz, Hendrik 3p A08.
Sada, Yurina 2p C12.
Saffari, Nader 3a A01.
Sakai, Takeharu 2a A03.

Sakai, Toshio **4a A06**.
Sakamoto, Masataka 3a C05.
Sakamoto, Maya 1p B05.
Sakamoto, Shin-ichi **2p P06**.
3a C01.
Salamone, Joe **2a A01**.
Sapozhnikov, Oleg **1a L1**.
1p A08.
Sapozhnikov, Oleg Anatol'evich
..... 4a B04.
Sato, Masayuki **2p C12**.
Sax, Nicolas **1p B05**.
Schanz, Daniel 3p A08.
Schofield, John Michael **2a A05**.
Scott, Julian 2a A04.
Seki, Hideki 3a C05.
Shanker, Kiran **1p C08**.
Shepherd, Micah R. 3p C11.
Shi, Chuang **4a C04**.
Shi, Weihua 2p C12.
Shimaya, Koji 1p C04.
Shimizu, Dai **3p C08**.
Shintaku, Yohei 1p C05.
1p C06.
Shirai, Koichiro 3p C07.
Shirota, Minori **3a A05**.
Shkolnik, Iosif E **1a C02**.
Shoab, Muhammad 1a C03.
Sievers, A. J. 2p C12.
Sinden, David **3a A01**.
Souquet, Jacques **2p B06**.
Sparrow, Victor 2a A01.
Stride, Eleanor 3a A01.
Sugimoto, Nobumasa 2a C04.
3p C08.
Sugiyama, Kazuyasu 2p A10.
Suslick, Kenneth S. **4a L6**.

T

Tabaru, Marie **2p B11**.
Takagi, Ryo 1p B07.
Takagi, Shu **2p A10**.
Takahashi, Takashi 2a A03.
Takahira, Hiroyuki **2p A12**.
Takao, Yuichi 2p C12.
Takeo, Minoru 1a A03.
Tamagawa, Masaaki **1p B06**.
Tanaka, Shigenori 2p A08.
Toker, Grigory **3p A06**.
Tokunaga, Yoshiaki 2p P09.
2p P11.
Tomita, Yukio **2p A08**.
Toyoizumi, Hitoshi 1a B03.
Tsuruoka, Fujio **2p P05**.

Tuziuti, Toru **2p P08.**
4a A04.

U

Ueda, Yuki **3a C05.**
Ulrich, Timothy J 3p B08.
Umemura, Shin-ichiro 1p B07.

V

Valière, Jean-Christophe 2p C09.
Van Den Abeele, Koen **3a B01.**
van Dongen, Koen WA 2a B04.
Ventikos, Yiannis 3p A07.
Verweij, Martin D **2a B04.**
Vilchinska, Nora A. **3p B10.**
Voloshchenko, Vadim Yur'evich
..... **2p P01.**

W

Wada, Yuji **2p P04.**
Watanabe, Masao 2p C07.
3a A02.
Watanabe, Yoshiaki 2p P06.
3a C01.
Watanabe, Yosuke **2a C04.**
Watanabe, Yukiko 1p B05.
Waxler, Roger 1p A04.
Weisman, Catherine 2p C08.
Wu, Ming 4a C01.

Y

Yagishita, Yoko 1p B05.
Yamaguchi, Jun 2p B09.
Yamamoto, Masafumi **2a A03.**
Yamanaka, Kazushi **1p C05.**
1p C06.
Yamashita, Hiroshi **1p A06.**
Yamashita, Kou 3a A05.
Yanagimoto, Kohei **3a C01.**
Yang, Jun **4a C01.**
Yang, Kai 3p A10.
Yano, Takeru **2p C06.**
2p C07.
3a A02.
Yasuda, Jun 1p B07.
Yasui, Kyuichi 1p C10.
4a A04.
Ye, Chao 4a C01.
Yoshikawa, Hideki 2p B11.
Yoshimura, Kazuyuki **2p C10.**
Yoshinaga, Takao **2p A07.**
Yoshizawa, Shin **1p B07.**
Yuldashev, Petr V 2a B02.

Z

Zabolotskaya, Evgenia A. 2p B10.
3a A03.
Zhang, Cui Ying 3p A10.
Zhang, De 3a B04.
Zhang, Dong **4a A01.**
Zhang, Ying 4a B05.
Zhu, Jinlin 4a B05.
Zhu, Qi Rong 3p A10.

Session Chair Index

A

Akiyama, I. 2p B06-09.
An, Yu 3a A01-05.
Atchley, A. A. 3a L4.

B

Biwa, S. 1a C01-03.
Blanc-Benon, Ph. 1a A01-03.
1p L2.
2a A01-05.
3p C06-08.

C

Choi, P. -K 4a A01-06.
Clement, G. T. 2p B10-12.

E

Enflo, Bengt O. 2p C06-09.

G

Gan, W-S. 4a C01-06.

H

Hamilton, M. F. 2a L3.
3p C10-12.
Hasegawa, H. 2a B02-05.
Hedberg, C. M. 1p C04-07.

I

Ishii, K. 3a C01-05.

J

Johnson, P. A. 4a B02-05.

K

Kamakura, T. 1a L1.
Kari, Leif 2p C10-12.
Kedrinskiy, V. K. 3p A06-08.
Khokhlova, V. A. 1p B05-07.
Kondoh, J. 1p B08-10.
Kurihara, E. 2p A10-12.

M

Makino, Y. 1p A04-06.
2a A01-05.
Matsumoto, Y. 4a L6.

N

Nakamura, K. 1a B01-03.
Nomura, H. 4a C01-06.

O

Ostrovsky, L. A. 3a B01-05.

S

Sapozhnikov, O. 3p B10-12.
Sugimoto, N. 3p L5.
Suslick, K. S. 3p A10-12.

T

Takahira, H. 2p A06-09.

V

Van Den Abeele, K. 3p B06-08.

W

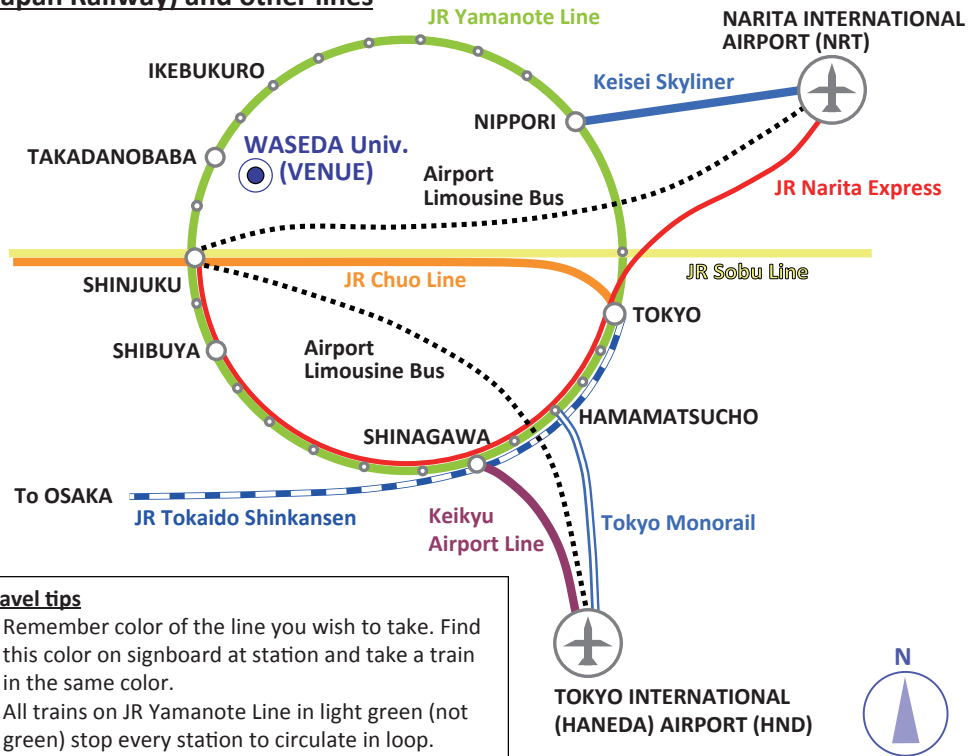
Watanabe, Y. 1p C08-10.

Y

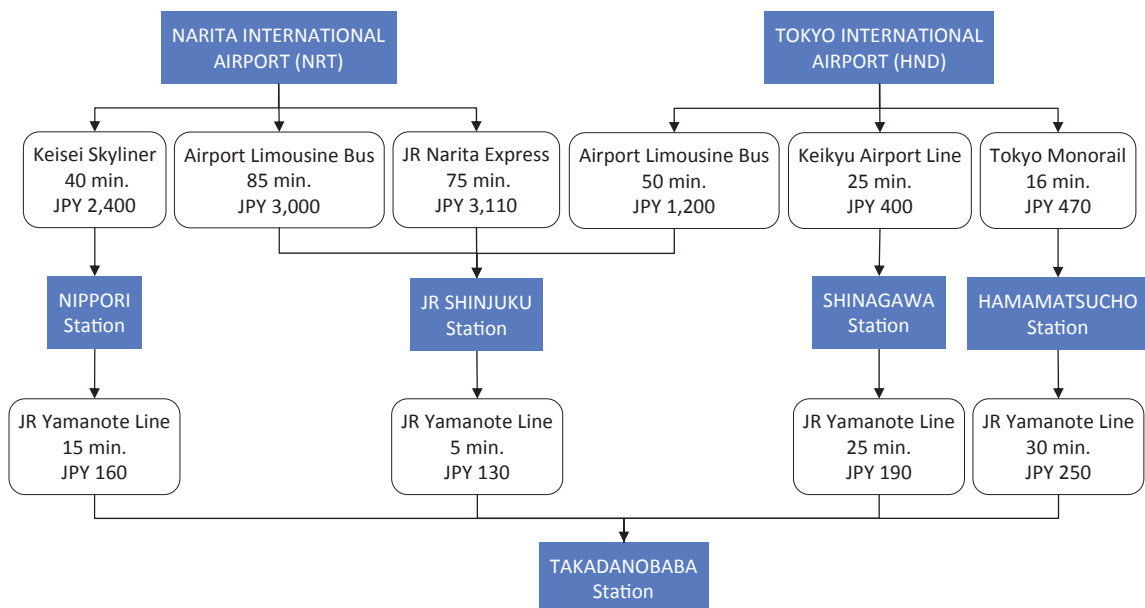
Yano, T. 1p A08-10.
Yoshimura, K. 2a C02-05.

▶ JR (Japan Railway) and other lines

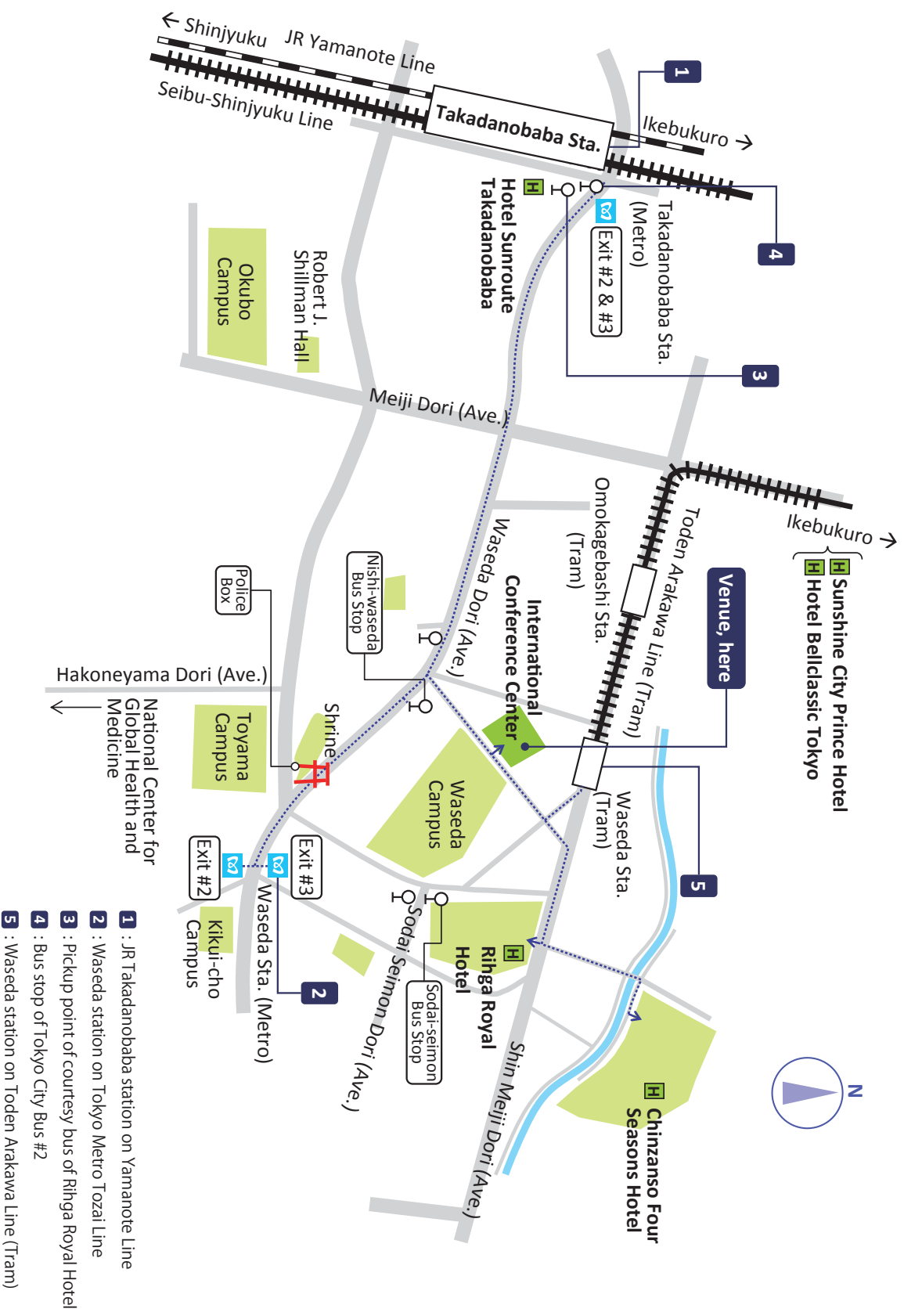
JR (Japan Railway) and other lines



▶ Access from Narita and Tokyo International Airports to Takadanobaba Station



▶ Local map of International Conference Center



- 1** : JR Takadanobaba station on Yamanote Line
- 2** : Waseda station on Tokyo Metro Tozai Line
- 3** : Pickup point of courtesy bus of Rihga Royal Hotel
- 4** : Bus stop of Tokyo City Bus #2
- 5** : Waseda station on Toden Arakawa Line (Tram)